VITELLOGENIN RECEPTOR AND NEUROPEPTIDE RECEPTORS INVOLVED IN REPRODUCTION OF THE RED IMPORTED FIRE ANT (*Solenopsis invicta* Buren)

A Dissertation

by

HSIAO-LING LU

Submitted to the Office of Graduate Studies of
Texas A&M University
in partial fulfillment of the requirements for the degree of

DOCTOR OF PHILOSOPHY

December 2011

Major Subject: Entomology

VITELLOGENIN RECEPTOR AND NEUROPEPTIDE RECEPTORS INVOLVED IN REPRODUCTION OF THE RED IMPORTED FIRE ANT (*Solenopsis invicta* Buren)

A Dissertation

by

HSIAO-LING LU

Submitted to Office of Graduate Studies of
Texas A&M University
in partial fulfillment of the requirements for the degree of

DOCTOR OF PHILOSOPHY

Approved by:

Chair of Committee,	Patricia Pietrantonio
Committee Members,	S. Bradleigh Vinson
	Craig Coates
	Ginger Carney
Head of Department,	David Ragsdale

December 2011

Major Subject: Entomology

ABSTRACT

Vitellogenin Receptor and Neuropeptide Receptors Involved in Reproduction of the Red Imported Fire Ant (*Solenopsis invicta* Buren). (December 2011)

Hsiao-Ling Lu, B.S., National Chung-Hsing University;

M.S., National Chung-Hsing University

Chair of Advisory Committee: Dr. Patricia V. Pietrantonio

Social insects have complex forms of social organization. Molecular mechanisms involved in the regulation of their reproduction are not fully understood. This dissertation investigated the vitellogenin receptor (**VgR**), short neuropeptide F (**sNPF)** receptor and two insulin receptors (**InRs**) in the red imported fire ant *Solenopsis invicta*, focusing on their possible roles in the regulation of queen reproduction. Knowledge of these receptors may provide novel ways to manipulate either reproductive castes or overall reproductive outcome, diminishing the fire ant impact as invasive pest.

Fire ant virgin queens have more abundant VgR (*Si*VgR) transcripts than newly-mated queens, but limited egg formation. To elucidate whether queen maturation involved changes in *Si*VgR expression, we investigated both virgin and mated queens. In both queens, immunofluorescence analysis of ovaries revealed differential *Si*VgR localization in early and late stage oocytes; however, mated queens showed higher *Si*VgR expression than virgin queens. In virgin queens, the *Si*VgR signal was first observed at the oocyte membrane beginning at day 12 post-emergence, coinciding with

the maturation period required before a mating flight. *Si*VgR silencing in virgins through RNA interference abolished egg formation, demonstrating that *Si*VgR is involved in queen ovarian development pre-mating.

The sNPF and insulin signaling pathways have been implicated in the regulation of food intake and body size, and these peptides also play a gonadotropic role in the ovaries of some insect species. To elucidate the sites of action of the sNPF peptide(s), the **sNPF receptor** tissue expression and cellular localization were analyzed in the queen brain, subesophageal ganglion (SEG), and ovaries by immunofluorescence. Results suggest that the sNPF signaling cascade may be involved in diverse functions, and the sNPF peptide(s) may act in the brain and SEG as neurotransmitter(s) or neuromodulator(s), and in the ovaries as neurohormone(s). In addition, to elucidate the role of insulin signaling pathway in the fire ant, two putative **InRs** were cloned. Transcriptional expression analyses show that the receptor abundance was negatively correlated with body size and nutrition status in fire ant immatures. In queens, the expression of InRs in different queen tissues correlates with tissue requirements for queen reproductive physiology and behaviors.

ACKNOWLEDGEMENTS

I would like to dedicate this dissertation to my father who passed away ten years ago and to my family in Taiwan. I especially appreciate the encouragement, love and support from my mother and the help from my brother and sister who took care of home and let me have no worries. All of their support allowed me to pursue my Ph.D. in a foreign country.

Without the help and assistance of many individuals, the work in this dissertation would not have been possible. I would like to thank, most especially, Dr. Patricia Pietrantonio, my committee chair and advisor. She not only provided funding for my assistantship, she also provided lots of advice on my writings and presentations throughout my studies and sought out the opportunity for me to write a book chapter with Dr. Vinson. Additionally, she provided insightful advice on being in an academic position. Thank you, Dr. Pat.

I would further like to thank my committee members, Dr. Vinson, Dr. Coates, and Dr. Carney, for their comments and help on the development and execution of my research. I am grateful for their efforts. I also thank all of my friends and lab mates who gave me all kinds of assistance. All of my friends, it is so good to have your company here in College Station. Maria, Chris, Brad, Cymon, Sunny, and Andy, thank all of you for your assistance and I enjoyed those days spent in the lab together.

This dissertation is also dedicated to the memory of my friend, Yi-Chun Yang, who passed away while pursuing her Ph.D.

TABLE OF CONTENTS

CHAPTER Page

LIST OF FIGURES

FIGURE Page

FIGURE Page

LIST OF TABLES

CHAPTER I

INTRODUCTION

Introduction

Ants comprise at least one third of the world's insect biomass and they are fundamental components of both agroecosystems and natural environments [1,2]. They play essential roles as natural predators, scavengers in nutrient cycling and some of them are of medical importance. Despite their wide geographic distribution in diverse environments, not much is known about the molecular mechanisms of their reproduction. Knowledge of reproduction at this level is also scarce for most insect species.

The red imported fire ant, *Solenopsis invicta* Buren (Hymenoptera: Formicidae) (herein referred to as the fire ant) is an aggressive pest and invaded several countries in the world. When the fire ant was accidentally introduced into the United States in the 1930's, it found an almost ideal environment and quickly became an important agricultural and urban pest species [3]. With respect to public health concerns, the venom of workers causes small pustules in the skin which can become infected and thus be life threatening for humans and animals.

This dissertation follows the style and format of *FEBS Journal.*

Fire ant queens have high reproductive ability. For example, a monogyne queen can produce 347 eggs within 2 hours [4]. However, more than 80 years after the initial fire ant invasion, knowledge of its reproductive physiology is still insufficient. Thus, this dissertation aims to contribute new knowledge on the physiology and underlying molecular mechanisms of fire ant reproduction. Scientific contributions to topics including vitellogenesis, hormonal regulation of insect reproduction, fire ant reproductive biology, and hymenopteran genome projects were made.

Vitellogenesis

To understand female reproduction, a first step is to understand oogenesis (the formation of eggs). Vitellogenesis is the key control process of oogenesis in oviparous animals. Vitellogenesis involves the synthesis and release of the yolk protein precursor, vitellogenin (Vg), from the fat body in insects [5-7] or the liver in vertebrates [8], and the incorporation of Vgs into the developing oocyte through the Vg receptor (VgR)-mediated endocytosis. Receptor mediated endocytosis is an ubiquitous mechanism for internalizing functionally important macromolecules, which was first described in animal cells [9]. During VgR-mediated endocytosis, Vg binds to VgR located at the oocyte plasma membrane and the ligand–receptor complex is internalized into the oocyte cytosol. After internalization, VgR releases Vg to be stored as vitellin (Vn), the nutritional source for egg development, while the VgR is recycled back to the oocyte surface [6,7,10-12]. This endocytosis process has been described in several insect

species. Regulation of the VgR expression is one of the key elements in this receptor-mediated mechanism.

The vitellogenin receptor (VgR)

Several sequences of VgRs from vertebrates have been reported, including those from birds, amphibians and fishes [13-17] and from invertebrates including ticks [18,19], shrimp [20], nematode [21], and insects. Insect VgR genes encode large proteins (180-214 kDa) which are about twice the size of vertebrate VgRs (95-115 kDa) [6]. In insects, the first VgR gene was identified from the fruit fly *Drosophila melanogaster* and was named yolk protein receptor (YPR) or *yolkless* (*yl*) [22]. Other insect VgRs were cloned from the mosquito *Aedes aegypti* (L.) [23], the fire ant *S. invicta* [24], the moth *Spodoptera litura* Fabricius [25], and three cockroach species (*Periplaneta americana* L., *Leucophaea maderae* (F.), and *Blattella germanica* (L.)) [26-28].

Insect VgR belongs to the low-density lipoprotein receptor (LDLR) superfamily [29]. This superfamily includes VgR, lipophorin receptors (LpR), and other LDLRs. Receptors in this superfamily are characterized by a highly conserved arrangement of modular elements which include: 1) the ligand-binding domain (LBD) comprising Class A cysteine-rich repeats, 2) the epidermal growth factor (EGF) precursor homology domain containing Class B cysteine-rich repeats and YWXD repeats, 3) an O-linked carbohydrate domain, 4) a transmembrane domain, and 5) a cytoplasmic tail [29,30]. Figure 1.1 shows the arrangement of those elements in insect VgRs and LpR, and other LDLR superfamily receptors in vertebrates. Insect VgRs include two copies of the

ligand-binding and EGF-precursor domains as compared to insect LpRs, vertebrate VgRs and LDLRs. Insect VgRs can be divided into three types (type I to III) based on the number of repeats in the first or second ligand-binding domains. Type-I includes cloned VgRs that have five Class A cysteine-rich repeats in the first LBD and eight such repeats in the second LBD. Insects with this type of VgR include cockroaches (*P. americana, L. maderae, B. germanica*), the mosquito (*A. aegypti*) and the fruit fly (*D. melanogaster*). All type-I VgRs contain an O-linked sugar domain except the VgR from the fruit fly. Type-II VgR includes fire ant VgR, and has four repeats in the first LBD and lack O-linked sugar domain. The predicted VgR from the wasp (*Nasonia vitripennis*) (our analyses of XP_001602954) and the honey bee (*Apis mellifera*) [31] also belong to type II VgR with no O-linked sugar domain. Until the present (2011), there are only two recognized types of insect VgRs (type I and type II) [32]; however, recently a moth VgR was cloned form *S. litura* and its gene structure is slightly different than type I or type II VgRs [25]. Similarly to the fire ant VgR, the *S. litura* VgR has four Class A cysteine-rich repeats in the first LBD and also lacks the O-linked sugar domain; however, there are only seven Class A cysteine-rich repeats in the second LBD [25]. Therefore, the moth VgR belongs to the type III VgR.

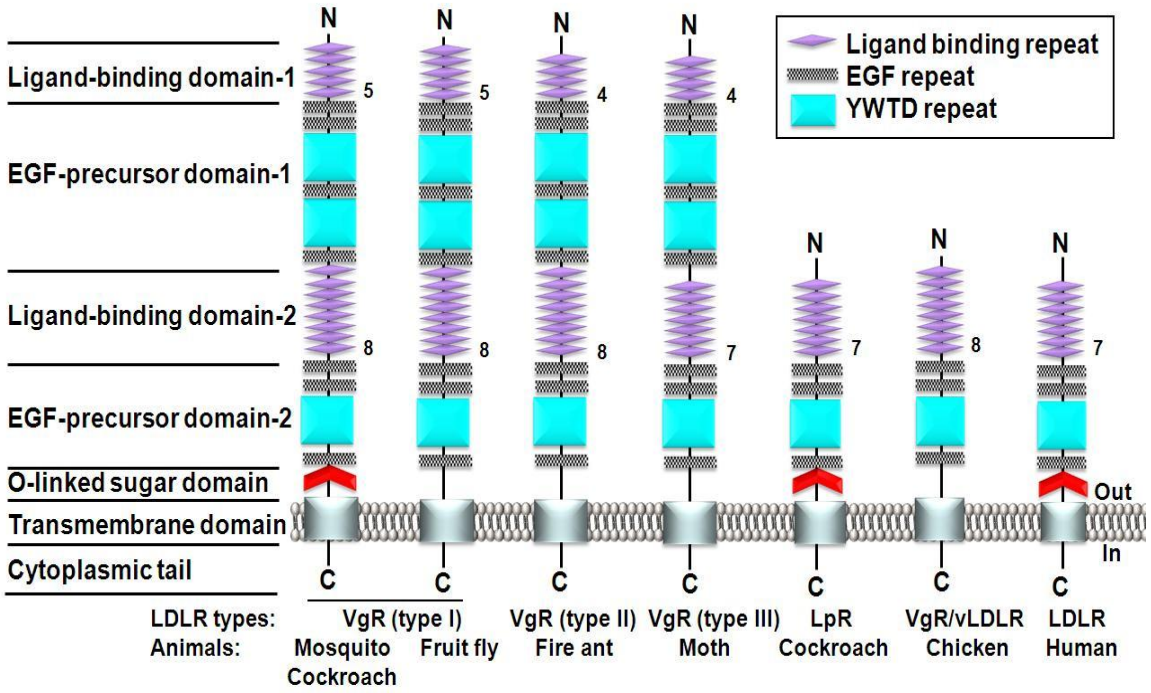

Figure 1.1 The arrangement of protein domains in vitellogenin receptors (VgRs) and lipophorin receptor (LpR) in insects, and other LDLR superfamily receptors in vertebrates. The common structural elements that are shared among LDLR superfamily members are listed on the left. Insect VgRs include two copies of the ligand-binding and EGF-precursor domains [22,24,26-28,33] in contrast to cockroach LpR (only the *B. germanica* LpR is shown; [34]), chicken VgR and vertebrate LDLR (summarized in [32]).

The fire ant VgR (*Si*VgR) was the third cloned and characterized VgR in insects. Previously Mei-er Chen in Dr. Pietrantonio's laboratory determined that the *Si*VgR transcript was detectable in female reproductive pupae (in pupae that will produce female reproductives) and its abundance increased with age in virgin queens. The *Si*VgR gene was only expressed in the ovaries of reproductive females (virgin and mated queens), and the transcript was significantly more abundant in virgin queens than in newly mated queens [24]. In addition, the overall *Si*VgR transcript abundance in virgin queens was higher than in newly mated queens throughout the colony foundation period [35]. The observation of the phenomenon of *Si*VgR transcripts being present at a high level during the pre-vitellogenic period but at a low level during the vitellogenic period was attributed to the fact that receptor proteins are believed to recycle during the latter [11]. *In vitro* endocrine regulation studies of newly-eclosed (day 0) virgin queen's ovary showed that after incubation with 10^{-6} M methoprene (JH analog) at 27 °C for 24 h, the *Si*VgR transcript was significantly up-regulated ($p<0.05$) compared to control ovaries (ovaries incubated in dimethylsulphoxide (DMSO), or in culture media only) [24]. Conversely, in ovaries of virgin queens there were no significant differences in relative *Si*VgR transcript abundance between the 20-OH-Ecdysone-treated, and negative control tissues incubated with ethanol or culture media only, indicating ecdysone does not induce oogenesis in the fire ant [35]. The study of a 1.5-Kb region upstream of the mosquito VgR gene ORF (potential promoter region of VgR gene) showed that it contains binding sites for the ecdysone regulatory hierarchy early gene products (E74 and BR-C) and transcription factors (GATA and HNF3/fkh) [36]. Since ecdysone does

not induce fire ant *Si*VgR expression in ovaries *in vitro* [35], other regulatory elements may involved in the regulation of *Si*VgR gene expression.

Hormone regulation of insect reproduction

Several hormones control insect vitellogenesis at different times (temporal regulation) and in different tissues (spatial regulation). Juvenile hormone (JH) and/or ecdysone are believed to directly induce vitellogenesis and ovary development [7,37]. In Diptera, such as mosquitoes and fruit flies, JH and ecdysone both stimulate Vg synthesis in fat body, while JH stimulates Vg uptake by the oocyte [38-41]. In addition, JH controls the formation of ovarian epithelial patency (space between follicular cells that allows Vg to pass through and reach oocyte membrane) by regulating follicle cell volume [42-45].

In Hymenoptera with a complex social structure, the role of JH and ecdysone remains unclear and appears to have diverged. In the fire ant, JH appears to regulate vitellogenesis and increases *Si*VgR transcripts in queen ovary while ecdysone has no effect [24,46]. In bumble bee, *Bombus terrestris*, juvenile hormone (JH) and ecdysone titers are involved in the regulation of ovary development and cast differentiation [47,48]. In contrast, in the queenless ant *Streblognathus peetersi*, JH suppresses ovarian function and ecdysone may stimulate Vg production [49]. Also, JH titers are low in female reproductive ants in the genus *Diacamma* [50]. However, a different situation is present in the honey bee, *A. mellifera*, and the stingless bee, *Melipona quadrifasciata,* in which JH and ecdysteroids are thought to have lost most of their gonadotropic function

in adult queens, and JH is suggested instead, to be involved in the regulation of foraging ontogeny [51-55].

In insects, gonadotropic neuropeptide hormones appear to operate in the central nervous system (central function) upstream of the direct inducers (JH and ecdysone) to stimulate or inhibit vitellogenesis, and also act directly on peripheral tissues [56]. Candidate neuropeptides are the **short neuropeptide F (sNPF)** peptide and **insulin-like peptides (ILPs)** which play a gonadotropic role in some insect species (Figure 1.2). In locust, sNPF increases ovarian growth [57]. In *Drosophila*, sNPF peptides [58] and NS3 (a nucleostemin family GTPase) [59] stimulate ILPs synthesis in the brain insulin-producing cells (IPCs); these ILPs subsequently affect insulin signaling in target tissues such as fat bodies. *Drosophila* sNPF and sNPF receptor have been shown to be the upstream regulators of expression of insulin signaling pathway [58]. The NS3 also regulates growth and body size and may act through the serotonergic neurons next to the insulin-producing neurons in the brain [59]. In insects including mosquitoes, fruit flies, and fire ants, the sNPF receptor transcript is also detected in peripheral tissues; however, specific receptor function in these tissues is still unknown. These unknown roles are represented with question marks and dashed lines in Figure 1.2.

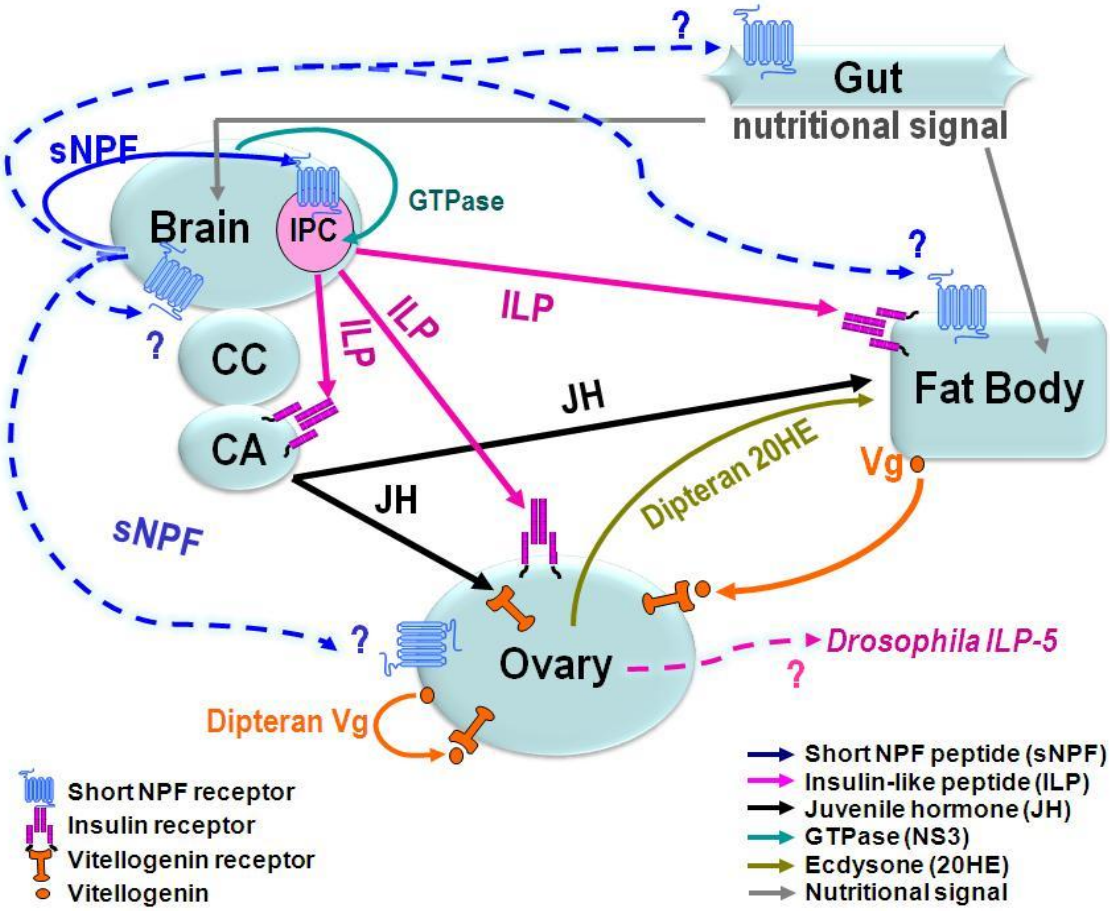

Figure 1.2. Hormonal control of insect vitellogenesis. JH stimulates ovarian growth and increases *Si*VgR transcripts in fire ant ovary [24]. In locust, short neuropeptide F (sNPF) increases ovarian growth and hemolymph Vg concentration [57]. In Diptera (fruit flies, mosquitoes), JH and ecdysone stimulate Vg synthesis in fat body while JH stimulates Vg oocyte uptake [41]. In *Drosophila*, sNPF and sNPF receptor have been shown to be the upstream regulators of expression of insulin signaling pathway [58], and a GTPase (NS3) also regulates growth and body size and may act through the serotonergic neurons next to the insulin-producing neurons in the brain [59]. The insulin-like peptides (ILPs) may then increase JH synthesis in CA. ILPs are also synthesized in the ovary, however, this pathway is still unclear. The *Drosophila* and mosquito insulin receptors are present in the ovary, supporting the ILP roles in the oocyte maturation and ovary development [60-63]. Bovine insulin peptides in combination with 20-hydroxyecdysone stimulate mosquito ovaries to secrete ecdysone [64], and activate Vg gene transcripts in the fat body [65]. Question marks and dashed lines represent unknown pathways. Previously only the *Si*VgR and the short NPF receptor sequences are known from fire ant. Receptors for these two candidate neuropeptide hormones (sNPFs and ILPs) are investigated in this dissertation. CC = corpora cardiaca; CA = corpora allata.

In Diptera (flies and mosquitoes), the ILPs regulate JH synthesis in the corpora allata in flies [66], stimulate ovaries to secrete ecdysone in mosquitoes, and activate Vg gene transcripts in mosquito fat body [64,65,67]. The presence of the insulin receptor in the ovary of dipterans supports these ILP roles in the oocyte maturation and ovary development [60-63]. In the fire ant, the sNPF receptor transcriptional expression level in the queen brain is related to queen feeding status [68].

In addition to gonadotropins (stimulatory hormones), other peptide hormones such as trypsin biosynthesis modulating oostatic factors (TMOF) inhibit the digestive enzyme trypsin, consequently lowering the level of free amino acids in the hemolymph as nutritional signals, which in turn decreases Vg synthesis in the fat body, suppressing ovary growth [69].

Two neuropeptide pathways are the focus of this dissertation: the sNPF and insulin signaling pathways.

Short neuropeptide F signaling pathway

Neuropeptides in the neuropeptide F (NPF) family have been identified or predicted from genomes of a broad range of invertebrate taxa, including insects [70-74]. Invertebrate neuropeptides in the NPF family are structurally and functionally related to the vertebrate neuropeptide Y (NPY) peptide. NPY is a highly conserved 36 amino acid residue polypeptide and is one of the most abundant neuropeptides in the vertebrate central nervous system. It has significant roles in the regulation of feeding behavior,

stress and obesity, blood pressure, anxiety, memory retention, and circadian rhythms [75-77].

In insects, the role of neuropeptides from the NPF family in physiological processes such as reproduction, feeding, and digestion, makes them an important subject of study. Neuropeptides in the NPF family are characterized by a conserved R(P/L)RFamide motif in the C-terminal sequence and are divided into long and short forms [78]. The long NPF peptides (referred to as "NPFs") range in size from 36 to 40 amino acid residues ending with –RPRFamide, and the short NPF peptides (sNPFs) range in size from 6 to 11 amino acid residues ending with –RLR(F/W)amide. The long NPF signaling pathway is involved in feeding and social behaviors, stress responses, and alcohol sedation sensitivity in the fruit fly *D. melanogaster* [79-87], in hindgut contraction in the blood-sucking bug *Rhodnius prolixus* [88], and in ovarian maturation in locusts [89]. Little information was available on the role of the sNPF signaling pathway until recent studies in *Drosophila*. Four *Drosophila* sNPF peptides (sNPF-1 to -4) are generated from the same sNPF precursor by enzymatic processing and modification. This sNPF peptide precursor was detected in about a thousand neurons in the CNS of 3rd instar larvae, and in about five thousand neurons in the CNS of adults [90,91]. *Drosophila* gain-of-function mutants with sNPF over-expression in the nervous system display increased food intake, resulting in flies larger than the wild type, while loss-of-function mutants exhibit reduced food intake [92]. In *Drosophila*, sNPF peptides are the upstream regulators controlling the expression of insulin-like peptides in the brain insulin producing cells [58,93]. It was suggested that the sNPF produced in the fly

brain binds to the sNPF receptor and activates the extracellular signal-related-kinase (ERK), which results in the turning on of the *Drosophila* insulin-like peptide genes in the insulin producing cells in the brain. The up-regulated *Drosophila* insulin-like peptides are secreted into the hemolymph and bind to the insulin receptor in target tissues which activates the Akt/FOXO/4E-BP pathway [58,93]. In this way, the sNPF peptides might modulate insulin signaling in target tissues including growth, carbohydrate metabolism, lifespan, reproduction, and JH biosynthesis in *Drosophila.* In other insects, the sNPF signaling pathway also appears to be involved in feeding regulation. For example, in the fire ants, the sNPF receptor transcripts in the queen brain were decreased by starvation suggesting that the sNPF signaling cascade may play a role in feeding regulation [68]. Moreover, during diapause, the adult Colorado potato beetle is devoid of sNPFs suggesting that the sNPFs might contribute to pre-diapause shifts in feeding behavior that lead to larger body size and reserve accumulation [94]. In the honey bee *Apis mellifera*, the sNPF and its receptor transcript expression levels were interpreted as associated with worker division of labor and feeding behavior [95,96]. The sNPF receptor transcript is up-regulated in brains of foragers under food-deprivation (without protein) suggesting that foragers are more sensitive to nutritional changes than nurses [96].

The sNPF signaling pathway appears to be involved in additional functions in insects. For instance, the Colorado potato beetle sNPF peptide, Led-NPF-1, was shown to stimulate ovarian development in the locust *Locusta migratoria*, suggesting a potential gonadotropin role of the peptide [57,78]. Functions such as cardio-inhibitory

activity on beetles [97] and an inhibition of locomotor behavior and the modulation of metabolic stress responses in the fruit fly [98,99] have also been discovered. In *Drosophila*, the diversity in the function of the sNPF pathway might be explained by the broad and abundant distribution of sNPF peptides discovered in the brain. In addition, the sNPF peptides have also been identified in the hemolymph of adult *Drosophila*, suggesting a potential neuroendocrine role [100]. However, the exact neuronal targets of the sNPF peptide in adult insect CNS or other tissues are unknown.

Several physiological events related to sNPFs in insects such as ovarian growth, body size control and adult diapause are all indicating that sNPFs may serve a role in the up-regulation of JH biosynthesis and also act directly on peripheral tissues. In contrast to the putative role of sNPF signaling pathway inducing or affecting insulin production, putative sNPF peptides discovered in the silkworm, *Bombyx mori,* have allatostatic activity (decreasing JH synthesis) in larvae [101].

The sNPF receptor belongs to the G-protein coupled receptor (GPCR) superfamily which is characterized by the standard feature of seven transmembrane regions, with the amino terminus located on the extracellular side and the carboxyl terminus on the intracellular side of the plasma membrane. Insect sNPF receptors have been cloned and characterized from *S. invicta*, *D. melanogaster*, and *A. gambiae* [68,102-104]. The sNPF receptor cloned from the fire ant was the first GPCR identified from any ant species [68]. Semi-Q RT-PCR analyses found that the fire ant sNPF receptor transcript is present in the brain, midgut, hindgut, Malpighian tubules, fat body, and ovaries of mated queens, and a particularly high level of receptor expression was

detected in the brain [68]. There is no available information about the localization of sNPF receptor in the brain or peripheral tissues in any adult insect; therefore, it is important to establish the localization of the sNPF receptor.

Insulin/insulin-like growth factor signaling (IIS) pathway

In insects, the IIS pathway regulates reproduction, growth, metabolism, and longevity [105]. Insect insulin receptors have been cloned from the fruit fly *Drosophila melanogaster* and the mosquito *A. aegypti*, and were named *DIR* and *MIR*, respectively [62,106,107]. Most of the functional studies were performed with *Drosophila*. Mutant *Drosophila* insulin receptor (*DIR*) flies showed female sterility, reduced juvenile hormone (JH) and ecdysone level, and in the ovary, decreased germline stem cell division- and cyst growth-rates. They also showed reduced cell number and cell size, developmental delay, growth-deficiencies and had a longer lifespan [108-112]. Similar to what was seen in the receptor (*DIR*) mutants, ablation of the medial neurosecretory cells in the brain, which expressed *Drosophila ILP*-1, -2, -3, and -5, reduced fecundity, and reduced follicle cell proliferation rate, germline stem cell division rate, metabolism and growth were observed, and also resulted in a longer lifespan [112-115]. In *Drosophila*, seven ILPs were found, and synergy, redundancy and compensation of the expression among these different ILPs were recently demonstrated [116,117]. These phenomena make it difficult to study the function of each ILP. Recently, scientists were able to perform the single deletion of each *Drosophila* ILP to study their individual functions. Flies with a single deletion of *ILP*-1 to -5 also showed poor fertility and a

reduced metabolic activity [118]. Reduced function of the *ILP*-7 expressing neurons by hyperpolarization results in sterility, due to a lack of oviposition [119]. Some of these phenotypes are also caused by mutations in downstream components of the IIS pathway, such as mutations in *chico* (insulin receptor substrate) [67,110,120,121], *Dp110* (a phosphoinositide 3-kinase, PI3-kinase) [122], *Akt* (a serine/threonine kinase) [123,124], or the negative control factor, *PTEN* [123]. For example, if female flies have a mutated gene for the insulin receptor substrate (*chico*), which normally is phosphorylated by the insulin receptor protein tyrosine-kinase activity, they are also sterile and the level of Vg and VgR gene expression are reduced [121]. In contrast, overexpression of ILPs results in bigger flies because of an increase in both cell number and size in individual organs, and to no surprise, this phenotype is insulin receptor-dependent [109,115].

There is a link between the IIS pathway and JH and ecdysone synthesis and/or release in insects. ILPs may be upstream regulators of JH and ecdysone acting on the neuroendocrine system and they may also act directly on peripheral tissues. Fruit fly *DIR* expressed in the corpus allatum regulates the expression of a key enzyme in JH synthesis suggesting that the IIS pathway is required upstream of JH synthesis [125,126]. Also, female flies with a *DIR* mutation have reduced JH and their ovaries are arrested at the pre-vitellogenic stage, and treatment with a JH analog (methoprene) restores vitellogenesis [66,111]. It appears that the activation of the insulin pathway elevates ecdysone synthesis in the prothoracic glands both in larvae of *Drosophila* and silkworm [127-131]. In the ovary and fat body of Diptera, insulin peptides (bovine insulin and *Aedes* ILP-3) appear to play a key role in the stimulation of steroidogenesis and yolk

uptake in the ovary [61,62,64,67,132,133] and of yolk protein synthesis in the fat body [65] which together, regulate vitellogenesis. In addition, knockdown of the expression of AaegPTEN6, an IIS pathway inhibitor in *A. aegypti*, increases egg production in the mosquito [134]. The presence of the DIR and MIR in the ovary of flies and mosquitoes, respectively, supports these ILP roles in the oocyte maturation and ovary development [60-63]. Recently, a mutual antagonistic relationship between insulin signaling and ecdysone signaling was discovered in the fat body of flies [128,135,136], providing evidence for more complex regulation mechanisms of the IIS pathway in development and growth.

In the honey bee, the IIS pathway is involved in caste determination, division of labor, and longevity. The IIS pathway in bees is correlated with longevity which is in agreement with findings from *Drosophila*. However, the traditional positive relationship between body size (nutrition) with the activation of the IIS pathway found in solitary insects like *Drosophila* is more complex in the honey bee [137] and the role of IIS pathway in regulation of bee reproduction is still unclear. Interestingly, two insulin receptor fragments were predicted in the honey bee genome. Recently, two insulin receptor fragments were also found in the draft genomes of several ant species [3,138-141]. The possible roles of two insulin receptors in the fire ant need further investigation.

Reproductive biology in the fire ant

Social insects have remarkable forms of social organization with the majority exhibiting reproductive division of labor between queen and workers [142]. Only a few females (queens) have the privilege of reproductive ability and longevity; most females become nonreproductive individuals (workers). The available knowledge on the physiology of fire ant reproduction was previously reviewed [143]. In fire ants, adult workers have no ovary and therefore are sterile; the queen has a pair of ovaries (polytrophic ovary) with each ovary consisting of 80 to 100 ovarioles [144]. Virgin queens (alate, normally are non egg-laying queens with small ovary) and mated queens (de-alate, egg-laying queen) differ dramatically in their behavior and physiology (see Figure 1.3). Correspondingly, factors and differentially expressed genes affecting muscle histolysis, reproduction, respiratory metabolism and immunity have been identified in the two types of queens [145-147].

In a mature colony, many hundreds of virgin queens take flight to mate when certain weather conditions are met. As outlined below, mating flights and colony foundation are controlled by complex gene networks which are regulated by hormones and modulated by environmental stimuli. Newly-emerged virgin queens within a colony require around two weeks of maturation time prior to flight and mating [143,144,148,149]. However, there is a high cost of reproduction [150] in fire ants because this mating-dispersal strategy implies a high risk of mortality because queens are eaten either by flying predators or other ants, or die when colony founding is

unsuccessful [144]. After a mating flight, the newly-mated queen lands, removes her wings (de-alation) and locates a place to found a colony.

Mated queens that begin to build a new colony do not continuously lay large number of eggs like a mated queen within a mature colony; rather, they produce typically 30-70 eggs between 24 h to 6 days post-mating, which will give rise to nanitics (first cast of workers). When these embryonated eggs begin to hatch (~7 days post-mating), mated queens produce trophic eggs (not embryonated) as food to feed the developing nanitic larvae until these first worker adults take over the nurturing work in the colony [144,151]. The mated queen's ovariole is suggested to be gradually activated: ovarioles are first activated after mating and then the number of vitellogenic follicles in each ovariole increases as the number of larvae in the colony increases [144]. We suggest that these changes in virgin queens transitioning to newly mated queens to finally be mature queens may be also associated with variations in *Si*VgR expression.

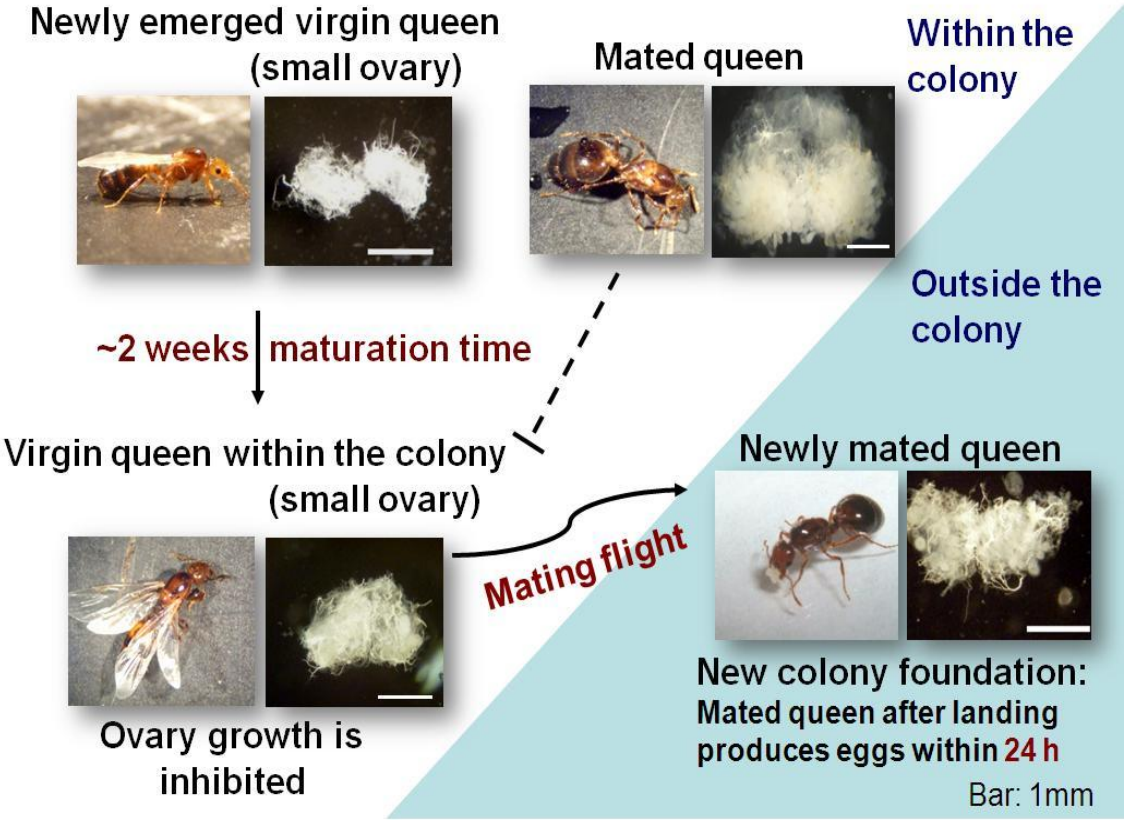

Figure 1.3. Biology of fire ant reproduction. The white area of the graph shows the queens present inside the colony and the blue area shows the events after mating flight outside the original colony and colony foundation. Virgin queens and mated queens differ in their behavior and physiology. Newly emerged virgin queens have small ovaries and these queens within a colony require around two weeks of maturation time prior to flying and mating. Within a colony, ovary growth in the virgin queens is inhibited by the primer pheromone released from the mated queen. On the other hand, newly mated queens produce eggs within 24 h after landing from a mating flight. Mating flights and colony foundation are likely controlled by complex gene networks which are regulated by hormones and modulated by environmental stimuli.

In fire ant queens, the ovarian development and the de-alating behavior is correlated with the elevation of JH (as measured in whole body and hemolymph), as follows. In a normal fire ant colony, a primer pheromone released from mated queens inhibits the reproduction of virgin queens. This primer pheromone received by the virgin queens' antennae suppresses their corpora allata activity and the corresponding production of JH and ovary development [46,145,152-156]. Application of JH I, II, and III or methoprene (JH analog) to virgin queens resulted in de-alating behavior, ovary development and increased fire ant VgR (*Si*VgR) transcript levels in the ovary; ecdysteroids seem to have no effect [24,46,55,155,157]. When separated from mated queen primer pheromone, virgin queens are capable of de-alating and becoming functional egg layers that produce only unfertilized (haploid) eggs that develop into males [1,158]. Isolation of virgin queens (unknown age) from queen primer pheromone leads virgin queens to start de-alation around 1-4 days post-isolation. Oviposition may occur around 5 day post-isolation, corresponding with peak production of JH, however, fully functional mated queens (egg laying mated queens within a mature colony) have higher JH biosynthesis rate and JH level than the virgin queens (0 day post-isolation) [158]. The development rate and the size of these virgin queen's ovaries are not comparable to that of newly-inseminated queens which develop dramatically one day after mating. Oviposition and oogenesis in isolated fire ant virgin queens are also associated with a higher dopamine (a biogenic amine) level in the brain which may up-regulate JH [159]. Taken together, these studies indicate that JH is involved in

behavioral (de-alation) and physiological (induction of ovary development) aspects of reproductive regulation in fire ant queens.

Hymenopteran genomes improve research in social insects

Ants and bees are important model species for studying social behavioral biology. In 2006, the honey bee genome sequence was released [160] which was the first genome project in social insects. The availability of honey bee genome sequences allowed scientists to clone genes of interest in other social hymenopterans more efficiently, specifically the fire ant [161]. For example, we were able to use predicted honey bee insulin receptor sequences to design degenerate primers to clone insulin receptors from the fire ant. Therefore, investigating the molecular mechanisms that regulate physiology and behaviors in social insects at a large scale of genes has become possible with the available genomic information from the honey bee. However, for shorter sequences like the sNPF peptide sequence, the honey bee genome is less useful because peptide sequences are difficult to predict.

Three years later, a database for ant genomic sequences named "Fourmidable" was released (http://fourmidable.unil.ch/) [3]. This database contains expressed sequence tag (EST) sequences from two ant species: the red fire ant *S. invicta* and the black garden ant *Lasius niger*. The information provided by this EST database allows scientists to identify and investigate gene expression differences in a broad scale. For example, genes associated with molecular changes in reproductive roles were studied in fire ant virgin queens. Out of 10,000 genes, 297 genes were up- or down-regulated after queen

orphaning (loss of their mother queen) which were identified from queen whole body by using microarrays [162]. These candidate genes included genes involved in JH metabolism and onset of reproductive development (for example, genes involved in olfactory signals).

In 2010, genomes of three parasitoid *Nasonia* species (*N. vitripennis, N. giraulti, and N. longicornis*) were released [163]. Almost immediately, the draft genome of six species of ants were released, including the fire ant [3], the Argentine ant *Linepithema humile* [138], the carpenter ant *Camponotus floridanus* [139], the ponerine ant *Harpegnathos saltator* [139], the leaf-cutter ant *Atta cephalotes* [140] and the red harvester ant *Pogonomyrmex barbatus* [141]. Most of these ant genomes were sequenced using the 454 pyrosequencing technology. For some of them, the assembly of sequencing results and the gene annotation were completed in less than one year.

The release of the fire ant draft genome helps research on this globally widespread and invasive species. There are more than 400 putative olfactory receptors identified in the fire ant genome [3]. This is the largest number of olfactory receptors reported so far in any insect species and points to the complex social behavior in the fire ant. Similarly, higher number of genes in the JH-binding protein (JHBP) and JH-epoxide hydrolases (JHEHs) families were annotated from the fire ant than from *Nasonia* and the honey bee [3]. This result indicates that the regulation of JH in fire ants is more complex than in wasps and bees.

With respect to reproduction, four adjacent copies of Vg genes (Vg-1 to Vg-4) were identified in the fire ant genome [3]. It was suggested that gene duplication

occurred twice in the fire ant from an ancestral Vg gene (from wasp and bees) and resulted in four Vg genes. The Vg-2 and Vg-3 are specifically expressed in queens while Vg-1 and Vg-4 are preferentially expressed in workers [3].

The insulin signaling pathway is an important and essential pathway in insects, and therefore it has been specifically investigated in many genome projects. In the fire ant genome sequences, two insulin-like peptides and two insulin receptors were predicted; however, these two receptor sequences were incorrectly predicted and therefore are still incomplete. There are two insulin receptor sequences in the genome of the honey bee [160]; however, we discovered that one of these two receptors (*Am*InR-2) is incompletely predicted and is missing half of the receptor sequence (β-subunit). Subsequently, incorrect predictions of the *Am*InR-2 orthologs from other ant genomes were also reported. In the genomes of the carpenter ant *C. floridanus* and the ponerine ant *H. saltator*, four and five genes similar to insulin receptor were annotated, respectively, based on annotations of the honey bee sequences (*Am*InR-2) [139]. However, we determined that only some of the predicted sequences in each species are similar in sequence and in predicted protein structure to the insect insulin receptor. These sequences are: "Cflo_05946 and Hsal_09512" (similar to honey bee *Am*InR-1, XM_394771; beebase number GB18331), "Hsal_01375" (similar to honey bee *Am*InR-2, XM_001121597; GB15492), and "Cflo_09206 and Hsal_11112" (similar to honey bee insulin-like growth receptor 1, XM_001121628). All of these sequences are still incomplete. Other sequences are wrongly annotated due to the wrong annotation of the honey bee genes. These genes are "Cflo_02109 and Hsal_08870" (similar to honey bee

insulin-like growth factor-2, XM_623411) and "Cflo_03027 and Hsal_02738" (similar to the honey bee insulin receptor precursor, XM_397038). The genes "XM_623411" and "XM_397038" in the honey bee are in fact the lysosomal enzyme receptor protein (LERP) and the venus kinase receptor (VKR), respectively. Therefore, the genome annotation needs to be interpreted with caution.

Dissertation objectives

This dissertation provides an integrative understanding of the complex reproductive physiology in fire ants, as well as the development of novel experimental tool (RNA interference) to accelerate discovery. The final goal of elucidation of the reproductive biology of the fire ant at the molecular level of integration is to discover new management methodologies or technologies. For target validation, we investigated candidate receptors: vitellogenin receptor, and neuropeptide receptors (sNPF and insulin receptors), the later controlling the signaling cascade of endocrine regulation of reproduction in fire ant queens. These receptors are candidates for disruption of egg production in queens and offer potential to manipulate the number of reproductives (queens and males) in colonies, thus, diminishing fire ant populations. Determination of the timing of *Si*VgR expression and its localization in ovaries is the first step toward a better understanding of the effectors involved in fire ant reproduction. We hypothesized that *Si*VgR expression can be silenced or reduced by RNA interference (RNAi). The successful disruption of fire ant ovary development by VgR RNA interference in queen ovaries will not only provide us a possible way to disrupt reproduction in fire ants, but

also allow the study of other genes' functions in queens and in other ant species. Prior to our study, RNAi had never yet been tested in ants. Elucidation of the localization, temporal expression pattern, and the possible roles on regulation of ovary development of sNPF receptor and insulin receptors will help to develop a more complete understanding of the regulatory networks involved in fire ant reproduction, providing the possibility to disrupt oocyte development and ovary development in the future.

In order to better understand the biological significance of the receptors involved in fire ant reproduction, four objectives were pursued in this dissertation, as follows:

Objective 1: *Si*VgR transcripts are abundant in virgin (alate) queens. However, there is no evidence that *Si*VgR protein, the actual functional component, is present, inhibited, or correctly localized in the oocyte membrane of virgin queens. Hypothesis: we hypothesize that changes in *Si*VgR expression and localization will occur during the period of maturation of virgin queens. The expression and localization profiles of the *Si*VgR protein in both virgin and mated queens were studied in this objective.

Objective 2: The vitellogenin receptor plays an important role in insect vitellogenesis. We hypothesize that RNA interference will be feasible in ants. Hypothesis: disruption of the *Si*VgR gene function in fire ant virgin queens by injection of doubled-stranded RNA should result in disruption of ovary development and egg formation.

Objective 3: The sNPF signaling pathway has been implicated to play a role in reproduction and body size control in some insect species. Hypothesis: if the sNPF receptor were indirectly involved in the regulation of reproduction and queen behavior

through the central nervous system (CNS), and/or directly involved in ovary development through the expression of receptor in the ovaries, expression of the receptor protein in the brain and/or ovaries should be observed. The expression and localization profiles of the sNPF receptor in queens were investigated in brain and ovary; the distribution of this receptor is unknown in the adult insect brain.

Objective 4: The insulin/IGF signaling pathway in solitary insects influences growth, reproduction, metabolism, and longevity, while in the honey bee, it is linked to division of labor, caste differentiation, and foraging behavior. Two insulin receptors are present in the honey bee. Limited information on this pathway is available in other social insects such as ants. To elucidate the role of IIS pathway in the fire ant, we cloned two putative insulin receptors (*Si*InR-1 and *Si*InR-2). Hypothesis: we hypothesize that the insulin receptor may be involved in reproductive division of labor and queen reproduction in fire ants. Therefore, the transcriptional expression of two fire ant insulin receptors was studied.

Studies of receptors involved in fire ant reproduction are presented in chapters, each covering a different aspect of the project. The *Si*VgR protein expression and localization studies are presented in Chapter II. Chapter III focuses on silencing *Si*VgR gene function by RNA interference. The studies of candidate upstream genes involved in the regulation of fire ant reproduction are presented in Chapters IV and Chapter V. Chapter IV includes studies on the localization of a sNPF receptor in queen brains and ovaries. In chapter V, we investigated the molecular characterization and transcriptional expression analyses of two insulin receptors in fire ants.

CHAPTER II

FUNCTIONAL AND SPATIAL ANALYSES OF THE VITELLOGENIN RECEPTOR IN FIRE ANT QUEENS*

Introduction

Vitellogenesis is a key process that controls reproduction in insects. The vitellogenin receptor (VgR) is responsible for egg formation during vitellogenesis in insects [6,7,12,37,164]. Although the ovary-specific expression and localization of VgR have been reported from *Drosophila*, mosquitoes, and cockroaches [22,26-28,33], there is a paucity of knowledge on VgR physiology in insects of high reproductive capacity, such as the queens of social hymenopteran insects. Most of the available knowledge on molecular mechanisms of reproduction in social insects is from the honey bee; however, bees have evolved mechanisms different from those in ants and wasps. Contrary to most insects, in bees, VgR is not ovary or queen specific [31]. In addition, JH and ecdysone are thought to have lost their gonadotropic functions in adult queen bees and JH is suggested to regulate the division of labor, social behavior and colony function [51-55]. In ant species in which mating flights are a strategic life-history trait for dispersal and reproduction, maturation of virgin queens occurs. However, the specific molecular

* Portions of this chapter are reprinted with permission from "Oocyte membrane localization of vitellogenin receptor coincides with queen flying age and receptor silencing by RNAi disrupts egg formation in fire ant virgin queens" by Lu, H.L., Vinson, S.B., Pietrantonio, P.V. 2009, *FEBS Journal* 276: 3110–3123. © 2009 Blackwell Publishing Ltd.

mechanisms that mark this transition and the effectors that control pre-mating ovarian growth are unknown.

In fire ant castes, the fire ant VgR (*Si*VgR) transcript was analyzed by northern blot and results showed that it was present only in the ovaries of reproductive females (virgin and mated queens) and was significantly more abundant in virgin queens than in newly-mated queens 24 hour after mating [24]. The transcript was not detected in fat body of reproductives, male or female, and was also not detected in mRNA extracted from the complete body of workers. The temporal profile of transcriptional expression analyzed by semi-Q RT-PCR showed that *Si*VgR mRNA increased with age in virgin queens; the amount being statistically significantly lower in the untanned pupae versus virgin queens 60 days after eclosion [24]. The temporal profiles of *Si*VgR transcription from field-collected newly mated queens was also previously examined [35]. The results showed that the *Si*VgR transcripts increased from days 0 to 10 and remained at the day-10 level until day-30 post-mating. *Si*VgR transcripts increased by day 35, then declined following nanitic emergence, at about day 40. The overall *Si*VgR transcript abundance throughout the study period of 35 days post-mating was lower than in virgin queens. Yet, it is still not known if this high expression of *Si*VgR transcript in virgin queen is accompanied by functional *Si*VgR protein expression. We hypothesized that the complex mechanism that precisely controls the maturation of virgin queens for flying and mating should include regulation of *Si*VgR expression. Here we investigated the temporal ovarian expression and subcellular localization of the *Si*VgR in fire ant virgin queens and mated queens within the colony, and in field-collected newly-mated queens.

Results

Anti-SiVgR antibody production

All VgRs are members of the low-density lipoprotein receptor (LDLR) superfamily [29]. Proteins of this superfamily share some common structural elements (See Chapter I). To select a highly specific sequence of *Si*VgR to be expressed as antigen for antisera production, which would not overlap with sequences of other LDLR superfamily members potentially expressed in the ant, structural domains from the fire ant VgR (AAP92450), the predicted honey bee VgR (XP_001121707), the wasp VgR (XP_001602954), the cockroach *B. germanica* lipophorin receptor (LpR) (CAL47125), and human LDLR (AAA56833) were aligned and their percent identity (%ID) and similarity (%SIM) were compared. The alignment showed that the second YWXD repeat region in the first epidermal growth factor (EGF) precursor homology domain is a highly variable region among LDLR family members (Figure 2.1A, arrow). After hydrophilicity and antigenicity analyses of the *Si*VgR amino acid sequence, a fragment corresponding to the second YWXD repeat region in the first epidermal growth factor (EGF) precursor homology domain (amino acids 648-887) was chosen to produce a *Si*VgR antigen. The recombinant protein of the bacterial culture (the BL21 (DE3) strain transformed with the pET28a-VgR plasmid) was purified under denaturing conditions (8 M urea) using TALON® metal affinity resin to produce this *Si*VgR antigen.

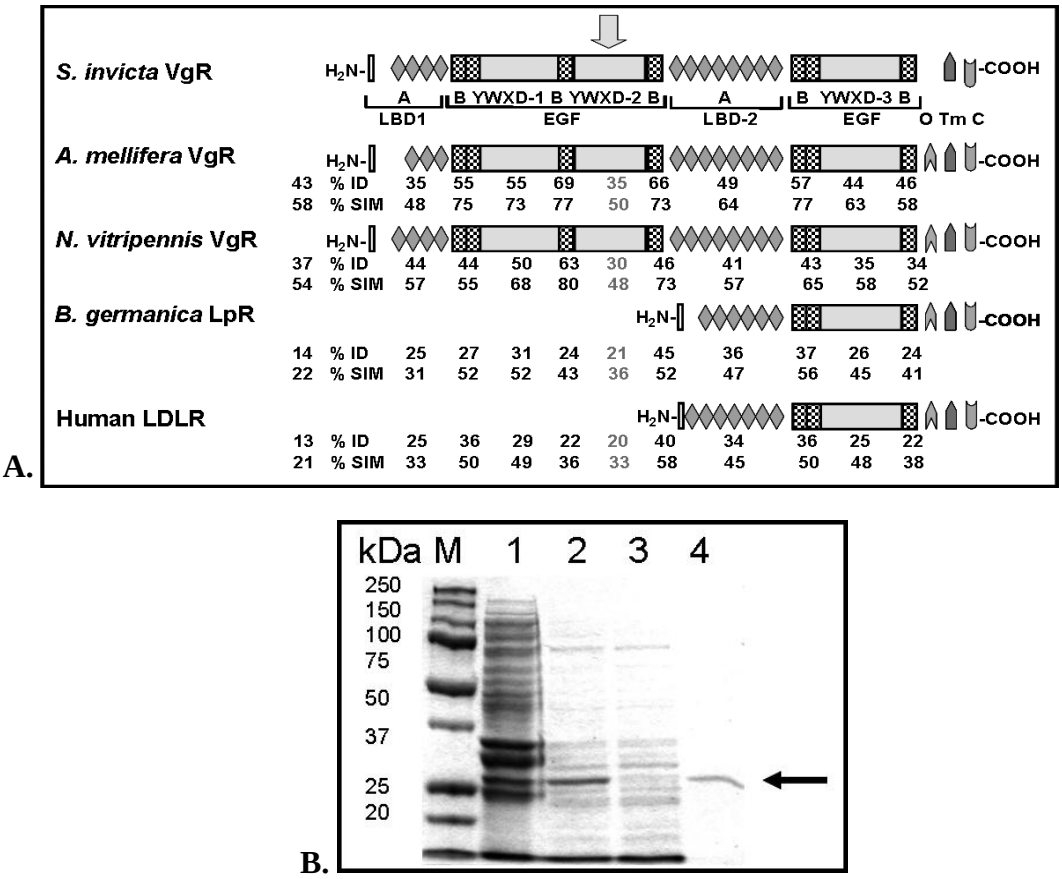

Figure 2.1. Expression of the recombinant antigen for anti-vitellogenin receptor (*Si*VgR) antibody production. A. Alignment and comparison of structural domains of Hymenopteran VgRs, cockroach LpR and human LDLR. Numbers below domains indicate percent identity (% ID) or similarity (% SIM). The second YWXD repeat within the first EGF precursor homology domain exhibited the lowest average similarity scores indicating it is a highly variable region among LDLR family members. The cockroach and human LDL receptors are shorter in the N-terminal half, therefore percentages of identity and similarity presented for the N-terminal region indicate values calculated between the C-terminal half of these receptors and the corresponding N-terminal half of the *S. invicta* receptor. Class A cysteine-rich repeat (A); Class B cysteine-rich repeat (B); ligand binding domain (LBD); EGF precursor homology domain (EGF) contains Class B cysteine-rich repeats (B) and YWXD repeats (YWXD); O-linked sugar domain (O); transmembrane domain (Tm); cytoplasmic tail (C). B. Bacterial culture from the BL21 (DE3) strain (transformed with the pET28a-VgR plasmid) was induced with 1mM IPTG for 8 h at 20 °C. Proteins were analyzed by 10% SDS-PAGE; numbers in parenthesis indicate volumes loaded. Lane 1, Insoluble proteins (pellet) after centrifugation of the lysed culture (5 µl); Lane 2, Soluble proteins (supernatant) from lysate after centrifugation (5 µl); Lane 3, Unbound proteins after batch binding with resin (5 µl); Lane 4, the purified protein in eluant (20 µl). M: marker.

The plasmid, pET28a-VgR, expressed the amino acid sequences 648-887 of *Si*VgR with only an additional N-terminal extension of 32 amino acid residues including the His-tag (6 residues) and T7-tag (11 residues) coding sequences. Purified proteins were analyzed by SDS-PAGE (Figure 2.1B) and the analysis showed that the plasmid pET28a-VgR expressed a recombinant protein (~30 kDa) after induction by 1mM IPTG, as expected (lanes 1 and 2). The eluant was collected, dialyzed and concentrated for the anti-*Si*VgR antibody production (Figure 2.1B, lane 4).

SiVgR ovarian expression in virgin and mated queens within the colony

To verify the ovarian-specific expression of *Si*VgR, membrane fractions of different tissues dissected from mated queens were analyzed by western blot (Figure 2.2). A band was recognized by the *Si*VgR antisera only in ovaries (lane 1). No signal was detected in the head (lane 2), fat body (lane 3), or gut (lane 4) of mated queens; nor was it detected in the abdomens of adult males (lane 5). No signal was detected using pre-immune serum, as expected (data not shown). This result shows that the antibody raised against a purified *Si*VgR recombinant fragment was highly specific. The estimated molecular weight of *Si*VgR was ~202 kDa, corresponding to the predicted molecular weight of 201.3 kDa [24]. The molecular weight of *Si*VgR is similar to that of insect VgRs from *A. aegypti* VgR (205 kDa) [23], *B. germanica* (202 kDa) [27], *P. americana* (200.5 kDa) [26] and *L. maderae* (215 kDa) [28], *D. melanogaster* Yl (210 kDa) [22], *A. mellifera* VgR (~ 205 kDa, visualized by ligand blotting) [165], and the moth *S. litura* [25], as well as VgRs from other invertebrates including the tick *D.*

variabilis VgR (196.6 kDa, predicted molecular weight) [18] and the shrimp *P. monodon* VgR (211 kDa) [20]. VgRs from locusts, *L. migratoria* (180 kDa) and *Schistocerca gregaria* (186 kDa), and also from the polychaetous annelid *Nereis virens* (190 kDa) have not been cloned, but their molecular weights are slightly smaller in size as determined by ligand blot analysis [166-168]. In other invertebrates, the estimated molecular weight of VgR (230 kDa) from the crab, *Scylla serrata*, is apparently higher [169]. In the nematode, *C. elegans*, the size of VgR is more similar to VgR from vertebrates and is only 110 kDa [21].

In queen pupae, a detectable level of *Si*VgR transcripts in the ovaries was observed previously; upon eclosion, these levels continued to increase in virgin queens up to 60 days of age [24]. It was of interest to determine whether receptor protein expression paralleled transcript abundance in these virgin queens. The *Si*VgR band was recognized by the anti-*Si*VgR antisera (Figure 2.3A) in western blots of ovary from virgin (lane 1) and mated (lane 2) queens. Analysis of relative band intensity showed that the *Si*VgR signal was much lower in virgin queens than in mated queens (virgin/mated queen = 0.578). No band was detected with pre-immune serum (lanes 3 and 4). The localization of *Si*VgR in queen ovaries was examined by immunofluorescence. Comparison of ovary cross sections from 13 day-old virgin queen (Figure 2.3B) and newly-mated queen (24 h post-mating) (Figure 2.3C), showed that both the number of developing oocytes and those exhibiting receptor immunofluorescence signal was lower in virgin queens than in newly-mated queens.

Correspondingly, the size of the ovary in virgin queens was also smaller, about half the diameter of that in newly-mated queens.

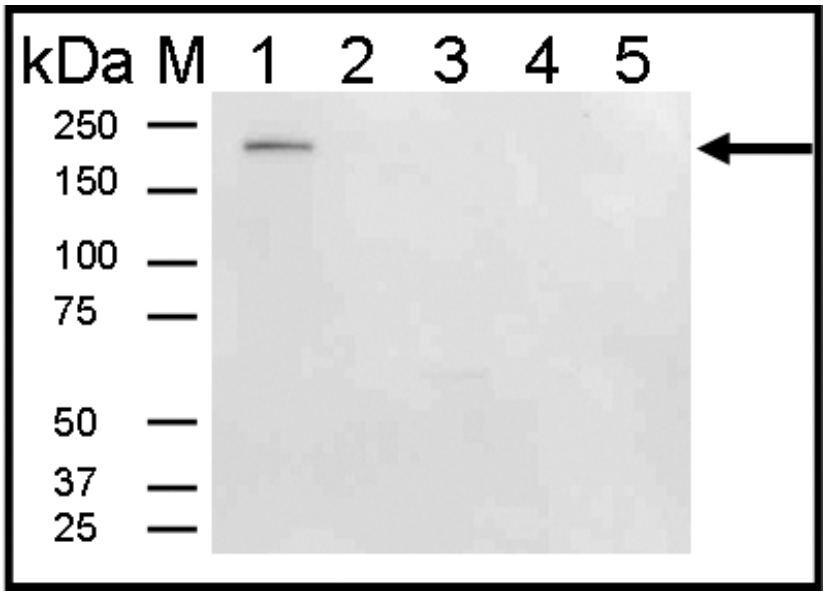

Figure 2.2. Tissue expression analysis of vitellogenin receptor (*Si*VgR) by western blot. Membrane proteins (10 μg) from ovary (lane 1), head (lane 2), fat body (lane 3) and gut (lane 4) of mated queens, and from abdomen of adult males (lane 5) were analyzed by western blot (primary antibody anti-*Si*VgR antisera, 1:1000). A band at ~202 kDa was detected only in ovaries from mated queens (lane 1). No signal was detected in other tissues (lanes 2-5). M: Marker.

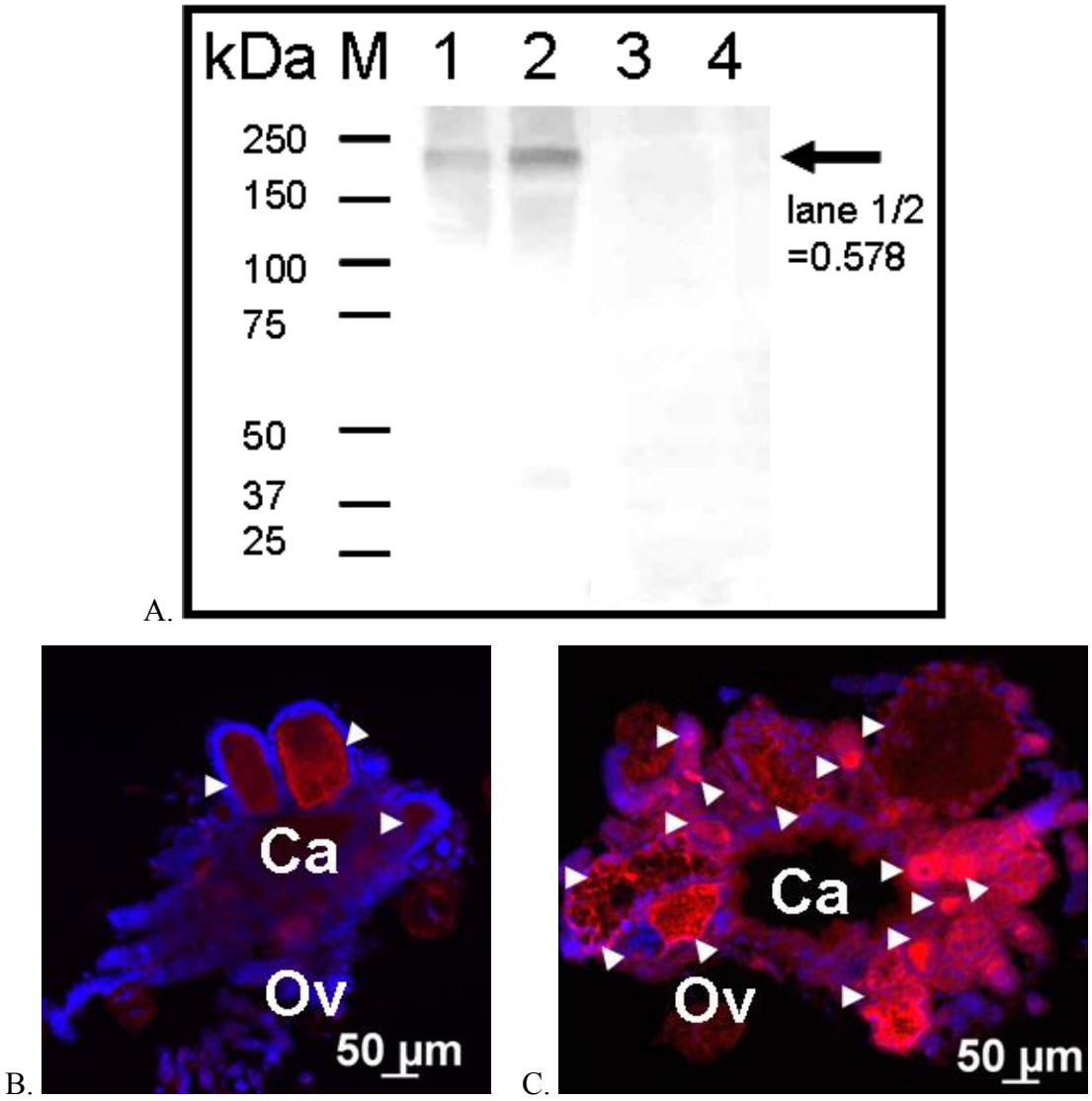

Figure 2.3. Vitellogenin receptor (*Si*VgR) expression in ovaries of virgin and mated queens within the colony and newly-mated queens: western blot and immunofluorescence. A. Membrane protein from ovaries of virgin queens (lanes 1 and 3; protein from 16 pairs of ovaries) and mated queens (lanes 2 and 4; protein from 4 pairs of ovaries) was analyzed by western blot (primary antibody: *Si*VgR antisera in lanes 1 and 2 and pre-immune serum in lanes 3 and 4; both antisera 1:1000 dilution). A band at ~202 kDa was recognized by the *Si*VgR antisera in ovaries from virgin (lane 1) and mated queens (lane 2, arrow). The relative *Si*VgR band intensity for virgin queens with respect to mated queen (lane 1/lane 2) is shown on the right. M: Marker. Cross sections of ovaries from (B) a 13 day-old virgin queen and (C) field collected newly-mated queens 24 h post-mating were analyzed by immunofluorescence, arrowheads show *Si*VgR signal. Ca: Calyx. Ov: ovary.

Temporal analysis of the subcellular distribution of SiVgR

To determine the earliest age at which *Si*VgR is expressed in the oocyte plasma membrane, ovaries of virgin queens from day 0 (the day of emergence) to day 14 were collected and analyzed by immunofluorescence. In ovaries of 9- to 11 day-old virgin queens, some of the oocytes and trophocytes appeared larger and showed intense *Si*VgR signal in the oocytes, however the signal remained evenly distributed in the oocyte cytoplasm; photographs representative of 11 day-old virgin queens are shown in Figure 2.4 (A). From 12 to 14 days old, ovaries exhibited a few late-stage oocytes with the *Si*VgR signal localized at the oocyte membrane; photographs representing this period from 12- to 13-day-old virgin queens are shown in Figure 2.4 (B and C). These results demonstrated the *Si*VgR expression begins before queen eclosion and suggest that the *Si*VgR-endocytotic machinery might achieve full functioning 12 days after queen eclosion. No signal was detected with pre-immune serum (Figure 2.4D), as expected.

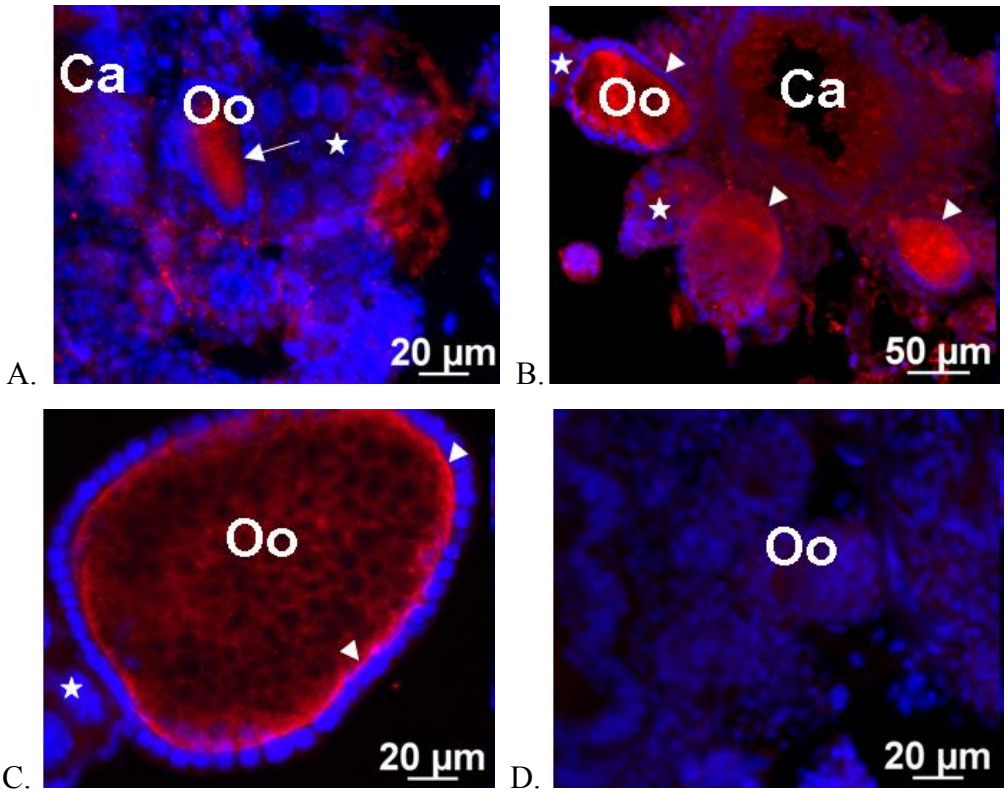

Figure 2.4. Temporal analysis of the subcellular distribution of vitellogenin receptor (*Si*VgR) in ovaries from virgin queens by immunofluorescence. *Si*VgR accumulated in the cytoplasm of early stage oocytes (Oo) (A, arrows), and in the plasma membrane of late stage oocytes (B-C, arrowheads). A. Oocytes from an 11 day-old queen, notice trophocyte nuclei stained in blue (stars). B. Oocyte from 12 day-old queen. C. Oocyte from 13 day-old queen. D. Negative control (pre-immune serum), no signal was detected in ovaries from a 9 day-old virgin queen. Ca: Calyx.

In mated queens, *Si*VgR protein was evenly distributed in the oocyte cytoplasm in early-stage oocytes (pre-vitellogenic stage oocytes located towards the distal end of ovariole) (Figures 2.5A and 2.5B, arrows). Consistent with VgR function, the *Si*VgR became progressively more clearly visible in the oocyte plasma membrane of late-stage oocytes (vitellogenic stage oocytes) (Figures 2.5B and 2.5C, arrowheads). No signal was detected with pre-immune serum (Figure 2.5D), as expected. Signal was also undetectable with antigen pre-absorbed antiserum (Figure 2.5E) while anti-*Si*VgR antiserum at the same dilution (1:2500) showed a strong signal (data not shown). Immunofluorescence with anti-(roach VgR) serum failed to reveal the *Si*VgR signal (Figure 2.5F). Complementary western blot analysis of endoplasmic reticulum membranes (microsomes) from mated queen ovaries revealed a single specific receptor band (Figure 2.5G), confirming that the cytoplasmic fluorescent signal observed in Figure 2.5 (A-C), corresponded to the *Si*VgR.

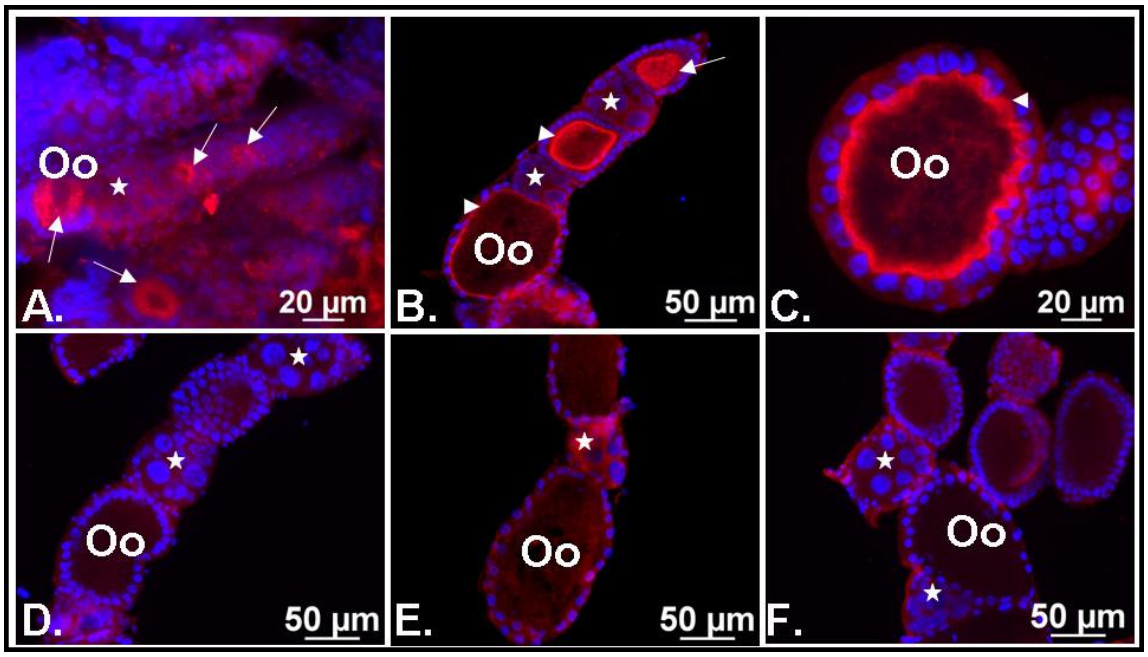

G.

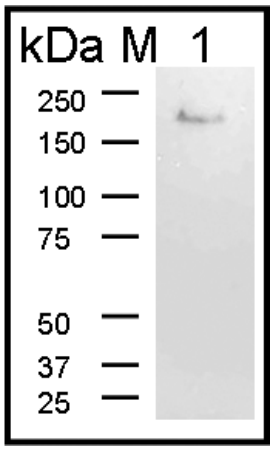

Figure 2.5. Vitellogenin receptor (*Si*VgR) expression in ovaries of fire ant mated queens within the colony analyzed by immunofluorescence. *Si*VgR accumulated in the cytoplasm of early-stage oocytes (Oo) (A and B, arrows), and in the membrane of late-stage oocytes (B and C, arrowheads). C. Cross section of a mature oocyte showing *Si*VgR signal in the membrane, as expected. No signal was detected in tissues incubated with pre-immune serum (D), with anti- *Si*VgR antiserum pre-absorbed with recombinant receptor antigen (E) and with non-specific antisera against cockroach VgR (F). Star, trophocytes nuclei. G. Ovarian microsomal proteins (10 µg) analyzed by western blot (lane 1). M: Marker.

SiVgR expression pattern in newly-mated queens

To investigate *Si*VgR expression in queens during the period of colony foundation, ovaries from queens at different ages post-mating were dissected and analyzed by western blot. Ovaries from virgin queens collected right before a mating flight were also analyzed. In newly-mated queens, the *Si*VgR immunoreactive band was highly noticeable from 8 h after field-collection and remained high until 10 days after field collection (mating) (Figure 2.6, lanes 2-6). Additionally, *Si*VgR was constantly expressed between 10 and 25 days after mating (Figure 2.6, lanes 6-9). However, *Si*VgR was not detectable in western blots from ovaries of virgin queens that were collected just before the mating flight began (Figure 2.6, lane 1). This might be due to the low receptor expression in virgin queens (only one ovary pair-equivalent protein was analyzed), which is confirmed by immunofluorescence (Figures 2.3B and 2.4). *Si*VgR protein abundance is almost complementary to that of *Si*VgR mRNA, which is higher in virgin than newly-mated queens [24]. Interestingly, *Si*VgR was also not detectable in ovaries from de-alate queens that had taken a mating flight but were not inseminated (no white spermatheca found). In these queens, the receptor was not detectable after 24 h of field-collection whereas mated queens showed high expression after that period (Figure 2.6, lane 10; compare with mated queen, lane 4). Therefore, we conclude that it is successful mating, and not participating in the mating flight per se, that induces high *Si*VgR protein expression in mated queens.

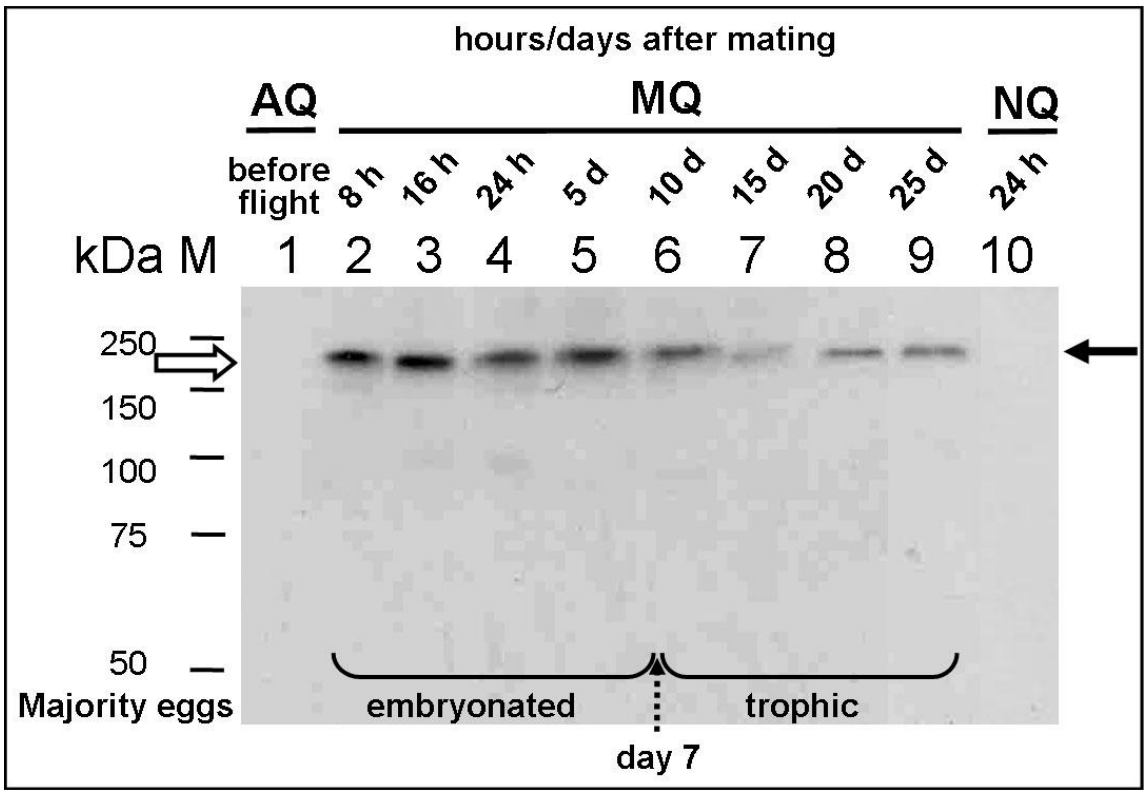

Figure 2.6. Western blot analyses of vitellogenin receptor (*Si*VgR) in ovaries from virgin and field collected newly-mated queens during the period of colony foundation. Total proteins from ovaries of queens at different time-points before and after mating were analyzed (equivalent to one pair of ovaries per lane). The strongest *Si*VgR signals were detected from 8 h until 10 days mated queen (MQ) after collection (lanes 2-6, arrow). *Si*VgR signals were also constantly detected 10-25 days after collection (lanes 6-9). No signal was detected from virgin (alate) queen (AQ) ovaries collected right before mating flights (lane 1) and non-inseminated de-alate queen (NQ) ovaries analyzed 24 h after being collected upon landing from mating flights (lane 10). Larvae of nanitics (first workers) start to emerge around 7 days after queen mating. n=5 ovaries per time point. M: Marker.

Discussion

SiVgR ovarian expression in queens

The molecular mechanisms of reproductive control in social insects are beginning to be understood, mainly through research on social Hymenoptera, specifically the honey bee [170,171]. Here we report the first such study on an invasive ant species, the red imported fire ant. The onset of reproduction in fire ants is under complex control, involving both environmental and endogenous factors. These stimuli may influence the readiness of virgin queens for a mating flight and upon mating, de-alation, the sudden increase in vitellogenesis and concomitant ovarian development, and the onset of egg-laying behavior. To begin to dissect the molecular mechanisms of reproduction in ants, we investigated the fire ant *Si*VgR temporal subcellular localization in the ovaries of both virgin queens and in mated queens.

Drosophila yolk protein receptor shares high sequence similarity and identity with insect VgRs [164], and therefore the polyclonal antibodies raised against *A. aegypti* VgR also recognize the *D. melanogaster* yolk protein receptor [172]. However, polyclonal antibodies against a VgR from cockroach failed to cross-react with the *Si*VgR (Figure 2.5F). Therefore, development of a specific *Si*VgR antibody was necessary. *Si*VgR immunoreactivity analysis indicated that *Si*VgR is only present in the ovary of queens, consistent with its role in Vg uptake for egg development (Figure 2.2). Reports on VgRs from other insect species analyzed by western blot with specific antibodies are of similar molecular weight as our result (~202 kDa) [22,23,26-28]. The antibody

developed is highly specific and does not cross-react or detect other LDLR family receptors (Figures 2.2 to 2.5). Receptor signal was not observed in membrane preparations from head, fat body, gut and male abdomens, verifying receptor tissue specific expression in the ovary (Figure 2.2). In the honey bee, occurrences of Vg and VgR in tissues other than the ovary in both queen and worker have been reported, suggesting an alternative role of Vg as a food storage protein or as an antioxidant [31,51,165,173].

Three Vg genes (*Vg-1*, *-2*, and *-3*) have been previously discovered in fire ants [147]. *Vg1* gene is expressed in all life stages and castes; *Vg2* and *Vg3* genes are only expressed in queens and their expression level is higher in mated queens than in virgin queens [147]. Therefore, besides the low expression of *Si*VgR protein in the virgin queens (in this dissertation), the low expression of Vg2 and Vg3 in virgin queens could also be another essential control component of fire ant ovary development. Recently, the fourth Vg gene (Vg-4) has been discovered in fire ants and it is only expressed in workers with lower expression level than the Vg1 gene [3]. However, we did not detect *Si*VgR expression in workers or queen tissues other than the ovary indicating that the fire ant Vg1 and Vg2 are only circulating proteins or must be incorporated through a receptor other than *Si*VgR in target tissues [24].

Chen in Pietrantonio's laboratory previously found that the *Si*VgR transcript level was higher in ovaries from virgin queens than from mated queens at 1-7 days post-mating (colony foundation period) [24]. Tian et al. who analyzed up-regulated transcripts in newly-mated queens versus virgin queens did not identify higher levels of

*Si*VgR expression in mated queens [147], supporting our findings. However, the *Si*VgR transcript level is lower in virgin queens than in egg-laying mated queens within a mature fire ant colony (Lu and Pietrantonio, unpublished data). We now report that despite the elevation of *Si*VgR transcript level with age in virgin queens [24], the *Si*VgR protein signal is much lower in the ovary of virgin queens than mated queens (Figure 2.3). These findings are consistent with the known reproductive inhibition by exposure to queen primer pheromone in virgin queens previous to the mating flight and indicate that the translational regulation of *Si*VgR expression is part of the orchestration of reproductive inhibition. Conversely, the mated queen within a colony has high *Si*VgR protein expression, in accordance with its role in continuous egg production. Honey bee VgR transcript level is also higher in the ovary of egg-laying queen within a mature colony than in virgin queens [31]. In cockroach, VgR transcript levels are also relatively high in the pre-vitellogenic stage ovaries and low in the vitellogenic stage; however, the expression of VgR protein was low in the nymphal stage and high during the vitellogenic periods [26-28]. In contrast, the level of mosquito VgR transcript and its protein start to rise in the ovary one day post-eclosion and continue to rise during the pre-vitellogenic and vitellogenic periods, reaching their peak at 24h after a blood meal and then decline [23,174].

Subcellular distribution of SiVgR

The subcellular localization of *Si*VgR signal was similar in virgin and mated queens, i.e. expressed in the cytoplasm of pre-vitellogenic oocytes and in the plasma

membrane of vitellogenic oocytes (Figures 2.3 to 2.5). Although this similar *Si*VgR subcellular distribution was observed in both virgin and mated queens, plasma membrane-localized *Si*VgR signal in virgin queens was not detected until 12 days post-eclosion (Figure 2.4), significantly later than in newly-mated queens (24 h post-mating) (Figure 2.3C). This age (12 days) coincides with the required virgin queen maturation time for flying and mating [143,144,148,149]. These results support the hypothesis that after virgin queen eclosion within a mature colony, oocyte development is partially suppressed possibly by the queen primer pheromone until virgin queens are ready for a mating flight. Queen primer pheromone may thus prevent virgin queens from competing with the mated queen for nutritional resources for reproduction (ovarial inhibition), but keeps virgin queens ready for reproductive success after a mating flight when the appropriate physical and environmental conditions become available [175,176]. In *Drosophila*, the yolk protein receptor transcript and protein are detected in germ line cells (pre-vitellogenic, stage 1 chamber) and receptor protein is evenly distributed throughout the oocyte during the pre-vitellogenic stages (stages 1-7) and increases remarkably at the oocyte membrane during vitellogenic stages (stages 8-10) [10]. Similar results were found in cockroach VgRs [26-28]. In fire ants, factors contributing to reproductive control via the *Si*VgR include: (a) functional *Si*VgR translational machinery which may be negatively regulated by low levels of JH in virgin queens; and (b) correct localization of the *Si*VgR protein in the oocyte membrane. Several proteins are involved with the correct transport of yolk protein receptor to the oocyte membrane in *Drosophila,* such as Boca (an endoplasmic reticulum protein) [177], Trailer Hitch (a

component of a ribonucleoprotein complex) [178], and Sec5 (the exocyst component in endoplasmic reticulum) [179]. Homologues of these genes in fire ants may be temporally down-regulated by levels of JH (or other hormones or factors) before 12-14 days of age in virgin queens in which *Si*VgR expression is cytoplasmic.

Our findings suggest *Si*VgR expression in mated queens during the colony foundation period is tightly synchronized with queen egg production (Figure 2.6). The high apparent expression of *Si*VgR at 8 h to 10 days post-mating is associated with the production of eggs that predominantly give rise to nanitics [151]. *Si*VgR signal declined after 10 days and was steady until 25 days post-mating. The eggs produced during this 15 day period (before the first worker adults emerged) are predominantly trophic eggs and during this period the number of eggs in the ovary is significant higher [180]. It is also known that size of trophic eggs is 4x larger than embryonated eggs [181]. However, the *Si*VgR signal in ovaries is lower in this period (Figure 2.6, lanes 7-9), perhaps suggesting that a large component of trophic eggs might not be Vg or that the Vg uptake may be more efficient in trophic eggs if limited *Si*VgR is present.

We also observed that ovaries of de-alate queens which were not inseminated remain small and show no *Si*VgR signal similar to these before mating (Figure 2.6, lane 10). This result implies that successful insemination of newly-mated queens, but not flight only, triggers vitellogenesis. In addition, the factors linked to this activation might not be involved in de-alation [182]. In *Drosophila*, the sex peptide (transported from male to female when mating) and its receptor are essential for triggering the post-mating

reproductive switch [183,184]. Sex peptides or other factors might play a similar role in fire ant reproduction.

In insects, JH level is regulated by neuropeptide hormones, biogenic amines and other factors [185]. In fire ant virgin queen ovaries *in vitro*, *Si*VgR transcript is upregulated by the JH analog methoprene [24]. In mosquito, JH is also assumed to enhance post-transcriptional control of VgR transcripts in ovary similarly to its effect on other transcripts in the fat body [37,186]. However, how VgR expression is hormonally controlled in virgin queens needs further investigation. In *Drosophila*, the insulin signaling pathway may regulate JH synthesis [66] and is necessary for vitellogenesis in adults [121] (please see Figure 1.2, Chapter I). In addition, the sNPF signaling cascade is involved in ovarian development in locust [57,78] and is the up-regulator of insulin signaling pathway in *Drosophila* [58]. It appears that JH is the main regulatory hormone for ovary development and de-alating behavior in fire ant queens and the *Si*VgR transcript in virgin queen ovaries is up-regulated by the JH analog methoprene *in vitro* [24]. Therefore, VgR regulation appears to be under complex control of nutritional signals which regulate JH through several neuropeptide pathways including sNPF and insulin pathways, and also perhaps male factors transferred during mating. This conclusion is not inconsistent with the diverse pleiotropic effects of JH and insulin signaling known to exist among insects.

In summary, *Si*VgR is queen and ovary specific and is critical for egg formation. It is successful mating, but not participating in the mating flight per se that induces high *Si*VgR protein expression in mated queens. In virgin queens, the receptor signal was

first observed at the oocyte membrane beginning at day 12 post-emergence, coinciding with the required two weeks of maturation before a mating flight. Thus the correct localization of *Si*VgR in the cell membrane in virgin queens appears to be a legitimate physiological marker for virgin queen readiness for a mating flight.

Materials and Methods

Insects

Polygyne (multiple-queens) colonies of *S. invicta* were obtained and maintained as described previously [24]. All colonies were collected in Brazos County, Texas, and tested for free of microsporidium *Kneallhazia* (*Thelohania*) *solenopsae* infection [187]. The laboratory colonies of *S. invicta* were housed in plastic trays (27 × 40 × 9 cm, Pioneer Plastics Inc.) covered with Fluon (Insect-a-Slip insect barrier, BioQuip Products, CA, USA). Each tray equipped with one nest (14 cm diameter Petri dishes half-filled with damp Castone®, Dentsply International Inc., York, PA, USA). Colonies were maintained at 27 ± 2 °C (16L: 8D photoperiod) and fed daily with 20% honey-water, cricket carcasses (Flukers, Port Allen, LA, USA), and an artificial diet [188]. Water was given *ad libitum*. Virgin queens and mated queens were collected from multiple polygyne colonies.

Virgin queens ready to begin a mating flight were collected from the top of mounds in the field and their ovaries were dissected after collection. Newly-emerged virgin queens from laboratory colonies were kept in a 3 cm diameter plate nest (half-

filled with damp Castone®) with holes on the lid to receive care from workers within the queenright colony and exposure to primer pheromone from mated queens. Newly-mated queens were collected from the field after mating flights (at about 3-4 pm). Queens were brought to the laboratory and maintained at 27 °C in glass tubes which acted as humidity chambers by preparing them half-filling them with water and cotton (please see Mei-er Chen's dissertation, Figure 5-1 [35]). These queens will not eat for about one month. Ovaries were dissected at 8, 16, and 24 h, and 5, 10, 15, 20, and 25 days after collection, respectively. During dissection, successfully mated queens were identified by observing an inseminated large and white spermatheca; only inseminated queens were used as "mated queens."

Anti- SiVgR antisera production

To select a highly specific sequence of *Si*VgR to be expressed as antigen for antisera production, structural domains of the hymenopteran VgRs, (fire ant VgR, AAP92450, predicted honey bee VgR, XP_001121707, wasp VgR, XP_001602954), *B. germanica* lipophorin receptor (LpR) (CAL47125), and human LDLR (AAA56833) were aligned and compared. The SMART (simple modular architecture research tool; http://smart.embl-heidelberg.de) [189,190] was used for identification of modular domains that were adjusted by eye, when necessary. The SignalP 3.0 (http://www.cbs.dtu.dk/services/SignalP/) and the SigCleave tools (EMBOSS; http://mobyle.pasteur.fr/cgi-bin/portal.py?form=sigcleave) were used to predict the cleavage sites of the signal peptide. Percentage identity and similarity for sub-domains

were determined by the EMBOSS Pairwise Alignment Algorithms of EBI (European Bioinformatics Institute; http://www.ebi.ac.uk/emboss/align).

After hydrophilicity and antigenicity analyses of the *Si*VgR amino acid sequence by DNASTAR software (DNASTAR Inc., Madison, WI, USA), a fragment corresponding to the second YWXD repeat region in the first epidermal growth factor (EGF) precursor homology domain (amino acids 648-887) was chosen to produce a *Si*VgR antigen. The *Si*VgR fragment was amplified from a *Si*VgR clone (from Mei-er Chen) by PCR and cloned into pCR®2.1-TOPO® vector using the TOPO TA cloning kit (Invitrogen, Carlsbad, CA, USA). Competent cells (Top10F', Invitrogen) containing the plasmid were grown in Luria–Bertani medium containing 100 μg/ml ampicillin and cloned products were isolated by QIAprep Spin Miniprep Kit (Qiagen, Valencia, CA, USA). The plasmid was cut with *Bam*HI and *Sal*I and the *Si*VgR fragment was subcloned into *Bam*HI and *Sal*I restriction sites in the pET32a(+) vector (Novagen, San Diego, CA, USA) with T4 DNA ligase (Promega, Madison, WI, USA). Competent cells (Top10F') containing this plasmid (pET32a-VgR) were grown in Luria–Bertani medium containing 30 μg/ml kanamycin and cloned products were isolated as above and sequenced (ABI PRISM Big Dye Terminator Cycle Sequencing Core kit; ABI 3100 Sequencer) by the Gene Technology Laboratory (Texas A&M University, College Station, TX, USA). To generate an expression plasmid, this *Si*VgR fragment was cut from the previously generated plasmid (pET32a-VgR) and subcloned into *Bam*HI and *Sal*I restriction sites in the pET28a(+) vector (Novagen) with T4 DNA ligase (Promega). This pET28a-VgR plasmid expressed the *Si*VgR fragment with an additional 32 amino

acid residues at the N-terminus, which included the His-tag sequences for its purification. Plasmid DNA was grown, purified, and sequenced as above for verification.

Escherichia coli strain BL21 (DE3) (Novagen) was then transformed with pET28a-VgR plasmid and one positive colony was grown in Luria–Bertani medium containing 30 μg/ml kanamycin. Isopropyl-thio-β-D-galactoside (IPTG) (1mM) was added to this bacterial culture (OD_{600nm}=0.6) to induce recombinant protein expression. After incubation at 20 °C for 8 h, the culture was centrifuged at 3,000 g for 10 min (Beckman Avanti 30 centrifuge, Beckman Coulter, Brea, CA, USA) and the pellet was lysed in wash buffer. Lysate was centrifuged at 10,397 g for 20 min (Beckman Avanti 30 centrifuge). Proteins in the supernatant were purified using TALON® metal affinity resin (Clontech, Mountain View, CA, USA) following the manufacturer's protocol with additional 8 M urea added in each step. Recombinant protein was eluted with 150 mM imidazole and analyzed by SDS-PAGE (Figure 2.1B). The eluant (~10 ml/each purification) was collected and dialyzed with decreasing concentrations of urea from 8 to 7, 6, 4 and 2 M in PBS at 4 °C, each step for 2 h in 10K MWCO SnakeSkin Dialysis Tubing (Pierce, Rockford, IL, USA). The *Si*VgR recombinant antigen (~30 kDa) was concentrated with a 10 kDa Amicon® Ultra-4 Centrifugal Filter (Millipore, Billerica, MA, USA) by centrifugation at 4,000 g (SX4750 rotor, Beckman Coulter, Brea, CA, USA). This antigen protein (~0.2 μg in each injection) was injected into two rabbits for antibody production (Robert Sargeant's Laboratory, Ramona, CA). Pre-immune sera

was collected to be used for negative controls. The specificity of anti-*Si*VgR antisera was confirmed using western blot analysis.

Tissue preparation and western blot analysis

Membrane proteins, microsomes (endoplasmic reticulum) or tissue homogenates were analyzed by western blot. Membrane proteins were extracted from virgin and mated queens and males of unknown age (Figures 2.2 and 2.3A). To confirm receptor tissue specific expression, membrane proteins (10 μg/lane) from the ovary, head, fat body, gut of mated queens, and abdomen of adult males were analyzed by western blotting. To compare receptor expression between virgin and mated queens (Figures 2.3 to 2.5), membranes of four pairs of ovaries from mated queens (45.4 μg/lane) and 16 pairs of ovaries (10.3 μg/lane) from virgin queens were analyzed. Membranes were prepared as previously described with modifications [22,23]. Tissues were dissected and homogenized in cold buffer A (25 mM Tris-HCl, pH 7.5, 1 mM EDTA, 1 mM EGTA, 1 mM dithiothreitol) with protease inhibitors (1 mM phenylmethylsulfonylfluoride, 1 mM benzamidine, 1.5 mM pepstatin A, 2 mM leupeptin). The homogenates were centrifuged at 800 g for 5 min and the supernatants were collected and centrifuged at 100,000 g (SW28 rotor, Beckman LE80K) for 1 h at 4 °C. After ultra-centrifugation, the pellets were re-suspended in 200 μl cold buffer B (50 mM Tris-HCl, pH 7.5, 2 mM $CaCl_2$) with protease inhibitors and stored at -80 °C. To confirm that oocyte cytoplasmic signal was specific for *Si*VgR, microsomes (10 μg/lane) from mated queen ovaries were prepared as described previously [191] and analyzed by western blotting (Figure 2.5G). To

determine receptor expression in mated queens throughout the colony foundation period (Figure 2.6), whole ovaries dissected from virgin queens (collected right before a mating flight), newly-mated queens at various times post-mating, and non-inseminated queens (24 h after collection) were placed in cold buffer A and stored at -80 °C. Five ovaries from each time point were homogenized in buffer A and total protein equivalent to one ovary was loaded per lane.

For western blots, proteins were separated on SDS-PAGE (7.5% gel, Bio-Rad, Hercules, CA, USA) and transferred to PVDF (polyvinylidene difluoride) membranes (Millipore). Membranes were blocked for 1 h at room temperature (RT) in 5% non-fat milk (Wal-Mart Store Inc.) in TBST (10 mM Tris base, 140 mM NaCl, 0.1% Tween-20, pH 7.4) and incubated for 1.5 h with rabbit anti-*Si*VgR antiserum (fourth bleed; 1:1000) in TBST. After 3 X 10 min washes with TBST, the membrane was then incubated with a horseradish peroxidase (HRP)-conjugated goat anti-rabbit IgG antibody (Jackson ImmunoResearch, West Grove, PA, USA; 1: 40,000) for 1 h. After the same washing steps, the membrane was visualized using the Enhanced Chemiluminescence System™ (Pierce) on X-OMAT film (Kodak, Rochester, NY, USA). To compare protein abundance, the intensity of the *Si*VgR band (Figure 2.3A) was determined using the ImageJ image processing program (http://rsb.info.nih.gov/ij/).

Immunofluorescence analysis

Ovaries from 10 each of mated queens, newly-mated queens (24 h post-mating), and virgin queens from day 0 (the day of eclosion) up to 14 days post-eclosion,

respectively, were dissected under PBS. Each pair of ovaries was divided into two, one individual ovary was included in the experimental group and the other used as a negative control. Ovaries were fixed for 4 h in 4% paraformaldehyde (Sigma-Aldrich, St. Louis, MO, USA) in PBS at 4 °C and serially dehydrated in 50%, 70%, 95%, 100% ethanol and xylene for 2 X 30 min each at room temperature. Tissues were then penetrated in Paraplast-Xtra (Fisher Scientific, Pittsburgh, PA, USA) at 60 °C for 4 h. Sections (12 μm) were cut with a rotatory microtome and placed on Superfrost Plus™ slides (Fisher) and dried for 2 days at 39 °C. Tissue sections were de-waxed for 2 X 5 min in xylene and rehydrated serially for 10 min, each in 100%, 95% and 70% ethanol and in water for 30 min at room temperature. After rinsing 2 X 5 min with PBST (PBS containing 0.05% Triton X-100), the slides were incubated in blocking solution (5% goat serum and 0.5% bovine serum in PBST) for 1 h at room temperature and then incubated overnight in a wet chamber at 4 °C with the anti-*Si*VgR antiserum (1:100) in blocking solution. The slides were also incubated overnight with the pre-immune sera (1:100), anti-*Si*VgR antiserum (4 μl) pre-absorbed for 3 h with 100 μg *Si*VgR antigen (1:2500), and the antisera against *B. germanica* VgR (a generous gift from Dr. M-D. Piulachs, Spain) (1:100) in blocking solution as negative controls. Washes were for 3 X 10 min in PBST, which were subsequently done in this fashion after each incubation step. Slides were incubated with biotinylated goat anti-rabbit IgG (Jackson ImmunoResearch, West Grove, PA, USA; 1:200) in blocking solution for 1.5 h and washed, followed by incubation with Alexa Fluor 546 Streptavidin (Invitrogen; 1:200) in blocking solution for 1 h. Sections were washed and mounted in Vectashield Mounting medium with

DAPI (4'-6-diamidino-2-phenylindole) for nuclear staining (Vector, Burlingame, CA, USA) and observed under a Carl Zeiss Axioimager A1 microscope with filters for DAPI (G 365 nm, FT 395 nm, BP 445 nm) and Alexa Fluor 546 (BP 546 nm, FT 560 nm, BP 575-640 nm). Sections were analyzed and images were obtained with an AxioCam MRc color camera (Carl Zeiss) and analyzed with AxioVision image program (Carl Zeiss).

CHAPTER III

DISRUPTION OF THE VITELLOGENIN RECEPTOR GENE FUNCTION IN VIRGIN QUEENS BY RNA INTERFERENCE*

Introduction

The formation of eggs in insects requires incorporation of relatively large amounts of proteins and lipids which uptake into oocyte involves the function of receptors of the low density lipoprotein receptor (LDLR) family. It is known that VgR mediates the uptake of Vg into the oocyte and this is a critical event in vitellogenesis. In fire ant, the transcripts and proteins of *Si*VgR are only expressed in the queen ovary [24,192]; adult workers (which are also females) have no ovary and are sterile. Therefore, we hypothesized that RNA interference (RNAi) mediated silencing of the *Si*VgR gene would lead to a phenotype of no (or impaired) egg formation in fire ant queens.

RNAi has been used as a research tool to disrupt the expression of specific genes in a wide range of organisms including plants, fungi, invertebrates and mammals [193,194]. One of common methodologies for RNAi is introducing the double-stranded RNA (dsRNA) into the organism to inhibit the expression of the target gene. The discovery of

* Portions of this chapter reprinted with permission from "Oocyte membrane localization of vitellogenin receptor coincides with queen flying age and receptor silencing by RNAi disrupts egg formation in fire ant virgin queens" by Lu, H.L., Vinson, S.B., Pietrantonio, P.V. 2009, *FEBS Journal* 276: 3110–3123. 2009, © 2009 Blackwell Publishing Ltd

dsRNA being the potent trigger for RNAi was first reported in the nematode *C. elegans* [195]. Subsequently, RNAi technology made it possible to knock down gene function on insects other than model organisms like *Drosophila*.

Studies on RNAi silenced genes expressed in the ovaries were reported from cockroaches [27,196], ticks [18,197], fruit flies [198-200], the mosquito (*A. aegypti*) [133], and the wasp (*N. vitripennis*) [201]. Previous research on RNAi treatments with VgR dsRNA in invertebrates have been shown effective to knock down VgR gene expression in ovary of the German cockroach, *B. germanica*, the American dog tick, *D. variabilis*, and the shrimp, *P. monodon*. Silencing VgR gene expression disrupts Vg uptake into the oocyte and thus leads to Vg accumulating in the haemolymph [18,20,27]. RNAi of VgR gene has not yet been tested in insects with polytrophic ovary. Silencing of lipophorin receptor (LpR, another receptor in the LDLR superfamily) in the ovary and the fat body of German cockroach also showed that dsRNA can be applied to silence genes expressed in ovary. The results showed that LpR RNAi treated females have lower receptor expression 6 days after treatment, and also contained less apolipophorin I in the ovary when compared with controls [27]. However, silencing of LpR has limited effect on egg formation or vitellogenesis.

In Hymenoptera, RNAi has been successfully used to knock down gene expression in the honey bee [202-204] and the wasp *N. vitripennis* [201]. In the honey bee, abdominal injection of eggs or newly emerged adult workers with Vg dsRNA (derived from a 504 bp Vg coding sequence) disrupts the expression of the Vg gene in the adult fat body [203]. Parental RNA interference (pRNAi) was applied in the wasp.

The dsRNA derived from the Otd1 gene was injected into female wasp pupae and the expression of Otd1 gene in the offspring embryos was tested [201].

Although when we started this project, there was no other report on silencing a gene in the ovary of the hymenopteran insects except the work from Lynch and Desplan [201], we hypothesized that silencing VgR gene expression should be feasible in the fire ant queen. RNAi technique would not only allow us to analyze VgR gene function in fire ants, but also would aid the study of other insect species in which it is not easy to produce transgenic insects, especially social insects in which at most only a few females have reproductive ability in a colony. To demonstrate that RNAi can be an effective tool for studying gene functions in queen ovary, we experimented to decrease transcript abundance for the Vg receptor and analyzed results by RT-PCR and histochemistry as well as by photography of ovaries.

Results

dsRNA synthesis

The purpose of this study was to silence the Vg receptor gene expression in fire ant ovary via microinjection of *Si*VgR-dsRNA. For this, high quality dsRNA from two regions of the *Si*VgR were synthesized *in vitro* using the MEGAscript™ RNAi Kit (Ambion). The *Si*VgR cDNA clone [24] and the enhanced green fluorescent protein (EGFP) clone [205] were used as templates for DNA amplification using gene specific

primers (Table 3.1) designed with the T7 RNA polymerase recognition sequence on both the sense and antisense strands for respective single stranded RNA synthesis.

A 691 bp product amplified from the *Si*VgR clone was used as the DNA template for *Si*VgR-dsRNA1 synthesis (Figure 3.1A, lane 1), and a 611 bp product from EGFP was used as a negative control DNA template for syntheses of the EGFP-dsRNA (Figure 3.1A, lane 2). After purification of DNA templates, the T7 enzyme was added to each transcript template for synthesis of the single stranded RNAs (ssRNAs) (Figure 3.1B, lane 1 and 5). The complementary ssRNAs were incubated at 75 °C for 5 min and then cooled-down to room temperature for the annealing of complementary ssRNA into dsRNA (Figure 3.1B, lane 2 and 6). Subsequently, the nuclease (DNase I and RNase) was added to digest DNA and ssRNA, but not dsRNA (Figure 3.1B, lane 3 and 7). In the last step, the dsRNA was purified (Figure 3.1B, lane 4 and 8) and the dsRNA was resuspended to 1 µg/0.5 µl in elution buffer.

Table 3.1 DNA primers used in PCR to generate the templates for double-stranded RNA synthesis for *Si*VgR and EGFP. Each of the primers incorporates the T7 promoter sequence at the 5' end (underlined).

Designation	Sequence	Orientation
For SiVgR- dsRNA1 template preparation		
T7-VgRi-f1	5'-TAATACGACTCACTATAGGGGCCATCTGC AATTATCAACGCCTTTCTTAACGTC-3'	Sense
VgRi-r1-T7	5'-TAATACGACTCACTATAGGGACCACATAC TGTGCATCGCGTGAATAAGGTGTC-3'	Anti-sense
For SiVgR-dsRNA2 template preparation		
T7-VgRi-f4	5'-TAATACGACTCACTATAGGGCGTGATCAGG TCAAAACGTATTTTCTTCATTT-3'	Sense
VgRi-r3-T7	5'-TAATACGACTCACTATAGGGGCCACAGTCA TCCTTTTTATCGCATACTAC-3'	Anti-sense
For EGFP-dsRNA template preparation		
T7-P164	5'-TAATACGACTCACTATAGGGACGTAAAC GGCCACAAGTTCAGCGTGTC-3'	Sense
P165-T7	5'-TAATACGACTCACTATAGGGTCACGAAC TCCAGCAGGACCATGTGATC-3'	Anti-sense

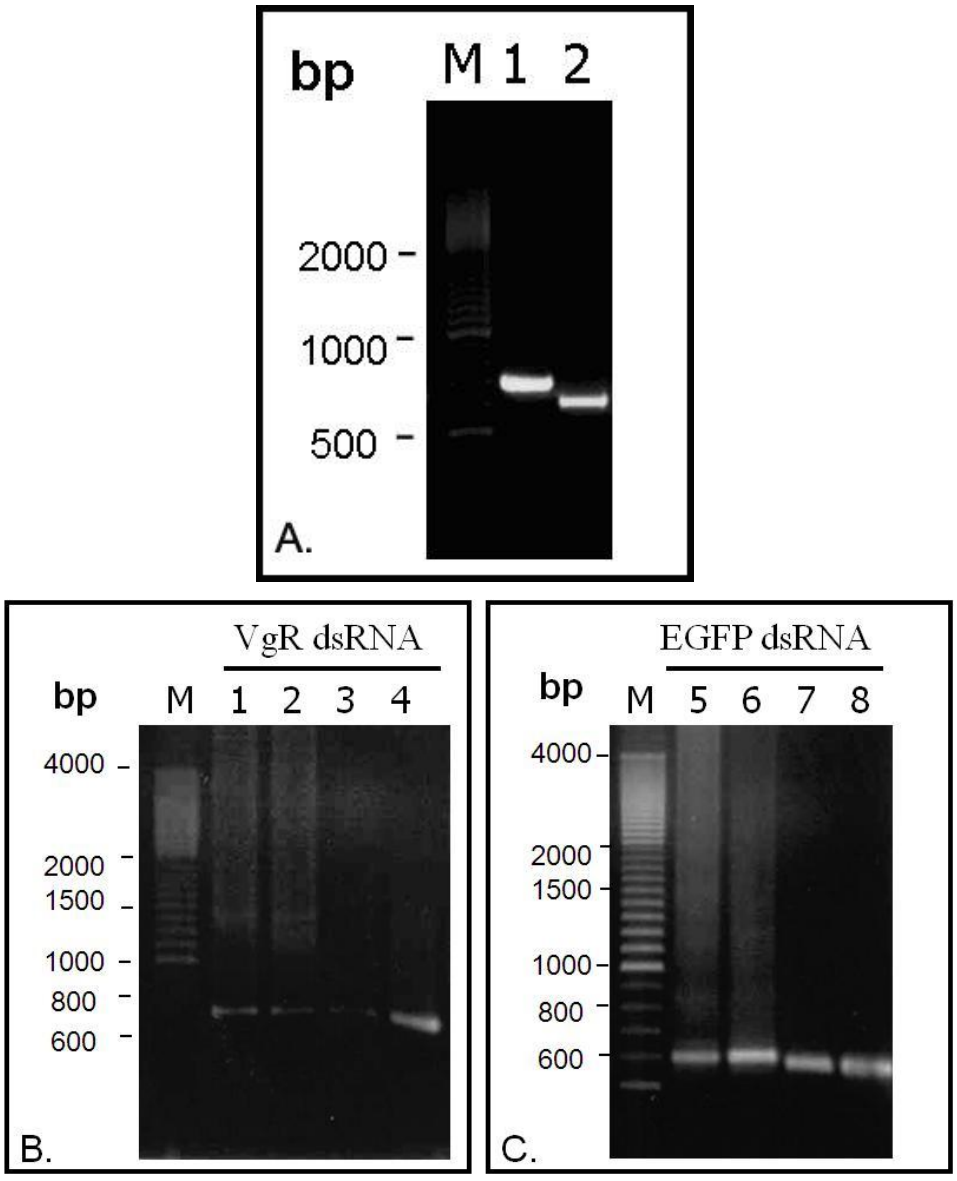

Figure 3.1. Syntheses and purification of dsRNA from *Si*VgR and EGFP for RNA interference. (A). *Si*VgR DNA template-1 (lane 1) and EGFP DNA template (lane 2) were PCR amplified and purified from the gel. (B): Single stranded RNA (ssRNA) of *Si*VgR and EGFP were transcribed from the DNA template respectively (lane 1 and 5). The complementary ssRNA were denatured and re-annealed into dsRNA (lane 2 and 6). Nuclease (DNase I and RNase) was added to digest DNA and ssRNA (lane 3 and 7) and the *Si*VgR-dsRNA1 and EGFP-dsRNA were purified by filter cartridge (lane 4 and 8). Notice that dsRNA quality and concentration increases greatly after annealing and purification. M: marker.

dsRNA injection and RNAi results evaluation

Red eye reproductive females were selected for dsRNA injection. Intra-abdominal injections (0.5µl) of elution buffer (negative control), EGFP-dsRNA (1 µg/0.5 µl, negative control), or *Si*VgR-dsRNA1 (1 µg/0.5 µl) were performed (Figure 3.2A). After injection, pupae were individually placed with a group of workers and brood from the same colony; food, water, and honey (20%)-water were provided (Figure 3.2B). Eclosion of red eye reproductive female pupae injected with dsRNA occurred 5-8 days after injection. In the first RNAi experiment, the alate rate of emergence was calculated in each treatment. Results showed that the rate of emergence was not significant different between treatments (71% in buffer injected alates, 69% in EGFP-dsRNA injected alates, and 63% in *Si*VgR-dsRNA1 injected alates; Figure 3.2D).

RNAi effects were analyzed by semi-Q RT-PCR and immunofluorescence at 0 (queen eclosion day), 5 or 10 days post-eclosion. Semi-Q RT-PCR analysis showed significantly reduced *Si*VgR transcripts in queen ovaries derived from *Si*VgR-dsRNA1 injected pupae (Figures 3.3A and 3.3B) and immunofluorescence revealed inactive ovarioles with stunted oocytes showing no *Si*VgR signal (Figures 3.3E and 3.3H). Conversely, clear *Si*VgR signal and the formation of eggs were observed in ovaries from buffer- (Figures 3.3C and 3.3F) and enhanced green fluorescent protein (EGFP)-dsRNA injected (Figures 3.3D and 3.3G) negative controls.

A.  B. 

C. 

D.

Injected	Buffer	EGFP	VgR
Injected pupae number	153	227	216
Emerged alate number	109	156	135
Alate emerged rate %	71	69	63

Figure 3.2. RNA interference treatments of fire ant queen pupae and laboratory setting. A: Red eye stage queen pupae were separated from colonies for microinjection. Intra-abdominal injections (~0.5 µl) of elution buffer, EGFP–dsRNA or *Si*VgR-dsRNA1 were performed using a Femtotip® sterile injection capillary needle (Eppendorf). B: After injection, queen pupae were individually placed with a group of workers (~100) and brood (~10); food, water and honey water were provided. C: Isolated cages containing individual queen pupae after RNA interference treatments. Pupae were individually injected with buffer, *Si*VgR-dsRNA1, or EGFP-dsRNA in each experiment. Insects were kept at 27 °C and maintained under a light/dark cycle of 16:8 hours. D. Comparison of emergence rate of buffer, EGFP-dsRNA, and *Si*VgR-dsRNA1 injection. The alate emergence rate is calculated as the number of emerged alates divided by the number of injected pupae. In total, 216 pupae were injected with *Si*VgR-dsRNA1, 227 pupae were injected with EGFP dsRNA, and 153 pupae were injected with elusion buffer only.

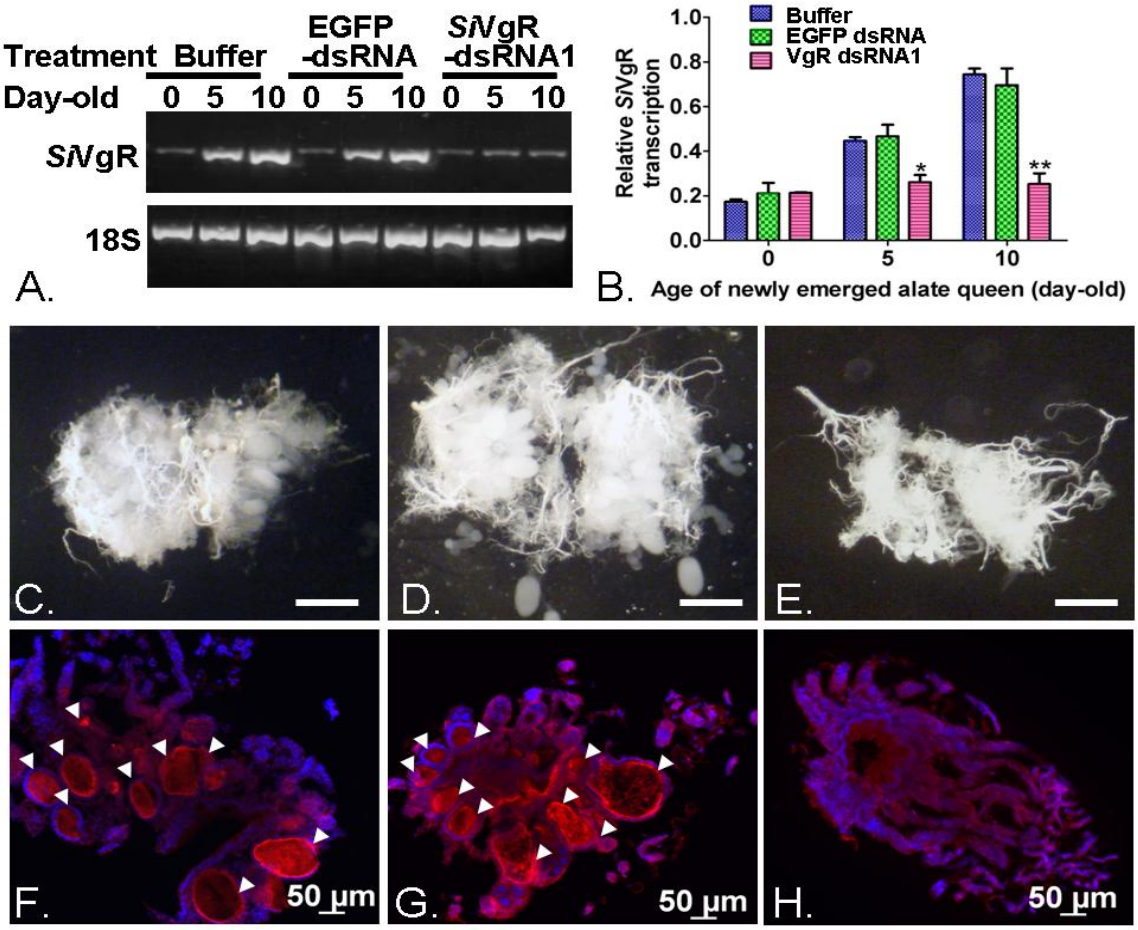

Figure 3.3. Results of RNA interference of vitellogenin receptor (*Si*VgR) in the fire ant virgin queens: semi-quantitative RT-PCR and immunofluorescence. The same amount of *Si*VgR-dsRNA1, EGFP-dsRNA, and buffer were injected into queen pupae and the results were analyzed with semi-Q RT-PCR and immunofluorescence. (A) Agarose electrophoresis of semi-Q RT-PCR amplified products (28 PCR cycles for *Si*VgR; 24 PCR cycles for 18S). Total RNA (0.5 µg) from four ovaries at each time point was used as a template. (B) Semi-Q RT-PCR shows the relative amount of *Si*VgR transcripts in comparison with amplified 18S transcripts in different treatments and age. The relative *Si*VgR transcript level of *Si*VgR-dsRNA1 treated ovaries is significantly lower than buffer- and EGFP-dsRNA- treated ovaries in 5 and 10 day-old virgin queens (*Tukey's multiple comparison test $P < 0.05$; **: $P < 0.01$). Ovaries from buffer (C), EGFP-dsRNA (D) and *Si*VgR-dsRNA1 (E) injected 10 day-old virgin queens were dissected and photos were taken under dissecting microscope. Bar, 0.5 mm. Ovaries from buffer- (F), EGFP-dsRNA- (G) and *Si*VgR-dsRNA1- (H) injected 10 day-old queens were analyzed by immunofluorescence. Arrowheads show *Si*VgR signal in control ovaries (F and G), but not in ovaries of queens where pupae had been injected with *Si*VgR-dsRNA1 (H).

Results from a second set of RNAi experiments using a different *Si*VgR target region (Figure 3.4) also showed that *Si*VgR transcripts in day-10 queen ovaries (derived from *Si*VgR-dsRNA2 injected pupae) were significantly reduced when compared with EGFP-injected groups. To eliminate the possibility of non-target effects within the same receptor superfamily, semi-Q RT-PCR analysis of a homologous LDLR (2.4 kb partial sequence obtained by Meier Chen in Pietrantonio's laboratory) gene expression showed that RNAi of *Si*VgR did not affect LDLR expression in the queen ovary (P=0.193, data not shown).

Analyses of oocyte size and *Si*VgR immunofluorescence signal showed *Si*VgR RNAi groups were significantly different from controls in days 0, 5 and 10 (Table 3.2). *Si*VgR silencing had a dramatic effect on pre-vitellogenic ovarian growth. An overall delay and inhibition of oocyte growth is demonstrated by the increase in the percentage of category II oocytes in the receptor silenced treatment, coupled with a decrease in this category in the controls, because more normal oocytes reached category III size during this period. This delay in growth was evidenced from the day of adult eclosion (D0), when about 64% of ovaries were inactive and devoid of receptor signal (category I oocytes) whereas 100% of control ovaries were growing and containing category II oocytes. The effect continued for 10 days, at which time 44% of ovaries still contained only inactive oocytes, devoid of *Si*VgR signal (category I), 52% of ovaries contained category II oocytes, but only 4% of ovaries contained large vitellogenic follicles (category III). In contrast, more than 61% of ovaries from both 10-day-old control groups contained at least one large vitellogenic follicle (oocyte > 20 μm; category III)

and the category II oocytes have began to decrease to 35-39% in controls, because oocytes had already grown.

A.

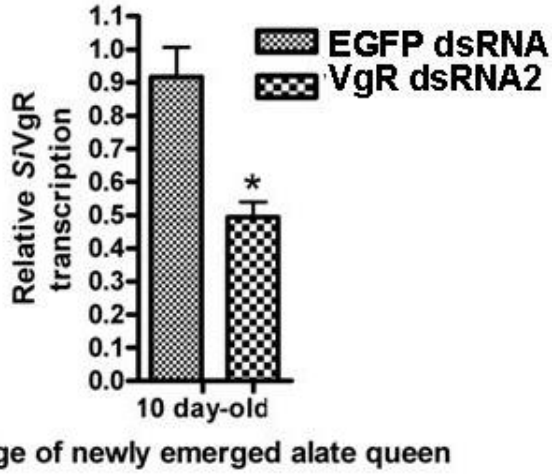

B. C.

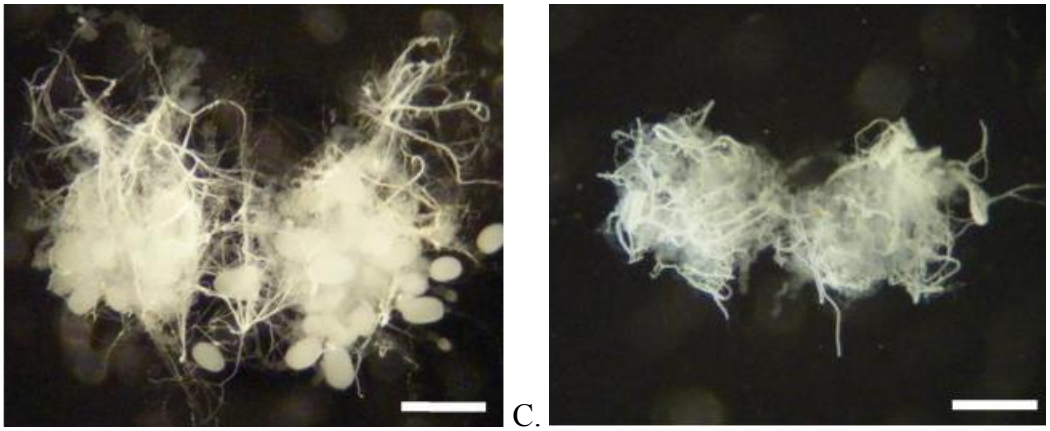

Figure 3.4. Results of silencing of the *Si*VgR gene by *Si*VgR-dsRNA2 targeting a second region of *Si*VgR gene. The same amount (1 μg/0.5 μl) of *Si*VgR-dsRNA2 and EGFP-dsRNA were injected into queen pupae and results were analyzed at day 10 by semi-Q RT-PCR. The relative *Si*VgR transcript level of *Si*VgR-dsRNA2 treated ovaries is significantly lower than in EGFP-dsRNA treated ovaries (asterisk means $P < 0.05$). EGFP-dsRNA (B) and *Si*VgR-dsRNA2 (C) injected 10 day-old virgin queens were dissected and ovaries were photographed under a dissecting microscope. Bar, 0.5 mm.

Table 3.2 Analysis of *Si*VgR silencing (RNAi) effect on ovaries from virgin queens at days 0, 5 and 10 post-eclosion. Percentage of ovaries exhibiting oocytes from categories I-III as defined by oocyte diameter and *Si*VgR immunofluorescence (ovary classification was mutually exclusive: ovaries were classified by the latest stage oocyte observed in each ovary). The category represents the oocyte growth stage and *Si*VgR signal. Category I: no oocyte development observed and no *Si*VgR signal observed; Category II: initial oocyte growth (oocyte size <20 μm) and *Si*VgR signal detected; Category III: at least one large vitellogenic oocyte (oocyte size >20 μm) and *Si*VgR signal detected. (Each pair of ovaries was separated into two individual ovaries, one for immunofluorescence analysis and the other for total RNA preparation followed by semi-Q RT-PCR).

Queen age	Day 0							Day 5							Day 10						
Categories	I		II		III			I		II		III			I		II		III		
Treatment	*n*	%	*n*	%	*n*	%	Total number	*n*	%	*n*	%	*n*	%	Total number	*n*	%	*n*	%	*n*	%	Total number
Elution buffer	0	0	9	100	0	0	9	0	0	8	53	7	47	15	0	0	12	39	19	61	31
EGFP–dsRNA	0	0	15	100	0	0	15	0	0	11	55	9	45	20	0	0	10	35	19	66	29
VgR–dsRNA1	7	64	4	36	0	0	11	10	56	7	39	1	6	18	12	44	14	52	1	4	27
Chi-square	18.545***							20.546***							43.059***						

***$P < 0.0001$.

Discussion

Test VgR RNAi on virgin queens

We developed an RNA interference protocol to disrupt fire ant vitellogenin receptor gene function in fire ant virgin queens. To our knowledge, this was the first report of successful post-transcriptional silencing of a VgR in Hymenoptera, as well as the first report of RNAi in any ant species when published [192].

In fire ant, the de-alating behavior and the onset of ovarian development in newly mated queen happen within 1 day after mating. Virgin queens are also capable of de-alating and becoming functional egg layers that produce only unfertilized eggs when they are separated from the mated queen primer pheromone. This indicates that the Vg receptor must have the function of uptake of Vg into the oocytes in isolated virgin queens. It is known that the Vg receptor protein is recycled during vitellogenesis in many insects. In order to silence gene expression before receptor protein accumulation occurred, microinjection of the *Si*VgR dsRNA fragment was into the female reproductive pupae stage. Two different pupae stages were tested previously which are white (red eye) pupae and dark pupae, respectively. Injection of dark queen pupae with *Si*VgR-dsRNA1 did not result in *Si*VgR silencing (data not shown). The selection of white pupae for injection of dsRNA appears to be critical for successful silencing of ovarian/embryonic genes in hymenopterans, as also shown earlier in the wasp, *N. vitripennis* [201].

To prevent dsRNA off-target effects, two methodologies were applied to designed dsRNA. First, *Si*VgR sequences selected for dsRNA synthesis were BLAST searched in GenBank and the Fourmidable database, and results showed no significant similarity to other genes. BLAST search allowed us to avoid sequences present in multiple genes, thus preventing the identification of false positives through off-target effects. In addition, the presence of CAN repeats (defined as ≥6 repeats of amino acids "Cysteine, Alanine, Asparagine") in the dsRNA have the potential to generate off-target effects [206,207]. The *Si*VgR regions we selected for dsRNA synthesis do not contain these repeats. Second, the RNAi effect was confirmed independently with two non-overlapping dsRNAs. *Si*VgR silencing experiments showed that dsRNA from two different receptor regions knocked down *Si*VgR gene function, which clearly proved a targeted effect of *Si*VgR RNAi on fire ant ovary (Figures 3.3 and 3.4).

VgR RNAi effects

In *Si*VgR-dsRNA1 injected pupae, receptor silencing effects were clearly detectable from day 0 to day 10 of virgin queen eclosion (Figures 3.3E and 3.3H and Table 3.2), although no effect was observed in negative controls. Although newly emerged virgin queens within a colony require around two weeks maturation time and then they are ready to fly and mate [143,144,148,149], the ovarian development in the isolated D10 virgin queens were obviously accelerated (D10 control groups in Figures 3.3C, 3.3D, and 3.4B). The RNAi silencing effect on *Si*VgR transcript and protein persisted for at least 10 days upon eclosion of virgin queens, until approximately the 15th

-18th day after dsRNA injection. However, the RNA silencing effect diminished somewhat with time because the percentage of ovaries that exhibited no *Si*VgR signal (category I) in the *Si*VgR-dsRNA1 injected group declined from 64% (day 0) to 44% (day 10) (Table 3.2). The delay in oocyte growth was evident in that for the control groups about 53% of ovaries had category II oocytes within the first 5 days, while the *Si*VgR-dsRNA1 group took 10 days to reach similar percentage (52%) of ovaries with category II oocytes. There was almost no change during the first 5 days in oocyte growth for the *Si*VgR-dsRNA1 group. In honey bees, the dsRNA can be detected endogenously more than 15 days after injection and the activation of RNAi can persist more than 21 days after dsRNA delivery [203]. The absence of the RNA dependent RNA polymerase in honey bee genome conflicts with this long lasting dsRNA result [208]; therefore, this long lasting dsRNA in bees may be due to low capacity of the Dicer enzyme system to process a great excess of injected dsRNA.

The VgR message is essential and critical for Vg uptake and egg development. Silencing of VgR in cockroach, ticks, and shrimp, disrupted Vg uptake into the oocyte and lead to Vg accumulation in the hemolymph [18-20,27]. In flies carrying the *Drosophila* female-sterile mutation of VgR, y*olkless* (*yl*), flies fail to accumulate yolk protein in oocytes and the receptor does not localize in the oocyte plasma membrane [10,22,209].

In summary, we have demonstrated that RNAi can be successfully applied to silence genes with ovarian expression in the fire ant. Silencing of *Si*VgR expression leads to impaired ovarian growth and oocyte development in virgin queens, providing

evidence that *Si*VgR may be a promising target for fire ant control. The development of RNAi techniques is particularly important for the control of invasive social insects in which the efficiency of production of transgenic insects would be decreased by the fact that only a few eggs will produce reproductive individuals.

Materials and Methods

Insects

S. invicta were reared as described in Chapter II.

Double-stranded RNA (dsRNA) synthesis

A *Si*VgR clone (cloned and published from our lab) [24] was used as a template for the synthesis of a 691 bp region of the *Si*VgR gene (amino acids 648-878) using primer set VgRi-f1 (5'-TAATACGACTCACTATAGGGGCCATCTGCAATTATCAACGCCTTTCTTAACGTC-3') and VgRi-r1 (5'-TAATACGACTCACTATAGGGACCACATACTGTGCATCGCGTGAATAAGGTGTC-3') (Table 3.1) which included the T7 promoter region (underlined). PCR amplification reactions contained approximately 2 µg of *Si*VgR plasmid template, 0.4 µM of each primer, 400 µM of dNTPs, 5 µl reaction buffer and 1 µl *Taq* polymerase (Promega) in a final volume of 50 µl. The PCR conditions were 94 °C for 3 min followed by 39 cycles of 94 °C for 30 s, 65 °C for 1 min, 72 °C for 1 min; 72 °C for 10 min. Products were visualized by agarose electrophoresis with GelStar™ dye (Lonza Group Ltd, Basel, Switzerland), cut from the

agarose gel, and purified using the QIAquick® Gel Extraction Kit (Qiagen). This PCR product was used as the DNA template for the synthesis of *Si*VgR-dsRNA-1.

To confirm the observed phenotype was due to specific silencing of the *Si*VgR mRNA, dsRNA synthesized from a second region of *Si*VgR gene was chosen for RNAi experiments. The *Si*VgR region corresponding to 677 bp fragment (*Si*VgR -92 to 585 bp, non-overlapping with *Si*VgR-dsRNA1 sequence [24]) was amplified using the *Si*VgR clone with primer set VgRi-f4 (5'-TAATACGACTCACTATAGGGCGTGATC AGGTCAAAACGTATTTTCTTCATTT-3') and VgRi-r3 (5'-TAATACGACTCACTA TAGGGGCCACAGTCATCCTTTTTATCGCATACTAC-3') (Table 3.1) which included the T7 promoter region as well (underlined). The PCR reaction was seen as above and this PCR product was used as the template for synthesis dsRNA named *Si*VgR-dsRNA2. These target regions were chosen because BLAST searches showed no significant similarity to other genes in the GenBank and in the fire ant expressed sequence tag (EST) database from Fourmidable (http://fourmidable.unil.ch/), thereby decreasing the possibility of off-target effects.

The EGFP cDNA (Accession #U55763) in the PinPoint™ vector (Promega) generously provided by Dr. Craig Coates (TAMU), was used as a template to amplify a 611 bp product using the primer set T7-P164 (5'TAATACGACTCACTATA GGGACGTAAACGGCCACAAGTTCAGCGTGTC3') and P165-T7 (5'TAATACGAC TCACTATAGGGTCACGAACTCCAGCAGGACCATGTGATC3') (Table 3.1). This PCR product was used as the DNA template for synthesis of the control EGFP-dsRNA.

Purified PCR templates (~2 μg) were used to produce dsRNA using the MEGAscript RNAi kit (Ambion, Austin, TX, USA) according to the manufacturer's instructions. The synthesis reactions for dsRNA proceeded at 37 °C for 8 h. After synthesis, reactions were denatured at 75 °C for 5 min and allowed to cool down slowly in a 65 °C water bath that was turned off, and reactions were incubated until they achieved room temperature (approximately for 5 h). All dsRNA was column-purified and eluted in 200 μl elution buffer provided with the kit. The dsRNA was diluted to 1 μg/0.5 μl in elution buffer and then aliquoted 10 μl per tube and stored at -80°C until use.

dsRNA injection

"Red eye stage" queen pupae (white in color) were separated from colonies for microinjection. Intra-abdominal injections (~0.5μl) of elution buffer (negative control), EGFP-dsRNA (negative control), or *Si*VgR-dsRNA1 were with a FemtoJet® Micro-injector (Eppendorf) using a Femtotip® sterile injection capillary needle (Eppendorf). After injection, pupae were individually placed with a group of workers (~100) and brood (~10) and food, water, and honey (20 : 80 v/v) were provided. Approximately 200 pupae were injected with *Si*VgR-dsRNA1 and EGFP-dsRNA respectively, and about 150 pupae were injected with buffer only.

Virgin queens at days 0 (the day of virgin queen emergence), 5 and 10 were collected (Figure 3.2D), and the ovaries from four queens were dissected at each time point. Photographs were taken under the dissecting microscope (Olympus, Center

Valley, CA, USA). Each pair of ovaries was separated into two individual ovaries, one for immunofluorescence analysis and the other for total RNA preparation followed by semi-Q RT-PCR. These experiments were replicated independently three times.

To confirm the observed phenotype was caused by specific silencing of the *Si*VgR mRNA, a second RNAi experiment was performed. Intra-abdominal injections (~0.5µl) of *Si*VgR-dsRNA2 or EGFP-dsRNA were as before and virgin queens were collected at day 10 after eclosion and ovaries from four queens were dissected. These experiments were independently replicated three times and evaluation was by photography and semi-Q RT-PCR (Figure 3.4).

Semi-quantitative reverse transcription polymerase chain reaction (semi-Q RT-PCR)

To evaluate the effect of *Si*VgR RNAi, total RNA from ovaries of virgin queens of different ages (0,5,10 day post-eclosion) was extracted with Trizol® reagent (Invitrogen) following manufacturer's instructions. To prevent potential genomic DNA contamination, RNA samples were treated with DNase I (Invitrogen) and DNase was removed with Trizol® reagent. cDNA was synthesized with SuperScript™ III First-Strand Synthesis System (Invitrogen) using 0.5 µg total RNA and random hexamers. PCR amplification reactions contained 2 µl of the diluted cDNA (1:2), 0.4 µM of each primer, 400 µM of dNTPs, 1× reaction buffer and 0.4 µl *Taq* polymerase in a final volume of 20 µl. PCR amplification of *Si*VgR product (*Si*VgR ORF from 1473 to 1927) was performed using primer set *Si*VgR-2.3-3-2, 5'-ACAAGAGCCATTCTCTATGACG GTCTTTC-3', and *Si*VgR-2.3-4r, 5'-CTGACCTGAGAGCGGATCAGATATTATATTC

AC-3', and the conditions were 94 °C for 3 min; 28 cycles of 94 °C for 30 s, 60 °C for 1 min, and 72 °C for 1 min; 72 °C for 10 min. The 18S ribosomal RNA gene transcript (GenBank accession number: AY334566) was used as an endogenous control. 18S rDNA amplification was performed using primer set 18S-f2, 5'-AAAAGCTCGTAGTT GAATCTGTGTCGCAC-3', and 18S-r2, 5'-TAGCAGGCTAGAGTCTCGTTCGTTAT CG-3'. Conditions for the amplification of 18S were identical to those for *Si*VgR except that 24 cycles were used. The optimal number of amplification cycles was determined empirically through preliminary runs. The PCR products (4 µl) were analyzed on 1% agarose gels containing GelStar® nucleic acid stain (BioWhittaker Molecular Applications, Walkersville, MD, USA). Gels were photographed with the Foto/Analyst® Investigator system (Fotodyne). To determine transcript abundance, the intensity of the amplified PCR bands was determined using ImageJ. Relative mRNA expression levels from each of the samples were presented as the ratio of the band intensities of the *Si*VgR RT-PCR product over the corresponding 18S RT-PCR product. The expression ratio from the same RT-PCR sample was averaged from two gels to limit the bias. In the RNAi experiment with VgRdsRNA1 (Figure 3.3), three replicates for each injection treatment and time point (D0, D5, D10) were analyzed using one way ANOVA followed by a Tukey multiple comparison test. In the RNAi experiment with VgRdsRNA2 (Figure 3.4), the results were analyzed by t-test. Statistical analyses were performed using SPSS version 15.0 (Chicago, IL, USA) and graphs were obtained using Prism™ 5.0 (GraphPad, San Diego, CA, USA).

To eliminate the possibility of non-target effects of dsRNA, the RT-PCR analysis of the expression of a homologous LDLR (2.4 kb partial sequence previously cloned by Mei-er Chen in Dr. Pietrantonio's laboratory, and it belongs to the same LDLR superfamily with VgR) was performed. PCR amplification of this LDLR product (795 bp) was performed using primer set LRP 2.4-14 (5'-AATCGCAGTTCATCCTGGTAC C-3') and LRP 2.4-15 (5'-ATTCCGTCGCAGATTGTTACGC-3') with Day 10 cDNA set obtained from the RNAi experiment with VgRdsRNA1 including injection treatments with buffer, EGFP-dsRNA or *Si*VgR-dsRNA1, respectively. All conditions for amplification of LRP fragment and the analysis of results were identical to those for VgR RNAi experiment except that 32 cycles were used for amplification.

Evaluation of RNAi effect by immunofluorescence

To objectively quantify the RNAi phenotypic effect, we classified ovaries from RNAi virgin queens into three categories based on oocyte size and *Si*VgR immunofluorescence results as ovaries containing follicles with: (I) no developing oocytes and no *Si*VgR signal, (II) initial oocyte growth (size <20 μm) with *Si*VgR signal, and (III) at least one large vitellogenic oocyte (size >20 μm) with *Si*VgR signal. The size of the vitellogenic oocyte (20 μm in diameter) was estimated based on the observation of the fire ant follicles compared to *Drosophila* oocyte in a stage 7 egg chamber, which is the last pre-vitellogenic stage. Ovaries from virgin queens at 0, 5, and 10 days old in each treatment were analyzed and compared. Total ovary numbers analyzed for injection treatments with buffer, EGFP-dsRNA or *Si*VgR-dsRNA1 were as

follows: for day 0 (9:15:11), for day 5 (15: 20: 18) and for day 10 (31: 29: 27). Non-parametric statistical analyses were performed by SPSS using Kruskal-Wallis test by assigning scores to the oocyte categories to compare treatments within each time point.

CHAPTER IV

TOWARDS DISCOVERING ROLES OF THE SHORT NEUROPEPTIDE F RECEPTOR IN FIRE ANT QUEENS: IMMUNOFLUORESCENCE EXPRESSION ANALYSES*

Introduction

Information processing through neuronal networks in the central nervous system (CNS) is achieved through the release of neurotransmitters and/or neuromodulators from presynaptic neurons and the receiving of those signaling molecules by their respective receptors in the postsynaptic neurons. Additionally, the released neuromodulators can also diffuse and reach out to receptors located at nonsynaptic regions within the CNS. Neuropeptides are a complex group of signaling molecules which can act as neurotransmitters or neuromodulators within the CNS, and also as circulating neurohormones in the hemolymph. In this way, neuropeptides influence numerous physiological processes in invertebrates [90].

The short neuropeptide F (sNPF) peptide belongs to the neuropeptide F (NPF) family. The sNPF peptide has been identified or predicted from genomes of some insect species; however, only few of the respective G protein-coupled receptors (GPCRs) have

* Portions of this chapter are reprinted with permission from "Immunolocalization of the short neuropeptide F receptor in queen brains and ovaries of the red imported fire ant (*Solenopsis invicta* Buren)" by Lu, H.L., Pietrantonio, P.V. 2011. *BMC neuroscience.* 12: 57. © 2011 BioMed Central Publisher.

been identified or fully characterized [72,74,95,210-215]. The sNPF peptide is involved in food intake and body size regulation in *D. melanogaster* and is the upstream regulator that controls the expression of insulin-like peptides in the larvae brain of this species [58,92,93]. In the fire ant and Colorado potato beetle (*Leptinotarsa decemlineata*), sNPF signaling pathways also appear to be involved in feeding regulation [68,94]. Interestingly, the Colorado potato beetle sNPF peptide, Led-NPF-1, was shown to stimulate ovarian development in the locust, suggesting a potential gonadotropin role of the peptide [57,78]; however, it is not known if this is the peptide's direct effect. In addition, the sNPF peptides have also been identified in the hemolymph of adult *Drosophila*, suggesting a potential neuroendocrine role [100]. Recently, the *Drosophila* sNPF peptide precursor was detected in many neurons located in the central nervous system [90,91]. However, the exact targets of the sNPF peptide in the adult insect CNS or other tissues are still unknown.

The sNPF receptor belongs to the GPCR Rhodopsin family and is an orthologue of the vertebrate NPY type 2 (Y2) receptor [102]. Insect sNPF receptors have been characterized from *S. invicta*, *D. melanogaster*, and *A. gambiae* [68,102-104]. Ligand-receptor binding assays of sNPF receptors from *D. melanogaster* and *A. gambiae* revealed that sNPF peptides that contain nine or more amino acids are more potent than those with eight or fewer amino acids [100,103,104,216]. *An. gambiae* sNPF-1 inhibited the production of forskolin-stimulated cAMP by sNPF receptor transfected cells, suggesting that the receptor may act via Gi/o signal pathway [104].

The fire ant sNPF receptor transcript is present in both central nervous system and peripheral tissues as determined by RT-PCR [68]. The *Drosophila* sNPF receptor transcript is present in both central and peripheral nervous systems as detected by *in situ* hybridization analysis of embryos and the RT-PCR analysis of larvae and adults [102,103]. The *An. gambiae* sNPF receptor transcript is also broadly expressed in different body parts, but the receptor protein is not detectable in the ovaries by western blot [104]. Studies in these three insect species clearly showed that sNPF receptor transcripts are expressed in different tissues. However, because of the presence of the sNPF receptor in the nervous system, the RT-PCR results for peripheral tissues shown in fire ants and *Drosophila* are not definitive to establish receptor tissue localization because the RT-PCR amplification could potentially arise from neuronal contamination. In addition, transcript presence may not be associated with receptor protein expression. Therefore, localization of the sNPF receptor is an important step in defining the functional sites of the sNPF. Importantly, to our knowledge, there is currently no report on sNPF receptor protein localization in the adult brain or ovaries of any insect species, and the role of sNPF in ovarian development is still unknown. The only immunolocalization report is from *Drosophila* larvae brain in which the receptor protein is immunolocalized in a few median neurosecretory cells [58]. Therefore, this study focuses on the immunolocalization of a sNPF receptor in the fire ant queen; possible roles of sNPF signaling pathway are discussed.

Results

Expression of sNPF receptor in brain and ovaries of fire ant queens

To demonstrate the specificity of the antibodies developed against the fire ant sNPF receptor, we first performed western blot analyses of membrane preparations of queen brains, postpharyngeal glands, and ovaries (Figure 4.1). In the membrane proteins from brains of virgin queens, only one band was specifically recognized by the anti-sNPF receptor antibodies (Figure 4.1A, lane 1). The estimated molecular weight of the sNPF receptor band was ~46.2 kDa, corresponding to the predicted receptor molecular weight of 44.8 kDa. No signal was detected using antigen-preabsorbed antibodies, as expected (Figure 4.1A, lane 3). Similar receptor expression levels were observed in the brains of virgin and mated queens (Figure 4.1B, lanes 1 and 2). The postpharyngeal gland in the head of fire ant queen, which occupies a large portion of the head overlaying the brain, was used as a negative control tissue. No signal was detected using either anti-sNPF receptor antibodies (Figure 4.1A, lane 2) or antigen-preabsorbed antibodies (Figure 4.1A, lane 4), as expected. In the ovaries, three putative sNPF receptor bands (~46.2-, 51.1- and 55.3- kDa) were detected in the mated queen (Figure 4.1B, lane 4), but not in the ovaries of virgin queens (Figure 4.1B, lane 3). These different size bands in the mated queen ovaries are likely due to different post-translational modifications (including phosphorylation and N-glycosylation), sites for which were predicted in the fire ant sNPF receptor protein sequence [68].

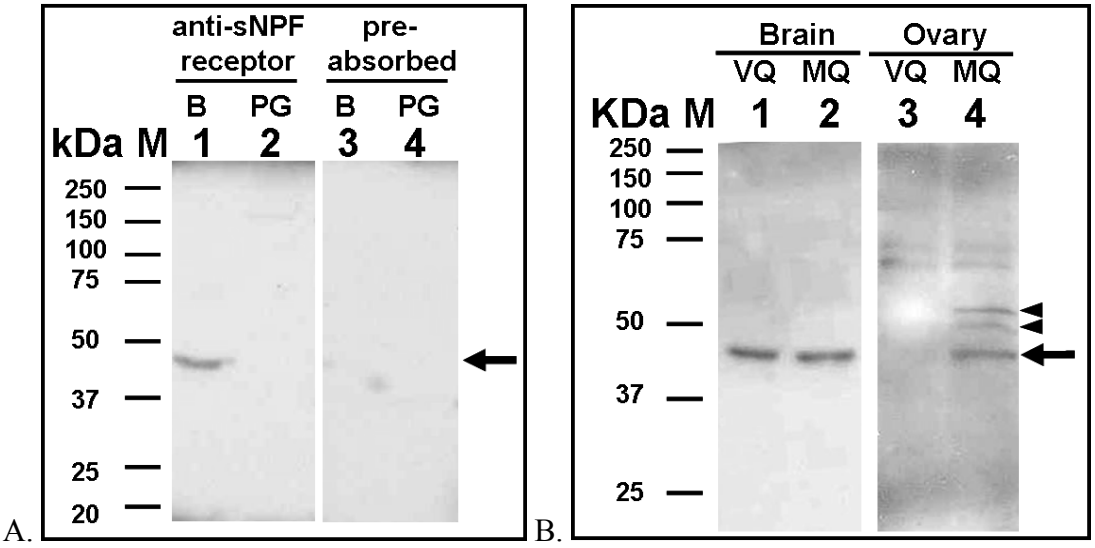

Figure 4.1. Western blot analyses of the sNPF receptor expression in membranes from queens. A: Membrane preparations (100 µg of protein per lane) of virgin queen brains and subesophageal ganglion (SEG) (lanes 1 and 3, labeled with B) and postpharyngeal glands (lanes 2 and 4, labeled with PG) were analyzed with anti-sNPF receptor antibodies (lanes 1 and 2) or with antigen-preabsorbed antibodies (lanes 3 and 4). Only one band (~46.2 kDa) was specifically recognized in the brain membranes by the anti-sNPF receptor antibodies (lane 1, arrow), and no signal was detected using antigen-preabsorbed antibodies, as was expected (lane 3). No signal was detected in the membrane proteins from the postpharyngeal glands (lanes 2 and 4). B: Membrane proteins from brains and SEG (100 µg, lane 1 and 2) and ovaries (50 µg, lanes 3 and 4) of virgin queens (VQ) and mated queens (MQ) were also analyzed with anti-sNPF receptor antibodies. Similar receptor bands (~46.2 kDa) were detected in the brains of virgin and mated queens (lanes 1 and 2, arrow). The same size band (arrow) was also detected in mated queen ovaries (lane 4), but not in those of virgin queens (lane 3). In addition, two putative receptor bands (~55.3- and 51.1-kDa, lane 4, arrowheads) were detected in the mated queen ovaries but not in those of virgin queen ovaries (lane 3). M, marker.

Distribution of the sNPF receptor in the fire ant queens

In the virgin queen brains and subesophageal ganglion (SEG), about 164 cells distributed in distinctive cell clusters (C1-C9 and C12) or present as individual cells (C10, C11) were immunolabeled with sNPF receptor antibodies. These cells or clusters were named as C1 to C12, clockwise, beginning from the mid-superior line in the anterior brain view and continuing to the posterior view of brain and the SEG. Clusters C1 to C6 (Figure 4.2A) are thus readily seen in the anterior view during brain whole mounts examination and C7 to C12, (Figure 4.2B) are seen in the posterior view while C5, C9 and C12 can also be seen dorsally (Figures 4.2C and 4.2D). Except clusters C1, C6 and C12 which are located centrally, other cells or clusters were bilaterally symmetrical. Most of these neurons are located in or near the important sensory neuropils. Strong sNPF receptor signals were observed in clusters C2, C3, and C12 (as shown in the figures on pages 85, 87 and 89). Three different sizes of cell bodies, small (~5 μm in diameter), intermediate (~5-10 μm in diameter), and large (~12 μm in diameter), were detected with sNPF receptor antibodies. The C6 cluster only contained small cells and C5 contained two large cells and one intermediate size cell, while C10-C12 cells were exclusively large. The rest of the immunostained cells in other clusters were of intermediate size. We did not observe different receptor distribution in the brains of virgin and mated queens. Therefore, results shown in these figures are only from virgin queens. All subsequent brain images show anterior or posterior brain views with the dorsal side up, unless otherwise mentioned.

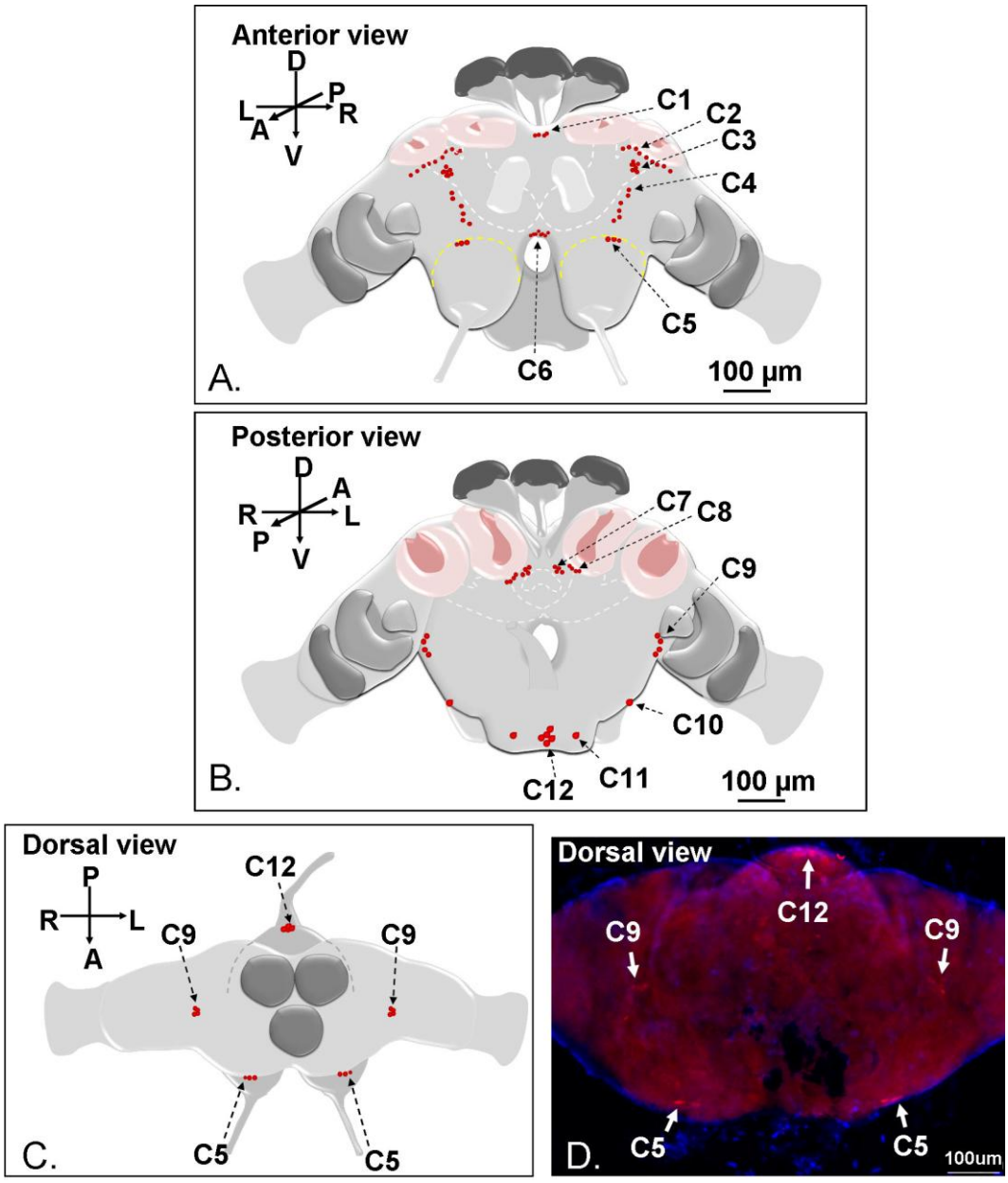

Figure 4.2. Summary of the localization of the sNPF receptor in the queen brain and SEG analyzed by immunofluorescence. A total of ~164 cells (shown as red dots) distributed in 12 cell clusters were identified. Six clusters of cells are seen in anterior view (A) and 6 clusters of cells are seen in posterior view (B) of the queen brain and SEG. Dorsal views of the brain (C and D) show the relative positions of clusters C5, C9 and C12 cells. D: Merged image of pictures obtained with red (receptor signal) and blue (DAPI labeled in nuclei) filters.

Clusters C1 to C6 were observed in the anterior side of the brain. Cluster C1 (cells ~5-10 μm) included three unpaired cells located in the superior medial protocerebrum (Figures 4.3B to 4.3D). These cells are reminiscent of the insulin-producing median neurosecretory cells in *Drosophila* larvae brains [58]. Cluster C2 (cells ~5-10 μm) is represented by two groups of ~25 cells each, which are located near the lateral calyces (lCa) of the mushroom bodies in the superior protocerebrum (Figures 4.3E to 4.3L). These cells surrounded the anterior half-side of the lateral pedunculi (lPed) that connects to the lCa (Figures 4.3E to 4.3H). Out of 25 cells in the cluster C2, seven cells that are located closer to the anterior surface of the lCa are likely to be the lateral neurosecretory cells (Figures 4.3E to 4.3L, arrowheads). The cluster C7 also is detected in the stacked confocal images (Figures 4.3F to 4.3G) obtained from the anterior view and will be described further in Figure 4.5 because it is more clearly visible from the posterior side of the brain. A monoclonal antibody against *Drosophila* choline acetyltransferase was used as a potential neuronal marker for cholinergic (acetylcholine-containing) neurons in the fire ant. Results showed that C2 cells labeled with sNPF receptor signals did not co-localize with these labeled by the monoclonal antibodies choline acetyltransferase, suggesting that they are not cholinergic neurons and may utilize neurotransmitters other than acetylcholine (Figures 4.3M to 4.3P). Other antibodies against *Drosophila* proteins (including anti-*Drosophila* fasciclin-II, anti-Repo, and anti-Alva antibodies obtained from DSHB [217,218]) also have been utilized to clarify the axon tracts or cell types; however, these antibodies failed to specifically recognize individual proteins in fire ant brains (data not shown).

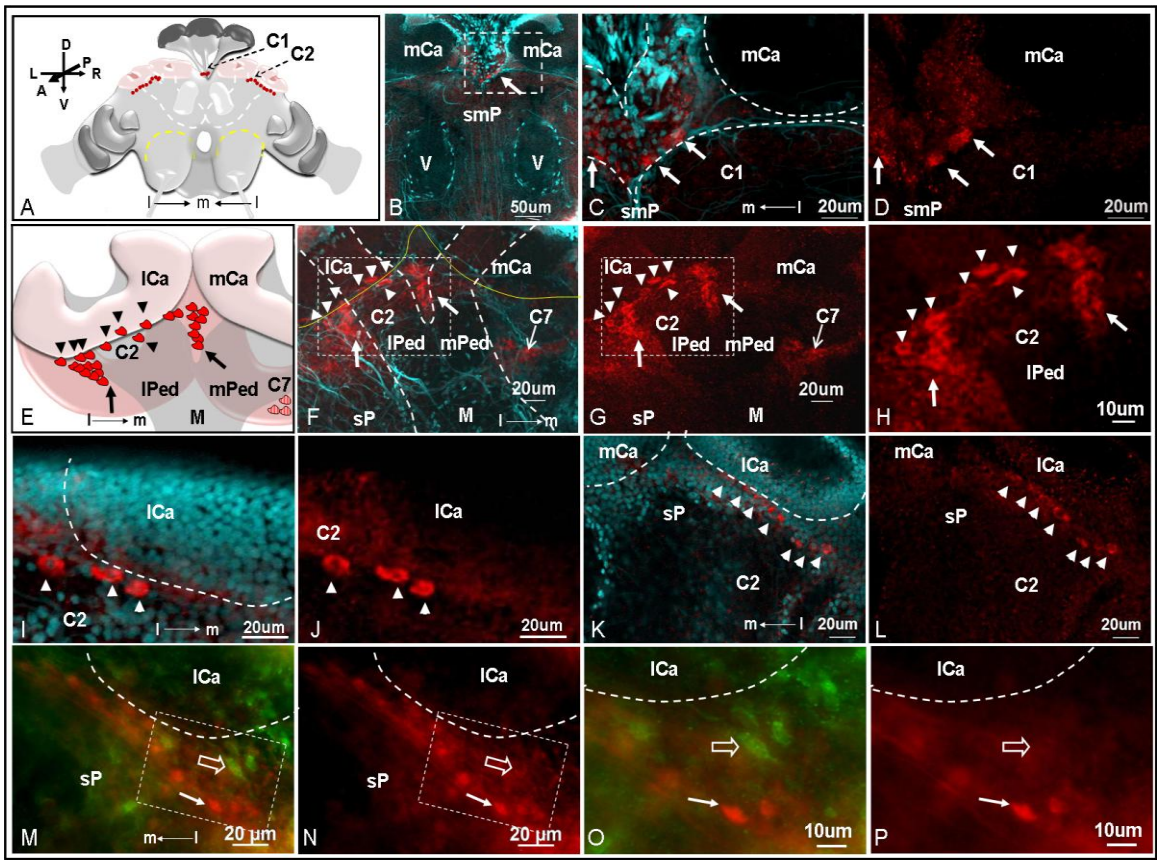

Figure 4.3. Distribution of C1 and C2 sNPF receptor immunolabeled clusters observed in the anterior queen brain. A: The relative position of cell clusters C1 and C2 in the anterior side of a queen brain are shown in a schematic. Confocal images obtained with single red channel for the receptor signal (D, G, H, J and L) or red merged with cyan (DAPI as a nuclear marker) (B, C, F, I and K) are shown. B: The cluster C1 (arrow) located in the superior medial protocerebrum (smP) is shown in a single confocal image. V: vertical lobe of the mushroom body. C and D: Higher magnification images of B show that three cells (arrows) are detected with sNPF receptor antibodies. mCa: median calyces. E-L: The cluster C2 (~25 cells) is located near the lateral calyces (lCa) of the mushroom bodies in the superior protocerebrum. The cluster C7 (F and G, thin arrow), seen faintly through the section (because it is close to the posterior side of the brain) will be described later in Figure 4.5. E: A schematic showing the relative position of C2 cells near the lCa. F and G: The cluster C2 cells surround the anterior half-side of the lateral pedunculi (lPed). H: Higher magnification image of G. I-L: Out of 25 cells in cluster C2, seven cells (arrowheads) located closer to the anterior surface of the lCa are likely lateral neurosecretory cells (arrowheads). Confocal stacked images thickness: 21.42 µm for C and D; 33.66 µm for F-H; 9.24 µm for K and L. M-P: Whole mount image obtained with Axioimager A1 microscope. M: Double labeling using antiserum against sNPF receptor (red, arrow) and monoclonal antibodies against *Drosophila* choline acetyltransferase (green, thick arrow) shows that the C2 cells were not co-localized with putative cholinergic neurons. N: Image of M with red filter. Higher magnification images of dashed rectangular areas in M and N are shown in O and P, respectively.

The cluster C3 cells are represented by two groups of eight cells each (cells ~5-10 μm), symmetrically located in the superior protocerebrum (Figures 4.4A and 4.4B). These cells are reminiscent of the Group 4 FMRFamide-like immunoreactive cells identified in the honey bee brain [219]. Two groups of six cells (cells ~5-10 μm) named cluster C4 were observed symmetrically located in the anterior protocerebrum, extending vertically between clusters C3 and C5 (Figures 4.4D and 4.4E). Cluster C5 contained three cells including two large cells and one intermediate cell, all horizontally aligned on the superior edge of antennal lobe (Figures 4.4E and 4.4F). Stronger signals were detected in the two larger cells. In the antennal lobe, anti-choline acetyltransferase antibodies (applied as potential markers for cholinergic neurons) recognized neurons located symmetrically in the outer-lateral and inferior areas (Figures 4.4G and 4.4H, arrowheads); however, no cell in the superior edge of the antenna lobe was immunolabeled with this antibody. Therefore, the C5 cells are different from the potential cholinergic neurons and may utilize neurotransmitters other than acetylcholine. The last cluster of cells observed from the anterior side of the brain was C6 which was composed of a group of ~30 small cells (cells ~5 μm). These cells were centrally located at the inferior medial protocerebrum right above the esophageal foramen, near the end of mushroom body median lobe (Figures 4.4I and 4.4J).

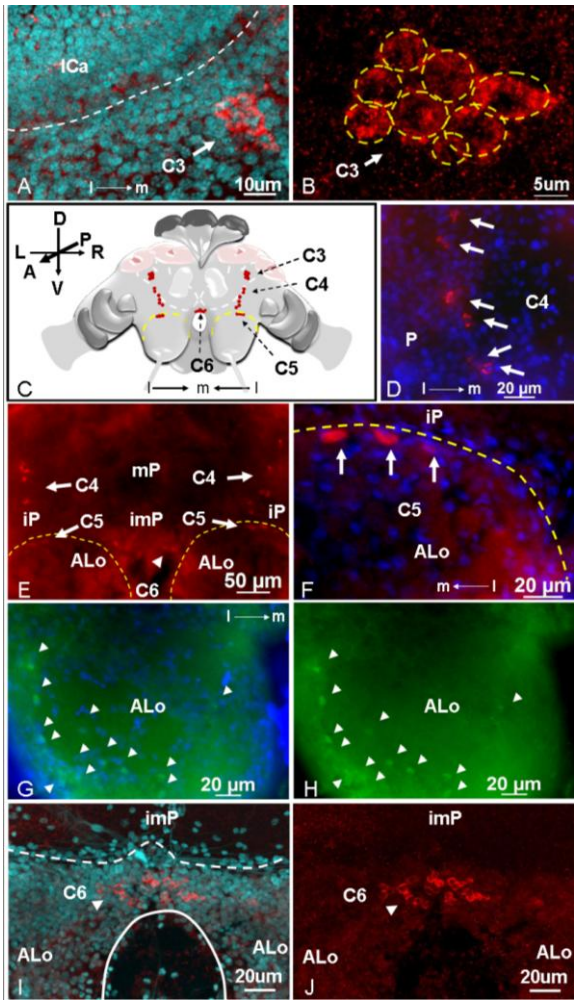

Figure 4.4. Distribution of C3 to C6 sNPF receptor immunolabeled clusters observed in the anterior queen brain. A: Merged confocal image of pictures obtained with red (receptor signal) and cyan (DAPI nuclear staining) channels. B: Image obtained with red channel. In A and B, the cluster C3 (arrow) includes a group of eight cells (B, dashed circles) located on each side of the superior protocerebrum (sP) near the lateral calyces (lCa). C: A schematic shows the relative position of clusters C3 to C6 in the brain. D-H: Whole mount images obtained with Axioimager A1 microscope (nuclei stained in blue with DAPI). D: The cluster C4 includes six cells distributed vertically in the protocerebrum (P). E: The anterior brain view shows the relative position of clusters C4 and C5 (arrows) on each side of the protocerebrum, and the cluster C6 (arrowhead) on the inferior medial protocerebrum (imP). mP, medial protocerebrum; iP, inferior protocerebrum (iP); ALo, antennal lobe. F: A higher magnification image of E showing that the cluster C5 contains three cells horizontally aligned on the superior edge of the antenna lobe which is nearby the inferior protocerebrum. G and H: Antiserum against *Drosophila* choline acetyltransferase showed that in the antennal lobes, the putative cholinergic neurons (green; arrowheads) are located symmetrically in the outer-lateral and inferior areas of both antennal lobes (left antennal lobe shown) and far from the sNPF receptor immunoreactive cluster C5. Confocal images I and J: I, merged of red and cyan channels and J, a red channel image. The cluster C6 includes a group of about 30 cells (arrowheads) located at the edge of the inferior medial protocerebrum above the esophageal foramen (I, white solid line). Thickness of stacked confocal images: 8.20 µm for A and B; 18 µm for I and J.

C7 to C12 were visible in the posterior side of the brain and SEG. Some cells belonging to the anterior cluster C2 that are located between lCa and medial calyces (mCa) were also visible from the posterior side of the brain (Figures 4.5B and 4.5C). Cluster C7 (cells ~5-10 μm) includes two groups of four cells symmetrically located above the central complex in the superior medial protocerebrum (Figure 4.5D), which is also named the pars intercerebralis in the honey bee. These cells could correspond to the cluster G4d octopamine-immunoreactive cells found in the honey bee brain [220]. Two groups of about 11 cells (cells ~5-10 μm) each, located in the superior protocerebrum right below the mCa of the mushroom bodies were named cluster C8 (Figures 4.5E and 4.5F). Cluster C9 includes two groups of 4 cells, each located in the inferior lateral protocerebrum; these are likely optical projection neurons (Figure 4.5G). In the posterior SEG, large cells (~12 μm) named C10, C11, and C12 were strongly immunolabeled with the anti-sNPF receptor antibodies (Figures 4.5H to 4.5L). C10 and C11 are represented each by a single cell on each side of the SEG, and cluster C12 is centrally located and includes 5 cells. The location of C10, C11, and C12 in the fire ant brain was very similar to the location of octopamine-immunoreactive neurons in the clusters G6b, LV (the lateral ventral), and VUM (the ventral unpaired median) in the honey bee brain, respectively [220].

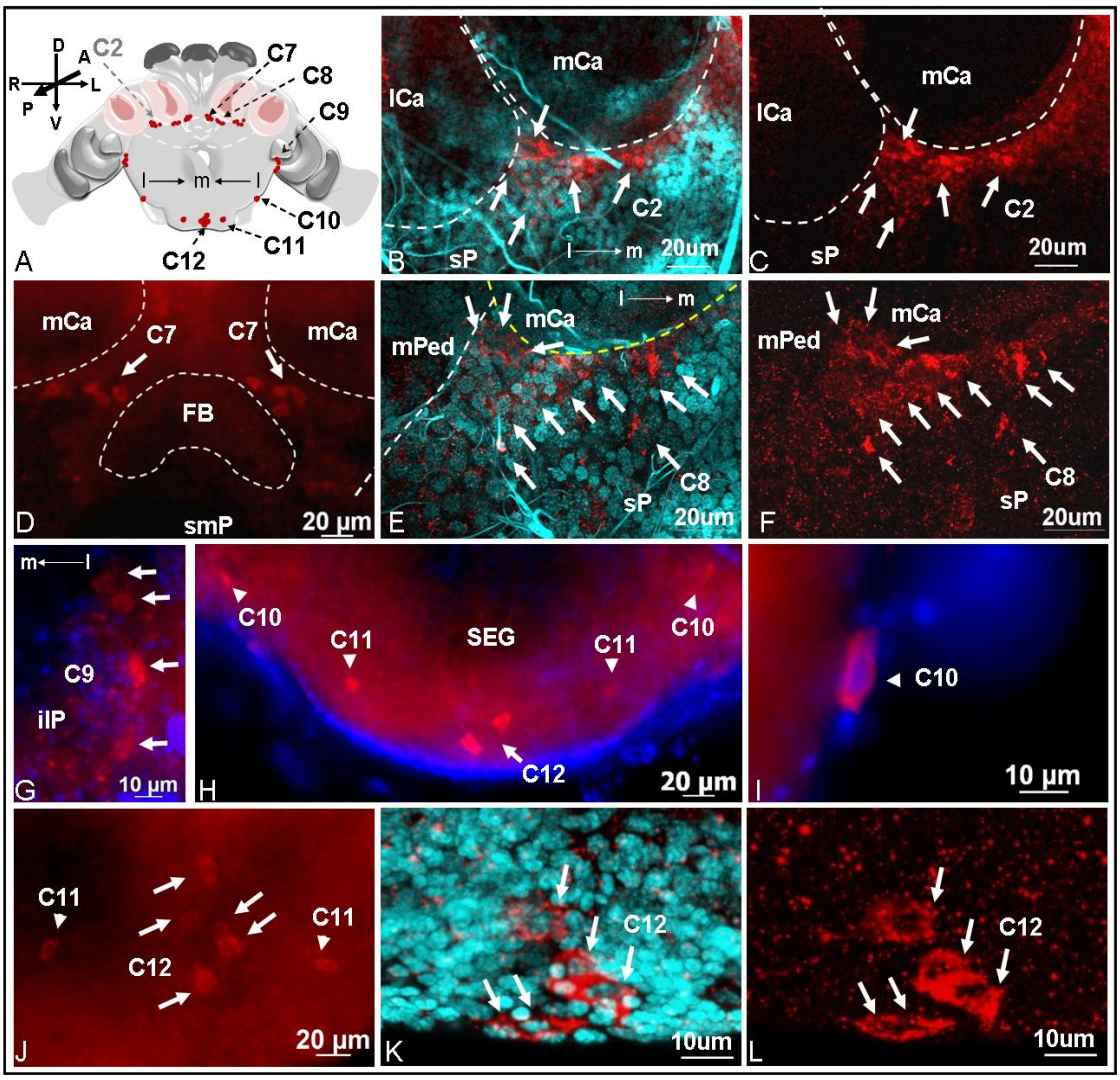

Figure 4.5. Distribution of C7 to C12 sNPF receptor immunolabeled clusters observed in the posterior queen brain and SEG. A: The brain schematic shows the relative position of cell clusters C7-C12. Confocal images obtained with red channel for receptor signal (C, F, and L) or merged images obtained with red and cyan (DAPI as nuclear stain) channels (B, E, and K). B and C: Some of the cells in the anterior cluster C2 (arrows) located between the medial calyces (mCa) and lateral calyces (lCa) of the mushroom body were also seen from the posterior part of the brain. D: The cluster C7 includes four cells (arrows) located above the fan-shaped body (FB) of the central complex in the superior medial protocerebrum (smP) (whole mount image obtained with Axioimager A1 microscope red filter). E and F: The cluster C8 is composed of ~11 cells and is located in the superior protocerebrum (sP) under the mCa. G-J: Whole mount image obtained with Axioimager A1 microscope (nuclei in blue). G: The cluster C9 is composed of four cells (arrows) located in the inferior lateral protocerebrum (ilP). H-J: C10 and C11 are represented by one cell each on each side of the subesophageal ganglion (SEG) (arrowheads) and C12 is composed of five cells (arrows) centrally located in the SEG. C10-C12 were strongly immunolabeled and their cells were larger in size (12 µm) and similar to the octopamine-immunoreactive cells in the honey bee. I: A C10 single cell is shown. J: C11 and C12 are clearly shown in a ventral view of SEG. K: A confocal stack of images shows C12 (five cells, arrows). Thickness of stacked confocal images: 12 µm for B and C; 14 µm for E and F; 19.6 µm K and L.

The localization of the sNPF receptors in the ovaries of fire ant queens

To discover the possible neurohormone role of the fire ant sNPF peptide(s), we performed immunolocalization of the sNPF receptor in the ovaries of virgin and mated queens. In the ovaries of both mated queens within a colony (Figure 4.6A, arrow) and newly mated queens 24 h after the mating flight (Figures 4.6B and 4.6C, arrows), sNPF receptor signals were detected in the posterior end of oocytes at the mid-oogenesis stage. Results clearly showed that the receptor signals localized in the oocyte membrane, and not in the membrane of follicle cells (Figure 4.6C). Such signal was not detected in late-oogenesis stage oocytes in which the nurse cells within the same follicle start to shrink in size (Figure 4.6A: F1 and F2, big stars).

Mated queens within the colony have more mature eggs in each ovariole than newly-mated queens; therefore, in the ovariole, the position of the oocytes with receptor signals depended upon the status of ovary development. The receptor signals were also detected in the early-oogenesis stage oocytes (oocyte size < 20 μm) of the mated (Figure 4.6D) and virgin queens (Figure 4.6E). Notice that the signal is present in the periphery of the oocytes. No signal was detected using either antigen-preabsorbed antibodies (Figures 4.6F and 4.6G) or a preimmune antiserum (Figure 4.6H), as expected. This result supports the direct function of the sNPF pathway in stimulating oocyte development previously discussed in addition to roles in the modulation of metabolism, growth, and feeding. To our knowledge, this is the first report that a GPCR may be associated with the oocyte pole.

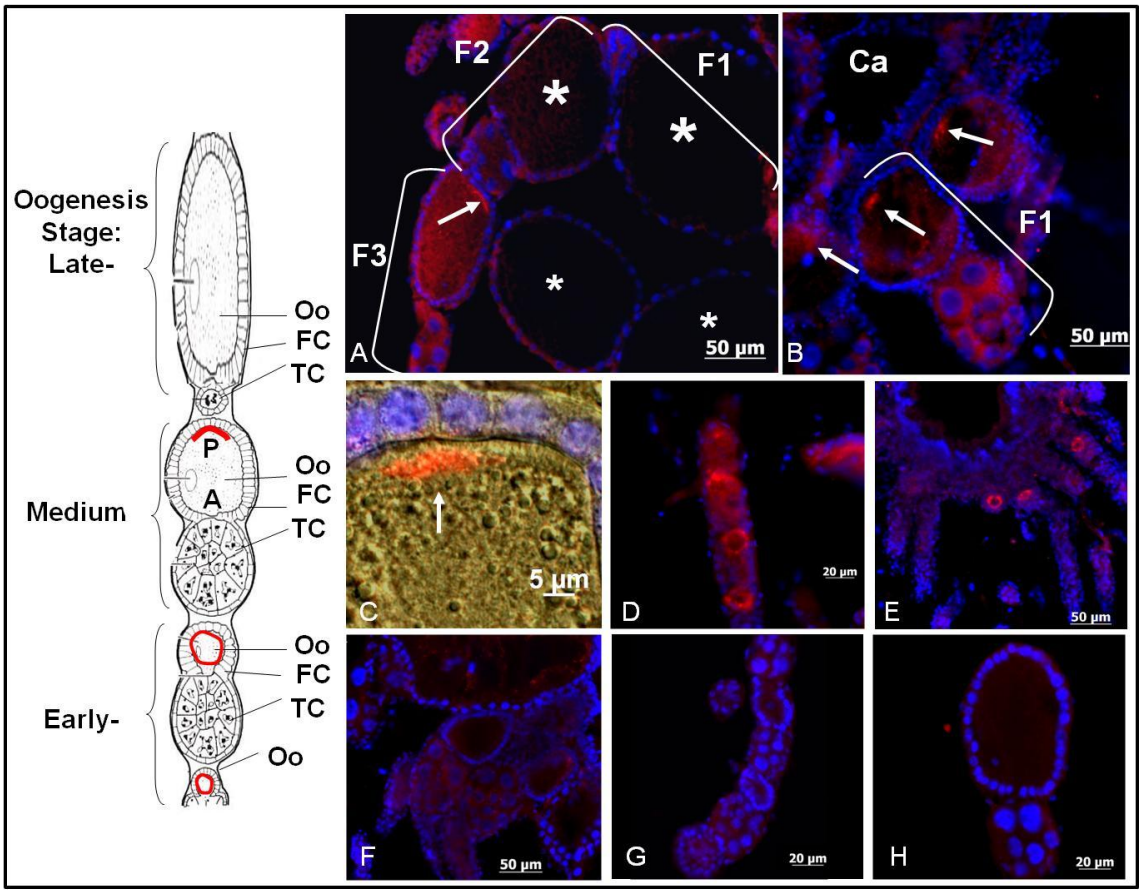

Figure 4.6. The immunolocalization analysis of the sNPF receptor in the ovaries of fire ant queens. A schematic (modified from [221]) on the left indicated receptor signals (red) were observed in mid- and early-oogenesis oocytes. A: In mated queens in a colony, the sNPF receptor signal was detected in the posterior end of oocytes at the mid-oogenesis stage (arrow, oocyte in follicle number three), but not in oocytes at the late-oogenesis stage in which nurse cells are reduced in size (big stars, oocytes in follicles number 1 and 2). F1, 2 and 3: follicle numbers counted from the calyx (Ca). B: In newly-mated queens (24 h after mating flight), the receptor signals were also detected in a similar stage of developing oocytes as in A. C: A higher magnification merged image of the oocyte posterior end from newly-mated queen ovaries shows a clearly receptor signal (red) in the oocyte membrane, but not in the follicle cells (nuclei in blue, DAPI label). D: The receptor signals were also detected in the early-oogenesis stage oocytes (oocyte size < 20 µm) of mated queens in a colony. E: In virgin queen ovaries, the receptor signals were detected in the early-oogenesis stage oocytes, similar to the mated queen oocytes shown in D. No signal was detected in negative controls using either antigen-preabsorbed antibodies (F and G) or a preimmune antiserum (H).

Discussion

Only one form of the sNPF receptor is present in the brains of fire ant queens

The only previous study in insects describing the molecular weight of the sNPF receptor was from *An. gambiae.* Two sNPF receptor bands of molecular weight 50- and 60- kDa were detected in western blot of heads of *An. gambiae* [104]. The authors indicated that the 60 kDa band might represent either another form of the receptor (because there are three predicted start codons in the receptor open reading frame), or alternatively, a post-translationally modified receptor. Unlike this mosquito, there was no evidence of an alternative start codon in the fire ant sNPF receptor cDNA [68]. Western blot analysis of the fire ant sNPF receptor (Figure 4.1) showed that only one band at 46.2 kDa was detected in membrane proteins preparations from brains of both virgin and mated queens, corresponding to the predicted receptor molecular weight of 44.8 kDa [68]. In addition, no differential receptor expression level between virgin and mated queen brains was found, suggesting that receptor abundance in the brains was similar in queens within a colony regardless their insemination status.

Expression of the sNPF receptor in diverse regions of queen brains

In the queen brain and SEG, we identified a total of ~164 sNPF receptor immunolabeled cells, distributed individually or in clusters. Most of these cells localized in important sensory neuropils such as the mushroom bodies, the antennal lobes, and the subesophageal ganglia. These results suggest that the sNPF receptor is

involved in the widespread modulation of neuronal activity and subsequently may affect various physiological processes and behavioral responses in fire ants. The pattern of the sNPF receptor immunolabeled cells in diverse regions of queen brains coincided with the sNPF peptide immunolocalization in the brain of *Drosophila*. In *Drosophila*, *in situ* hybridization and immunohistochemistry analyses have demonstrated that sNPF transcript or peptide precursor are present in a significant number of neurons in the brain beyond any other neuropeptide found in insects studied so far. In both larvae and adults of *Drosophila*, sNPF peptide precursor was detected in the mushroom bodies, the SEG, and some neurosecretory cells in each hemisphere; in addition, this precursor was also present in the fan-shaped body (a substructure of the central complex), the antennal lobe, a few clock neurons, the optical lobes, the tritocerebral neuropil of the adult brain, as well as in the thoracic-abdominal ganglia of the larvae, and some endocrine cells in the larval midgut [91,92,98,99,222-226]. It was suggested that sNPFs are likely to signal locally (no volume transmission) as co-transmitters because, first, these sNPFnergic neurons do not co-express a transcription factor (DIMM) that is present in most of the neurosecretory cells that release amidated peptides, and secondly, these sNPF neurons co-localized with other neurotransmitters [91,227]. Only a few neurons that co-express both sNPF and DIMM in adult flies are likely to act on target cells located at a distance (volume transmission) [90]. There is a paucity of information on the localization of both sNPF and its receptor in other insect orders. Only recently the expression of the sNPF transcript was analyzed in the honey bee worker brain, and found bilaterally only in a few lateral neurosecretory cells (4-6 pairs). This expression pattern contrasts with the

wide distribution of the sNPF in neurons of fruit flies described above. Further, the sNPF peptide has not yet been isolated from fire ants and there is no available sNPF peptide sequence identified from the recently released fire ant draft genome [3]. The lack of a cognate peptide has hampered our attempts to prove sNPF receptor functionality in a heterologous expression system. We have identified sNPF receptor immunolabeled cells distributed in many important sensory neuropils in queen brains suggesting that sNPF peptide function may be more complex and perhaps integrative in fire ant queen brains. However, because our immunolabeling did not stain the terminals of the sNPF receptor-labeled neurons we cannot conclude on the nature of these potential networks.

sNPF receptor localization in the protocerebrum of the fire ant brains

In the brain of fire ant queens, we detected three unpaired sNPF receptor immunolabeled cells (cluster C1) located in the superior midline protocerebrum (Figures 4.3B to 4.3D), where the median neurosecretory cells are located in the honey bee brain [228]. In *Drosophila* larvae, the sNPF receptor was also localized in some of the seven insulin-producing median neurosecretory cells and was verified to act as an upstream regulator of the insulin signaling pathway [58]. In *A. aegypti*, however, insulin-like peptides were detected in two clusters of lateral neurosecretory cells in the dorsal protocerebrum, but not in median neurosecretory cells [229]. It would be interesting to know if the regulatory role of the sNPF signaling pathway on insulin production in different insects is conserved and thus, to investigate by immunohistochemistry if cells in cluster C1 also produce insulin in fire ant queens.

The majority of the sNPF receptor immunolocalized cells were near the mushroom body in fire ant queens. In insects, the mushroom body is the main center for sensory processing, learning and memory, and the integration of other complex behaviors [230]. In Hymenoptera, especially ants, the mushroom bodies are particularly developed and may occupy ~40% of the brain volume [231,232]. The insect brain structure most similar to the fire ant brain is from the honey bee. Both insects have large mushroom bodies composed of two calyces (lateral and medial calyces), each with a peduncle which gives rise to median and vertical lobes. The calyx is a place where olfactory and visual sensory signals originate from the primary sensory neuropils (i.e. the antennal and optic lobes) connected to the intrinsic neurons named the Kenyon cells. The Kenyon cells consecutively integrate and pass on information within the brain [230]. We have identified several sNPF receptor immunolabeled cells near the mushroom body calyx (clusters C2, C3 and C8) and near the (output) end of the mushroom body median lobe (cluster C6) in the queen brains. Based on the comparison of the location of cluster C2 cells with the position of lateral neurosecretory cells in the brains of honey bees [228], it is likely that some of the C2 cells might belong to lateral neurosecretory cells (Figures 4.3E to 4.3L, arrowheads). Other neurons in clusters C2 (Figures 4.3E to 4.3H, arrows) and C8 (Figures 4.5E and 4.5F) were similar in location to the Clawed II Kenyon cells found in the honey bee which are perikarya lying outside the calyx [233,234]. This suggests the hypothesis that the sNPF peptide regulates Kenyon cells functions in fire ant queens.

Cells in the cluster C3 (Figures 4.4A to 4.4B) between the medium and lateral calyces of the mushroom bodies are tightly grouped together, reminiscent in location and aspect to the group 4 FMRFamide-like immunoreactive cells identified in the honey bee brain which have their fibers projected to the lateral protocerebrum [219], but the function of FMRFamides in this area of the bee brain is still unknown.

We can only speculate about the potential brain location of ligand (sNPF) producing neurons that may project towards the sNPF receptor identified neurons. According to the previous results obtained from *Drosophila*, none of the local and projection interneurons of the antennal lobe expressed sNPF peptide [91]. Therefore, in fire ants the sNPFnergic neurons that targeted these cluster C2, C3 and C8 near the mushroom bodies might not originate from the antennal lobe. One of the candidate sNPFnergic neurons that projected into this area is the clock neuron (a subset of LNds and s-LNvs) identified in *Drosophila* [223]. It is possible to hypothesize that in fire ant queens, the clusters C2, C3, and C8 may be involved in circadian activities controlled by the clock neurons.

The cluster C6 located in the inferior medial protocerebrum is very close to the end of mushroom body median lobe (Figures 4.4I and 4.4J). These C6 cells may represent the targets of axon outputs of sNPFnergic Kenyon cells in the queen brains. In *Drosophila*, the sNPF peptides are the only neuroactive substance that has been clearly identified in large subpopulations of intrinsic Kenyon cells, and strong sNPF signals are detected in the end (output) of median and vertical lobes in the mushroom bodies [91,224]. However, in fire ant brains, we did not detect other receptor signals near the

end of the vertical lobe. This might be due to the largely variant number of Kenyon cells between insect species. For example, in the honey bee each mushroom body has ~170,000 Kenyon cells [235], much more than in *Drosophila* (~2,500 Kenyon cells) [236]. As a result, the expression of sNPF peptide in the Kenyon cells may also be different between insect orders. In *Drosophila* CNS, besides the mushroom bodies, the sNPF peptides were also localized in the SEG [91]. Thus, it is possible that the C6 cells in the fire ant are targeted by the sNPFnergic neurons from both mushroom bodies and SEG.

The central complex has been proposed as a higher center for locomotor control that regulates several aspects of walking and flying behaviors [237]. The cluster C7 localized above the fan-shaped body of the central complex (Figure 4.5D) is similar to the cluster G4d octopaminergic neurons in the honey bee brain [220]. Octopamine treated honey bees exhibited increased flying and reduced walking behaviors [238]. In *Drosophila*, octopamine is also associated with locomotor behaviors [239]. Interestingly, a recent study showed that *Drosophila* sNPF peptides expressed in the fan-shaped body of the central complex was associated to the fine tuning of locomotor activity [99]. Female flies with reduced sNPF peptide expression in the fan-shaped body increased their walking distance and their mean walking speed. Thus, the relationship between the sNPF receptor and locomotor activity (which is regulated by sNPF and octopamine in *Drosophila* or other insects) deserves further investigation in fire ants. If these were related, it will contribute to the understanding of worker foraging behavior, expansion of established colonies and in regulation of queen mating flights. Knowledge of these

mechanisms that contribute to colony growth and dispersal may open the possibility of controlling this invasive pest.

In the optic lobs, we detected sNPF receptor signals in four cell bodies (cluster C9) in the inferior lateral protocerebrum in the fire ant (Figure 4.5G). No other sNPF receptor signal above background staining was obtained in the optical lobe. In the desert ant, *Cataglyphis albicans*, the optical projection neurons located in the similar inferior lateral protocerebrum region have their dendrites extended to the optic lobes, and their axons projected into the mushroom bodies [240]. Therefore, in fire ants, cluster C9 cells may function as the optical projection neurons that gather optical information signaling. In the brain of adult flies, both the sNPF transcripts and peptides are localized in the optic lobes [91,92].

sNPF receptor localization in the antennal lobe of the fire ant brains

The antennal lobe is the primary olfactory neuropil. In the antennal lobe, the axons of olfactory receptor neurons from the antennal and the maxillary palps invade into the glomeruli where they synapse with dendrites from interneurons. In queen brains, the cluster C5 cells were horizontally aligned on the superior edge of the antennal lobe. There are two large cells and one intermediate size cell in the cluster C5 (Figure 4.4F). It is possible that these C5 cells act in functionally different ways, and belong to different types of interneurons. In insects, three types of interneurons have been distinguished in the antennal lobe: 1) local interneurons that locally interconnect with glomeruli; 2) projection neurons that innervate single or several glomeruli and project axons through antennocerebral tracts into the protocerebrum; 3) centrifugal neurons that

are a diverse grouping of neurons with axons projected into the antennal lobe and dendrites reaching to other areas of the nervous system [241]. Cells in the cluster C5 could be local and/or projection interneurons. It is speculation; however, this localization of the sNPF receptor in queens is in a pattern matching the sNPF peptide distribution in *Drosophila*. In *Drosophila*, the sNPF precursor was immunolabeled in axons of the olfactory receptor neurons (ORNs) projecting from the antenna and the maxillary palps which terminate in 13 glomeruli, with the glomerulus DL3 being particularly strongly stained [225]. In the fly's anterior dorsal antennal lobes, the projection neurons have their dendrites invade into a subset of glomeruli, including sNPF-labeled glomeruli, and have their axons projected through the inner antennocerebral tract (iACT) to the mushroom body and the lateral horn of the protocerebrum [242]. In the fire ant queens, if sNPF peptide(s) were also expressed in antennal ORNs, it is possible that the chemosensory and olfactory information transmitted through these peptides might be delivered to the projection interneurons in the cluster C5 and be further transmitted for integration to the higher brain centers. In addition, the putative cholinergic neurons were only localized in the lateral and inferior antennal lobes of the fire ant queen (Figures 4.4G to 4.4H); therefore, C5 cells are likely to utilize neurotransmitters other than acetylcholine.

sNPF receptor localization in the SEG of the fire ant brains

The SEG is the primary center for controlling insect mouth parts. Important modulatory neurons, such as ventral unpaired median (VUM) neurons have their cell

bodies in the SEG [243]. In the honey bee, octopaminergic VUM cells innervate the neuropils of the SEG, the mandibulla, the antennal lobes, the mushroom bodies, and some other parts of the brain [244]. The sNPF receptor immunolabeled cells C10 and C11, and the cluster C12 in the SEG of the fire ant brain (Figures 4.5H to 4.5L) were comparable to the octopaminergic neurons G6b, LV, and VUM in the SEG of the honey bee brain, respectively [220]. In honey bee workers, octopamine modulates diverse behaviors including locomotor activity, dance, division of labor, foraging, hygiene, defense, and nestmate recognition [238,245-251]. In fire ant workers, it was also found that octopamine levels in the brain affect nestmate recognition acuity [252]. However, the function of octopamine in the queen brain of both insects is still unknown. It will be of interest to test if these sNPF receptor immunolabeled cells in the fire ant SEG are involved in regulation of feeding and/or are octopaminergic neurons.

The expression of the sNPF receptor in fire ant ovaries

Receptors that influence ovarian growth are critical for egg-laying species, as they play a role in oocyte development regulation. Recently some GPCRs involved in meiosis arrest and fertility in vertebrate oocytes were identified [253-256]; yet to our knowledge, no GPCR function has been found associated to the polarity of oocytes in insects. Only few receptors from other receptor superfamilies are involved in the follicle polarity, such as follicle cell-bound EGF receptor involved in the transduction of oocyte anterior/posterior polarity, and Frizzled, involved in the planar polarity signaling [257,258]. In fire ants, the sNPF receptor signal detected in the posterior end of the

oocytes during mid-oogenesis from both mated queens (Figure 4.6A) and newly-mated queens (Figures 4.6B and 4.6C) opens the possibility that the sNPF receptor may be involved in oocyte polarity. To our knowledge, this is the first report of GPCR that has been found associated with an oocyte pole in insects. We also detected the sNPF receptor signals in the periphery of early-oogenesis stage oocytes from both mated and virgin queens, most likely in the plasma membrane, indicating the sNPF receptor may participate in the regulation of initial oocyte growth (Figures 4.6D and 4.6E). However, we did not detect putative receptor bands in membrane preparations from virgin queen ovaries by western blot (Figure 4.1B, lane 3). This might be due to a limited number of developing oocytes with corresponding low receptor expression levels in the virgin queens which prevented receptor protein detection. In the past we had a similar experience with respect to the lack of detection in western blots from virgin queen ovaries with the antibody against the vitellogenin receptor which labeled the ovaries in immunohistochemistry but failed to detect the protein in western blots (Chapter II, Figures 2.3 and 2.4). In addition, because two weak bands were also detected by western blot in the 60-75 kDa range in both virgin and mated queen ovaries (Figure 1B, lanes 3, 4), we are not ruling out the possibility that the fluorescence signals in the early-oogenesis stage oocytes could represent non-specific antibody binding, to those two higher size bands. If this is the case, then only the signal in the oocyte posterior end in the mated queen would be specific sNPF receptor signal.

Different results on sNPF receptor expression were obtained in the mosquito. In *An. gambiae* sNPF receptor immunoblot analysis showed that the receptor protein was

not detectable in the ovaries of non-blood fed females [104]. Based on our results, we concluded that this might be due to the fact that the females were not blood fed and therefore the ovaries were underdeveloped. In *Drosophila*, sNPF receptor transcripts were detected in the ovaries of females of unknown age, and the expression level was higher than in the head and body parts [102]. However, in the Flyatlas transcriptome data bank which utilized mRNA from 7 day-old adult fly (http://www.flyatlas.org/), the sNPF receptor mRNA level in the ovaries was very low when compared to whole flies [259]. All together, it seems that the level of sNPF receptor protein abundance in the ovaries depends upon the level of the ovary development, mated status, the age of the insects and is perhaps different between solitary and social insects.

In summary, we presented the first comprehensive histochemical analysis of the distribution of the sNPF receptor in the adult insect brain. The sNPF receptor signals present in several neuropils in fire ant queen brain and SEG might link the receptor signaling pathway to behaviors such as foraging, learning, and food consumption. The localization of the sNPF receptor will allow testing new hypothesis about the potential regulatory role of this pathway in insulin-producing cells or octopaminergic cells. In addition, the localization of the sNPF receptor in the developing oocyte points to a direct, potentially novel effect of sNPF on the insect ovary. Still, several questions remain to be answered to fully understand the role of sNPF pathway in neuron circuits, in the endocrine control of reproduction, and in other, yet unknown functions. More interestingly, the localization of the sNPF receptor in the developing oocyte points to a direct, potentially novel effect of sNPF on the ovary in insects.

Materials and Methods

Insects

S. invicta were reared as described in Chapter II.

Anti-short neuropeptide F (sNPF) receptor antibodies

To determine the antigenic regions of fire ant sNPF receptor (GenBank: DQ026281) for anti-peptide antibody production, the hydrophilicity and antigenicity profiles of sNPF receptor amino acid sequence were analyzed using DNASTAR and ExPAsy software. Additionally, the N-glycosylation and phosphorylation sites were avoided in the selection for the antigenic region. Due to a very short N-terminal sequence present in the receptor before the first transmembrane region (total 23 residues), it is difficult to design an antibody against receptor N-terminus. Therefore, only one amino acid region located toward the receptor C-terminus encompassing residues 331 to 347 of sequence "CRGDKIDNGNNTMQETL" was selected for antibody production. Polyclonal anti-peptide antibodies were developed in New Zealand female rabbits by Pacific Immunology (CA, USA) and affinity purified. The synthetic peptide was conjugated with keyhole limpet hemocyanin (KLH) for antibody production. After purification, the specificity of the antibodies was verified by ELISA (tested by Pacific Immunology, CA) and western blot.

Membrane preparations and western blot analysis

Membranes for western blot analyses were prepared as described previously with minor modifications [192]. Briefly, brains (with SEG) and the postpharyngeal glands from about 200 virgin queen heads were dissected in phosphate buffered saline (PBS). In addition, brains (with SEG) and ovaries from about 200 virgin queens and 200 mated queens were also dissected in PBS. These tissues were homogenized in cold buffer A (25 mM Tris⁄HCl, pH 7.5, 1 mM EDTA, 1 mM EGTA, 1 mM dithiothreitol) with Complete Protease Inhibitor Cocktail® (ROCHE) and centrifuged at 10,000 g for 5 min. The supernatants were collected and centrifuged at 100,000 g (SW28 rotor, Beckman LE80K) for 1 h at 4 °C. After ultracentrifugation, the pellets were re-suspended in 200 µl cold buffer B (50 mM Tris ⁄ HCl, pH 7.5, 2 mM $CaCl_2$) with protease inhibitors and stored at -80 °C.

For western blot analysis, 40 µl membrane proteins (100 µg) with 10 µl 5X SDS gel-loading buffer (250mM Tris-Cl, 0.5 M dithiothreitol, 10% SDS, 0.5% bromophenol blue, 50% glycerol) were heated at 95°C for 5 minutes. Samples were separated on SDS-PAGE (10% gel, Bio-Rad) and then transferred to PVDF membranes (Millipore). Membranes were blocked 1h at room temperature in blocking solution (5% non-fat milk in TBST, 10 mM Tris base, 140 mM NaCl, 0.1% Tween-20, pH 7.4) and incubated overnight with rabbit anti-sNPF receptor antibodies (1:500) in blocking solution at 4 °C. Pre-absorbed anti-sNPF receptor antibodies and pre-immune serum were used as negative controls. Pre-absorbed antibodies were produced by incubating anti-sNPF receptor antibodies (4 µg in 10 ml blocking solution) with peptide antigen (500 µg)

overnight at 4 °C the day previous to their use. After 3 X 10 min washes with TBST, the membrane was then incubated with a of HRP-conjugated goat anti-rabbit IgG antibody (1:40,000) for 1 h. After the same wash steps, the membrane was visualized by the Enhanced Chemiluminescence System™ (Pierce) on film (Kodak).

Brain and SEG whole mount immunofluorescence analysis

Whole mount immunofluorescence was performed as previously described with modifications [260]. Brains of both virgin and mated queens were dissected in PBS and transferred into freshly prepared 4% paraformaldehyde in PBS for 2 h at 4 °C for fixation. All subsequent steps were carried out with slow agitation. The fixatives were removed by 3 x 10 min washes with 70% ethanol, on ice. After rinsed in PBS-0.1% Tween (PBST) 2 x 5 min at room temperature, tissues were incubated in 12 μg/ml protease K (Sigma-Aldrich) in PBS for 10 min at room temperature. Tissues were then rinsed in PBST 2 x 5 min and then blocked in PBST with 10% normal goat serum (NGS) (Sigma-Aldrich) for 24 h at 4 °C. After blocking, tissues were incubated with primary antibody for 48 h at 4 °C. The primary antibodies diluted in PBST-2% NGS included the anti-sNPF receptor antibodies (diluted 1:500) and the anti-*Drosophila* choline acetyltransferase monoclonal antibodies (diluted 1:5; ChAT4B1 obtained from Developmental Studies Hybridoma Bank, University of Iowa). For negative controls, anti-sNPF receptor antibodies (1:100 dilution) pre-absorbed with the antigen peptide, and pre-immune serum from rabbit (1:1000 dilution) were used as the primary antibody. Anti-sNPF receptor antibodies (4 μg in 1 ml PBST-2% NGS) were pre-absorbed with

500 μg of antigen peptide overnight at 4 °C incubation one day before used. Commercial monoclonal antibodies (Developmental Studies Hybridoma Bank, University of Iowa, Department of Biology, Iowa City, IA) against other *Drosophila* proteins Dachshund (Mabdac1-1-s), Elav (Elav-9F8A9**),** Repo (8D12 anti-Repo**)**, and fasciclin II (1D4 anti-Fasciclin II**)** were also tested as a primary antibody simultaneously, however, none of the results showed specific immunolabeling of these proteins in fire ant brain. After incubated with primary antibodies, tissues were washed 4 x 20 min in PBST and incubated in a 1:200 dilution of Alexa Fluor 546 goat anti-rabbit IgG or Alexa Fluor 488 goat anti-mouse IgG (Invitrogen) overnight at 4 °C. Tissues were then washed 6 x 30 min in PBST and mounted on slides with Vectashield™-DAPI (Vector, Burlingame, CA, USA) for nuclear staining. Results were observed under a Carl Zeiss Axioimager A1 microscope. Images were obtained with an AxioCam MRc color camera (Carl Zeiss) and analyzed with axiovision program (Carl Zeiss). Confocal images were taken using FV1000 Confocal microscope (Olympus) in the Microscopy and Imaging Center (TAMU) and images were analyzed with the Olympus FV10-ASW program (Olympus). Naming of the brain structures was done following previous publications on honey bee [234]. Orientation of neuronal structures was given according to the body axis.

Ovary immunofluorescence analysis

Ovaries of virgin and mated queens within colonies, and ovaries of field-collected newly-mated queens (24 h after the mating flight) were dissected in PBS and

fixed in 4% paraformaldehyde for 4 h at 4 °C. The procedures of ovary paraffin wax blocks and de-waxing and rehydration of ovary sections (12 μm) were as previously described [192]. Sections were blocked with 5% goat serum in PBST (0.05% Triton X-100) 1 h at room temperature and then incubated overnight in a humid chamber at 4 °C with the anti-sNPF receptor antibodies (1:1000 dilutions) in the blocking solution. Negative control sections were also incubated overnight with the pre-absorbed anti-sNPF receptor antibodies (1:1000 dilution) or the pre-immune sera (1:500 dilution) in blocking solutions. The preabsorbed anti-sNPF receptor antibodies were produced as described above.

CHAPTER V

INSECT INSULIN RECEPTORS: INSIGHTS FROM SEQUENCE AND CASTE EXPRESSION ANALYSES OF TWO CLONED HYMENOPTERAN INSULIN RECEPTOR CDNAS FROM THE FIRE ANT

Introduction

In invertebrates, there is a single insulin pathway which is ancestral to the two mammalian insulin and insulin-like growth factor (IGF) signaling (IIS) pathways and their functions are conserved between both animal groups [261-263]. In mammals the two pathways coordinate many physiological processes including growth, reproduction, blood glucose metabolism, stress resistance, and aging [261-263]. Insulin peptide functions primarily in glucose homeostasis and IGFs mainly regulate growth. Phylogenetic analyses of mammalian insulin receptors indicate that gene duplication occurred twice in mammals, resulting in three receptor genes that evolved from the invertebrate ancestral receptor gene [261]. Mammalian receptors belong to the class II Receptor Tyrosine Kinase (RTK) family, and are: the insulin receptor, the IGF-1 receptor, and an orphan receptor named insulin receptor-related receptor. Each of these receptors is synthesized as a single precursor that undergoes proteolytic cleavage to yield two subunits, α and β. The functional receptor is composed of two units, each unit composed of a transmembrane ß-subunit bound to an extracellular α subunit. The tetrameric receptor can be present as a hybrid with α and β subunits belonging to the

insulin receptor and/or the IGF-1 receptor. Five types of functional receptors were found to regulate downstream signaling pathways [263].

In insects, the IIS pathway has been shown to be the key integrative pathway regulating insect reproduction, development, metabolism and aging [105,264,265]. Most of these functional roles are supported by studies from fruit flies (please see Chapter I). However, social insects (the honey bee) evolved different mechanisms than solitary insects like *Drosophila*. First, the direct relationship between feeding and activation of the IIS pathway resulting in increased body size observed in *Drosophila* is more complex in bees. In bees, the IIS pathway plays a key role in caste differentiation (queen vs. worker) [137,266,267]. Caste differentiation is nutritionally based and additionally regulated by the TOR pathway; different castes not only differ in size (as expected from IIS regulation in dipterans) but also in development of specific body structures [268]. Manipulation of diet in early developmental stages resulted in caste-specific differential expression of genes in the IIS pathway, particularly for the *Am*ILP-1 and *Am*InR-2 [267]. In the 3rd instar larvae, a peak of receptor transcript in both *Am*InRs was observed in queen larvae but not worker larvae, and it may be responsible for growth rate boosting in queen larvae. This demonstrates a more dynamic and complex role of the IIS pathway in caste differentiation [137]. Furthermore, knockdown of the insulin receptor substrate in queen larvae causes development of worker morphology, proving that queen development requires IIS signaling [266]. Second, endocrine regulation of reproduction is not fully understood in honey bees and neither is the role of the IIS pathway in this process. JH and ecdysone are thought to have lost their

gonadotropic functions in bee queens, and JH is believed to regulate worker division of labor (e.g., nurses vs. foragers) and social behavior [51-55]. The IIS pathway is also involved in bee reproduction and longevity. Opposite to what would be expected based on the involvement of the IIS pathway in reproduction in dipterans, the expression levels of honey bee insulin receptor-1 (*Am*InR-1) in larval ovaries is also lower in queens than in workers [137]. Corona *et al.* proposed that higher nutrition in adult queens results in the transcriptional down-regulation of the IIS pathway (*Am*ILP-1, *Am*InR1 and *Am*InR2) in the head by unknown mechanisms, with the concomitant downstream down-regulation of JH synthesis resulting in a higher vitellogenin (Vg) level [269]. Vg as a signaling molecule maintains the repression of the *Am*ILP-1 in the head, achieving a longer life, yet with high reproductive capacity [269]. A complete understanding of the IIS pathway role in adult bee reproduction is missing.

The knowledge of insect insulin receptors is rapidly evolving, and until recently it was believed that insects only had one insulin receptor gene. The release of the honey bee genome revealed two insulin receptor genes (*Am*InR-1, XM_394771; *Am*InR-2, XM_001121597)[160]; however, the latter is incorrectly predicted. Draft genomes from several ant species including the fire ant were released in the last few months [3,138-141]. In some of them, more than one insulin receptor genes were specifically annotated (Hymenoptera Genome Database). However, none of these sequences have been verified by cDNA cloning, and the biological data on insulin receptors is lacking. It appears that two different insulin receptors are present in social insects and this may have biological significance.

Ants comprise at least one third of the world's insect biomass and are important in tropical and warm-temperature forests [1,2]. Their recognized importance is reflected in that draft genomes from several ant species including the fire ant were released in the past year [3,138-141]. Similarly to bees, in some ant genomes more than one insulin receptor gene was specifically annotated; however, none of the predicted full open reading frame sequences have been verified by cDNA cloning. In summary, knowledge on the role of the IIS pathway in ants is lacking. There is only one study on the queenless ponerine ant, *Diacamma* sp., in which both castes, gamergate (dominant egg layers) and workers, have reproductive capacity. Insulin receptor transcripts were found in the ovaries of adult day-7 future gamergate but not in workers of the same age, suggesting that this receptor plays a role in ovarian development and reproductive differentiation [270]. We investigated the red imported fire ant *Solenopsis invicta* Buren, an invasive species that potentially threatens urban and agricultural landscapes in one half of the terrestrial masses worldwide [271]. Unlike the honey bee, JH regulates vitellogenesis and reproduction in fire ant queens [24,46,46,158]; fire ant workers are completely sterile, like in most ant species. Therefore, the fire ant provides an evolutionary simpler system, intermediate between *Drosophila* and honey bees for the study of the diverse roles of the IIS pathway. We obtained the cDNA sequence of two insulin receptors from fire ant queens and, as a result, we corrected the incomplete prediction of the *Am*InR-2 in the honey bee genome. In fire ants, we also investigated the transcriptional expression of both receptors in different developmental stages, castes and queen tissues.

Knowledge of the expression profile of the insulin receptors will help in understanding the likely multiple functions of the IIS pathway in the fire ant.

Results

Cloning of fire ant insulin receptors

The goal of this study was to investigate the IIS pathway in fire ants through the estimation of insulin receptors relative transcript abundance during different life stages and in various queen tissues. Because this work began previous to the release of the fire ant draft genome, we first analyzed the insulin receptor sequences known from other insects to perform a multiple sequence alignment for primer design. We discovered that the honey bee *Am*InR-2 sequence was incompletely predicted and we corrected it. In the honey bee genome, an IGF-1 receptor (*Am*IGF1R, XM_001121628) had been previously annotated from the same contig where *Am*InR-2 is located [160]. After further examination of the contig sequence, we found that the *Am*InR-2 and *Am*IGF1R are likely fragments of the same gene because *Am*IGF1R is missing the α-subunit sequence and *Am*InR-2 is missing the ß-subunit sequence. Therefore, we corrected the prediction of *Am*InR-2 sequence (Third party annotation GenBank: BK008012) and utilized this new prediction to perform sequence alignment, primer design and subsequent cladistic tree analyses.

Sequence alignments of insulin receptors revealed that residues in the ligand binding (LB) domain and the tyrosine kinase (TK) domain were highly conserved. To

clone fire ant insulin receptors, degenerate primers sets were designed first for the TK domain to amplify initial receptor fragments from mated queen ovary cDNA. The cloning was completed through RLM-RACE cDNA reactions. Two insulin receptor homologues (likely paralogs) were obtained and designated *Si*InR-1 and *Si*InR-2, respectively. *Si*InR-1 has a complete cDNA length of 5919-bp and contains an open reading frame (ORF) that encodes a 1432-residue protein with a predicted molecular weight of 163.2 kDa (GenBank accession number JF304723, Figure 5.1). The complete sequence of the *Si*InR-2 cDNA has a length of 6795-bp and contains an ORF encoding a 1702-residue protein with the predicted molecular weight of 193.1 kDa (JF304722, Figure 5.2).

Insulin receptor cDNA sequences analyses

Several conserved domains found in insect insulin receptors are present in the *Si*InRs (Figure 5.3). In *Si*InR-1, the cleavage site for the signal peptide was predicted at residue Q^{24} (Figure 5.1, vertical arrow). In the *Si*InR-2, the N-terminal sequence analyzed by TMHMM and SMART programs does not reveal a signal peptide sequence, but a hydrophobic region is predicted at residues 162-184 (Figure 5.2; box, underlined). This is a putative membrane anchoring sequence such as in DIR [106]. Analyses of the region downstream to the anchoring sequence with the Signal IP program predicted a putative cleavage site at residue N^{198} (Figure 5.2, vertical arrow). This result suggests that upon cleavage, the mature α-subunit of *Si*InR-2 may start at this site.

The first predicted domain in the extracellular region of the *Si*InRs α-subunit is the LB domain which contains two ligand-binding loops (L-1 and L-2), with one furin-like cysteine rich region (Fu) between them. The ligand-binding loop contains leucine-rich repeats which are important for ligand binding. Downstream of L-2, there is the fibronectin type 3 (Fn3) domain (Figure 5.1, in bold) containing three Fn3 repeats which are important for the formation of two disulphide bonds when the α- and β-subunits dimerize. In *Si*InR-2, the tetrabasic sequence "RRRR" (residues 907-910) found in the second Fn3 repeat is a conserved putative site for receptor post-translational processing into α- and β-subunits. This region was analyzed by the PeptideCutter program (ExPASy) which identified three potential cleaving enzymes for this tetrabasic sequence: Arg-C proteinase, clostripain, and trypsin. Unlike *Si*InR-2, such a tetrabasic conserved feature is not present in *Si*InR-1; however, three putative cleavage sites ($K^{759}K^{760}$, $K^{795}K^{796}$, and $K^{845}K^{846}$) were identified in the second Fn3 repeat of *Si*InR-1. This domain in *Si*InR-1 was similarly analyzed and the program predicted that trypsin may act on these KK sequences. The second site sequence $K^{795}K^{796}$ is conserved in *Am*InR-1, indicating this site might be the common processing site for the hymenopteran InR-1. A single transmembrane domain is predicted downstream of the third Fn3 region in both *Si*InRs.

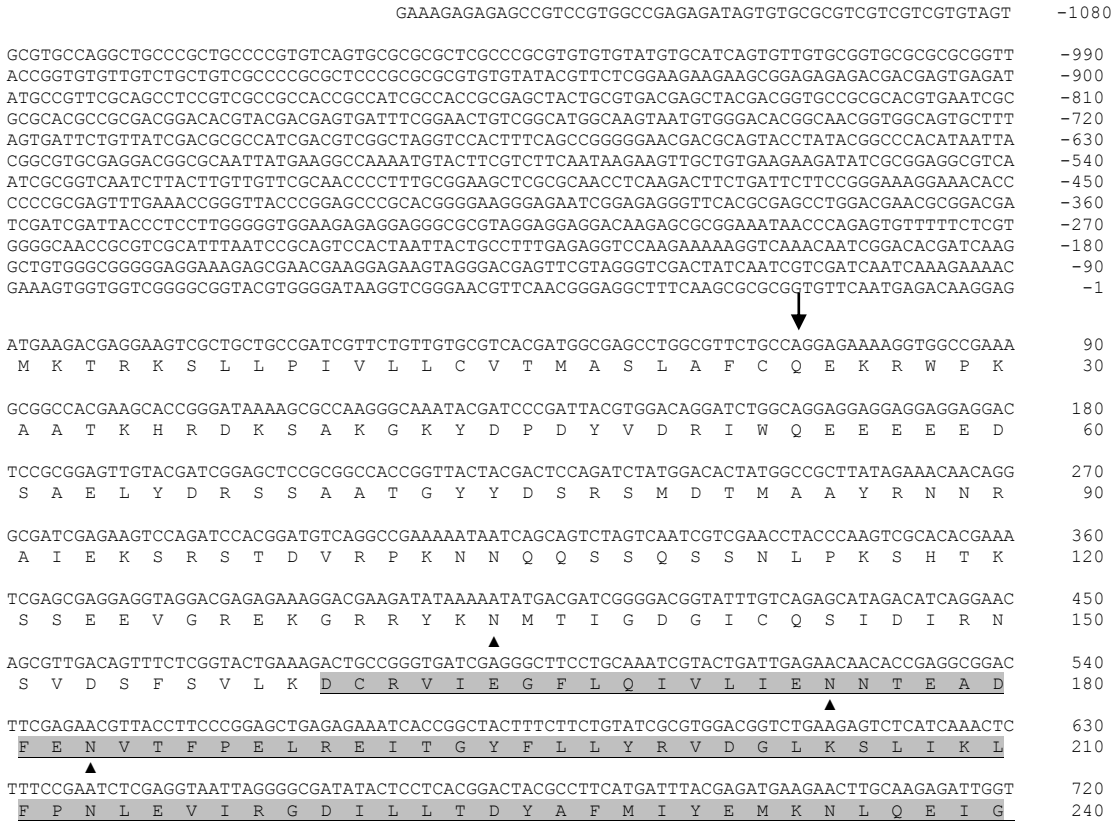

Figure 5.1. cDNA sequence of *Solenopsis invicta* insulin receptor-1, *Si*InR-1, cloned from the ovaries of fire ant mated queens. The amino acid sequences encoded from ORF of *Si*InR-1 (GenBank accession number JF304723; 5919bp: 5'UTR, 1135bp; ORF, 4296bp; 3'UTR, 488bp) are shown. The cleavage site at the N-terminus is indicated by a vertical arrow. Predicted ligand-binding loops (L-1 and L-2) in the LB domain in α-subunit are underlined and highlighted. The fruin-like cysteine rich (Fu) region in between is highlighted. Three fibronectin type 3 (Fn3) repeats were labeled with (bold letters without an underline). The putative cleavage sites are indicated by a dash underline with highlight. A single transmembrane region in the β-subunit is shaded and the juxtamembrane motif (NPXY) next to the transmembrane region is boxed. The highly conserved tyrosine kinase domain in the β-subunit is indicated with bold and underlined letters. Within the tyrosine kinase domain, there are a protein kinases ATP-binding region signature (double underlined), a tyrosine protein kinases specific active-site signature (FVHRDLAARNCMV; boxed), a Mg^{2+} binding region (DFG; boxed), and a triple tyrosine cluster (YXXXYY; boxed). Several modifications were predicted and labeled under the residues, including N-glycoslytion sites indicated by black triangle (▲), protein kinase C (PKC) phosphorylation sites labeled by black circle (●), cAMP-dependent protein kinase phosphorylation sites labeled by star (*), casein kinase II phosphorylation sites labeled by white diamond (◊).

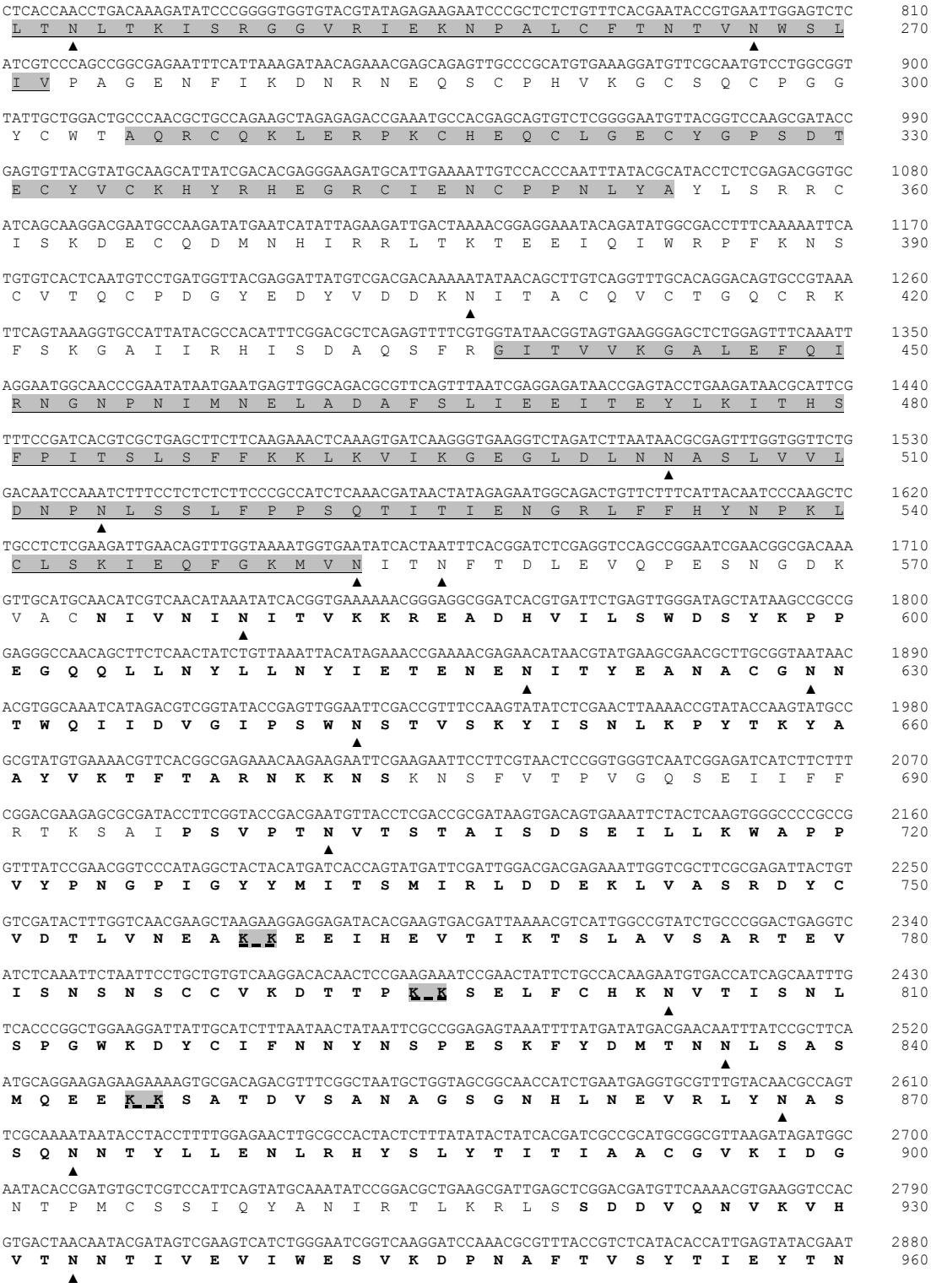

Figure 5.1. Continued.

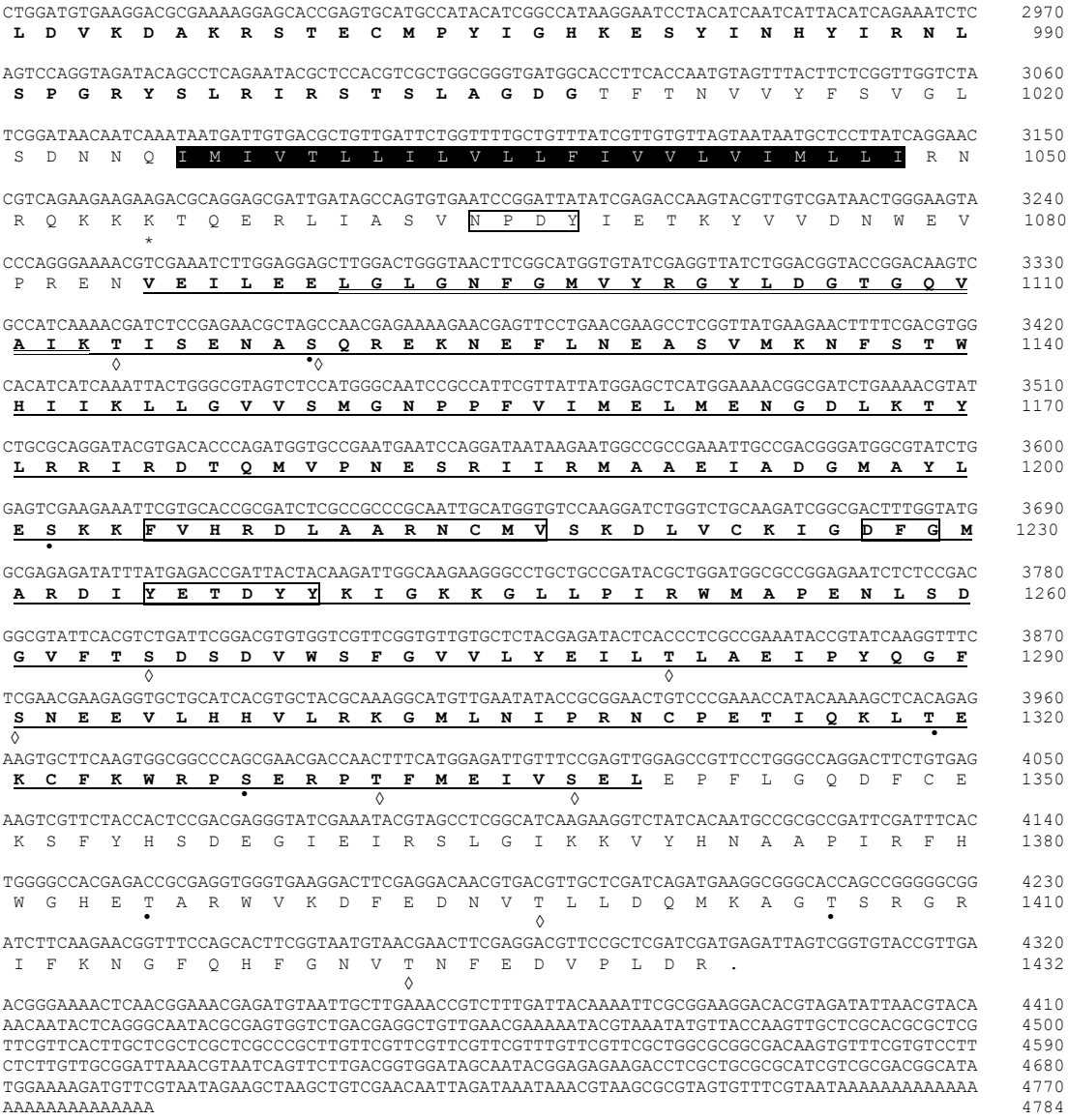

Figure 5.1. Continued.

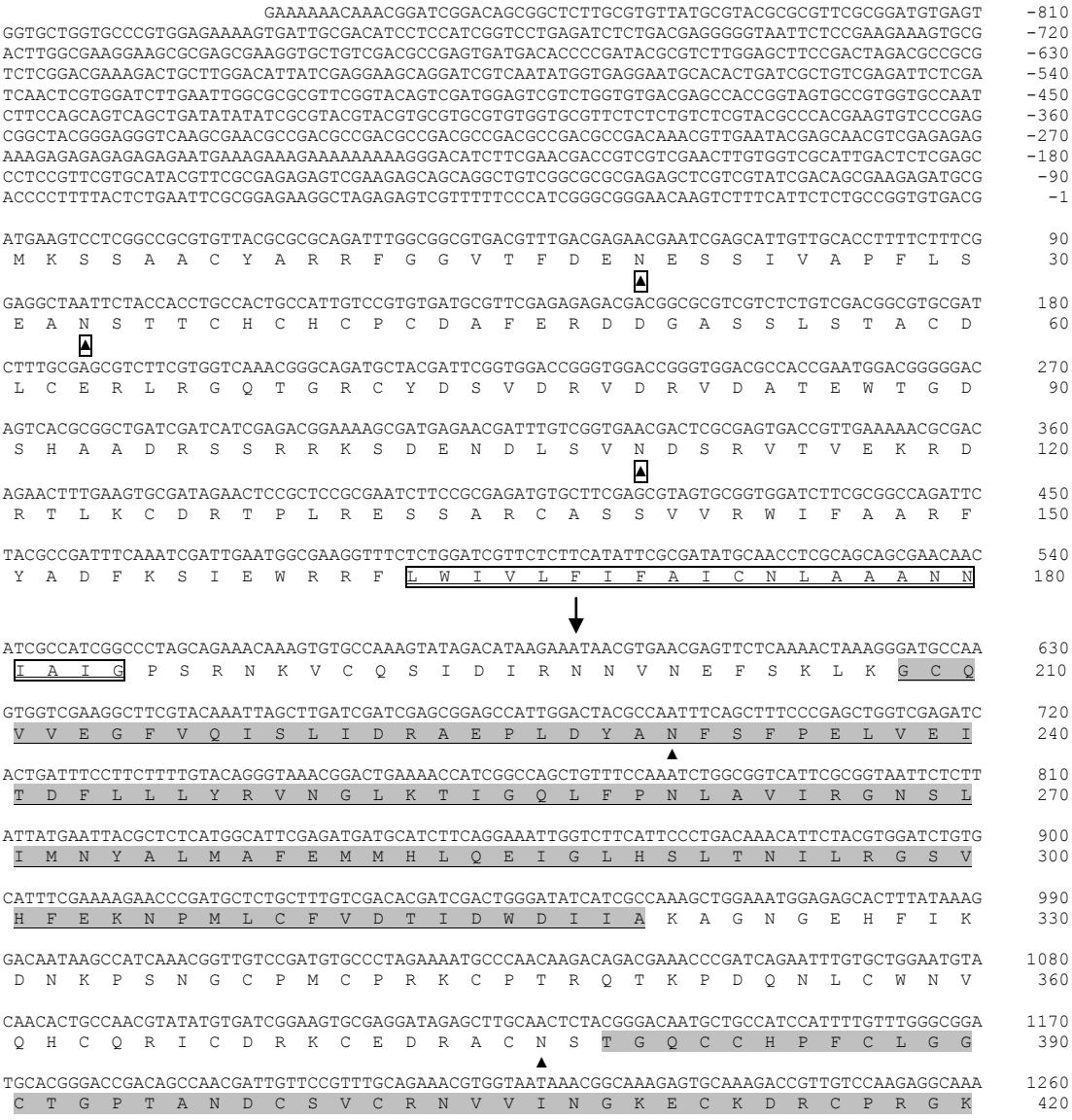

Figure 5.2. cDNA sequence of *Solenopsis invicta* insulin receptor-2, *Si*InR-2, cloned from the ovaries of fire ant mated queens. The amino acid sequences encoded from ORF of *Si*InR-2 (GenBank accession number: JF304722); 6795bp: 5'UTR, 876bp; ORF, 5106bp; 3'UTR, 813bp) are shown. Labeling of features are the same as in the *Si*InR-1 sequence (please see figure legend below Figure 5.1), except that a hydrophobic region was predicted in *Si*InR-2, amino acid residues 162-184 (boxed with underline), as a putative membrane anchoring sequence. Three prediction of N-glycoslytion sites near N-termius of the *Si*InR-2 were separately labeled with boxed black triangle (▲) because these modifications were predicted before the signaling peptide cleavage site, and therefore may not present in receptor protein.

Figure 5.2. Continued.

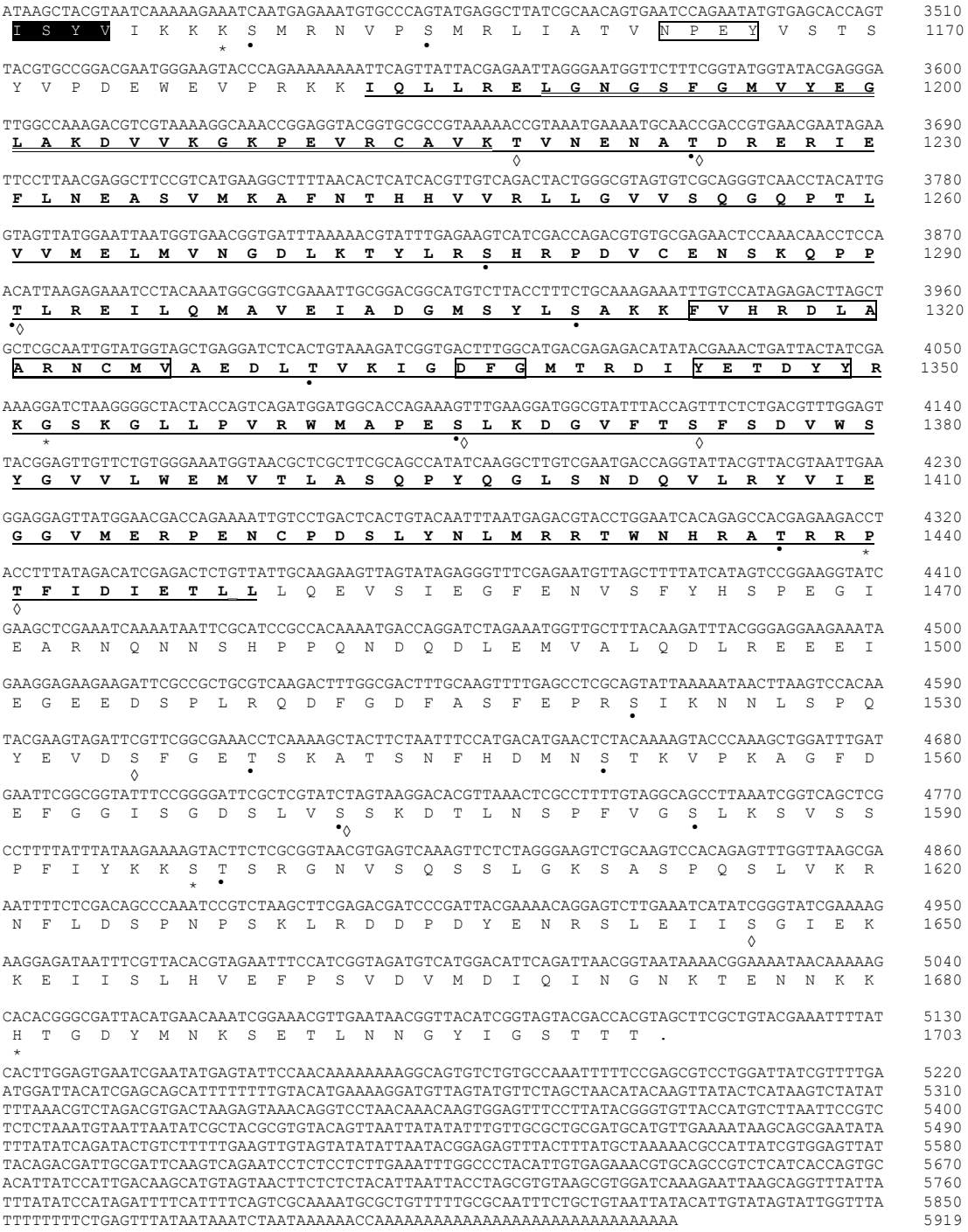

Figure 5.2. Continued.

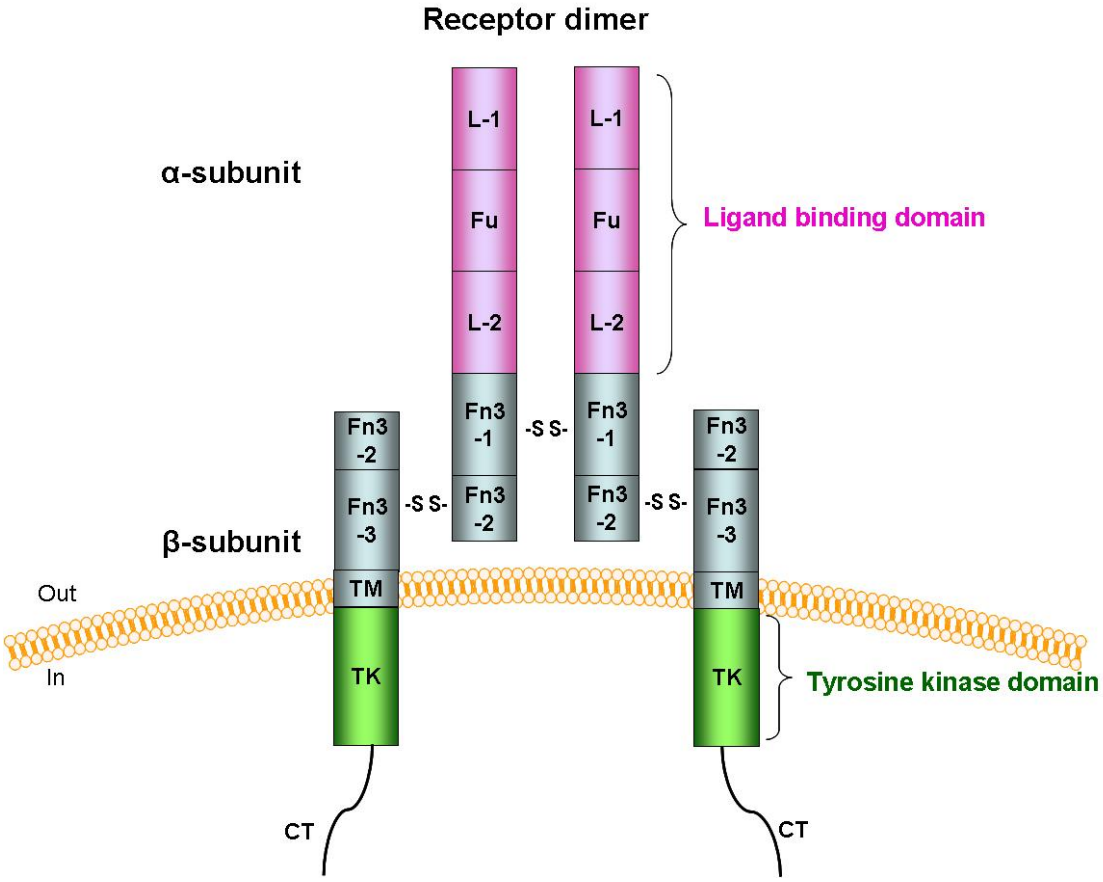

Figure 5.3. Diagram of quaternary structure and the protein domain organization of the insulin receptor. LBD-1 and LBD-2, ligand binding domains contain leucine-rich repeats; Fu, furin-like cysteine-rich domain; Fn3-1, Fn3-2, Fn3-3, fibronectin type 3 domains; TM, transmembrane domain; TK, tyrosine kinase domain; and CT, carboxy-terminal tail. Disulfide bonds are shown.

The first feature in the intracellular region of both *Si*InRs is the juxtamembrane motif "NPXY" (Figures 5.1 and 5.2). This NPXY motif in *Drosophila* DIR binds to the N-terminal region of the insulin receptor substrate and is important for the efficient phosphorylation of this substrate which is critical for triggering downstream signaling events [272]. Following NPXY, there is a TK domain which is responsible for signal amplification (Figures 5.1 and 5.2). Within the TK domain of both receptors, there are four conserved features including, 1) the protein kinases ATP-binding region; 2) the tyrosine protein kinases specific active-site signature; 3) the triple tyrosine cluster (YXXXYY), and 4) the Mg^{2+} binding site (DFG). The triple tyrosine cluster constitutes the major autophosphorylation site for the mammalian insulin receptor [273].

Seven insect insulin receptor sequences (*Si*InR-1; *Si*InR-2; *DIR*; *MIR*; *Nv*IR; *Am*InR-1; *Am*InR-2, this study) were analyzed with prediction tools in order to identify common sites for potential post-translational modifications (Table 5.1). Among the predicted N-glycoslytion sites, three are conserved among these insulin receptors (group 1: residues N^{183}, N^{619}, and N^{933} in *Si*InR-1 corresponding to N^{231}, N^{693}, and N^{1026} in the *Si*InR-2). Likewise, conserved protein kinase C (PKC) and casein kinase II (CKII) phosphorylation sites were found in all insulin receptors compared (Table 5.1). These conserved sites may be important for the regulation of insect insulin receptor functions. In hymenopteran receptors (groups 2 and 3), some sites were only conserved in the group 2 (*Si*InR-1 and *Am*InR-1) or in the group 3 (*Si*InR-2, *Am*InR-2, *Nv*IR) (Table 5.1, shaded).

Table 5.1. Conservation of predicted sites for post-translational modifications in *Si*InR-1 and *Si*InR-2 and in other insect insulin receptors. The analyses resulted in four groups of predicted sites: 1) conserved among all analyzed insulin receptors (*Si*InRs, *Am*InRs, *Nv*IR, *DIR*, and *MIR*); 2) conserved only between InR-1 of hymenopterans *Si*InR-1 and *Am*InR-1); 3) conserved only among hymenopteran InR-2 (*Si*InR-2, *Am*InR-2, and *Nv*IR); 4) conserved among *Si*InR-2, *Am*InR-2, *Nv*IR, *DIR*, and *MIR*. In the table, the number above each residue indicates its position in the corresponding sequence of *Si*InR-1 or *Si*InR-2. For receptors in group 1 underlined residues are those conserved among all sequences, and for clarity these residues are not repeated in comparisons of groups 2-4. Residues listed in group 4 are also listed in group 3 in parenthesis. Residues in gray boxes highlight conservation only within the hymenopteran insulin receptors. No: no other conserved residue(s) found.

Post-translational modifications	Conservation among insulin receptor groups:	Receptor corresponding residues/position	
		*Si*InR-1	*Si*InR-2
N-glycoslytion sites	1) All analyzed insulin receptors	$\underline{N^{183}\ N^{619}\ N^{933}}$	$\underline{N^{231}\ N^{693}\ N^{1026}}$
	2) *Si*InR-1, *Am*InR-1	$N^{135}\ N^{175}\ N^{514}\ N^{553}\ N^{629}\ N^{804}$	No
	3) *Si*InR-2, *Am*InR-2, *Nv*IR	No	$N^{648}\ N^{790}\ N^{808}$
	4) *Si*InR-2, *Am*InR-2, *Nv*IR, *DIR*, *MIR*	No	No
Protein kinase C phosphorylation sites (S/T)	1) All analyzed insulin receptors	$\underline{S^{1120}\ S^{1319}}$	$\underline{T^{1224}\ T^{1437}}$
	2) *Si*InR-1, *Am*InR-1	No	No
	3) *Si*InR-2, *Am*InR-2, *Nv*IR	No	$S^{1277}\ S^{1522}$ ($T^{1331}\ S^{1366}\ S^{1584}$)
	4) *Si*InR-2, *Am*InR-2, *Nv*IR, *DIR*, *MIR*	No	$T^{1331}\ S^{1366}\ S^{1584}$
Casein kinase II phosphorylation sites (S/T)	1) All analyzed insulin receptors	$\underline{S^{1120}\ S^{1265}\ T^{1332}}$	$\underline{T^{1224}\ S^{1374}\ T^{1441}}$
	2) *Si*InR-1, *Am*InR-1	$T^{1281}\ S^{1291}\ S^{1338}$	No
	3) *Si*InR-2, *Am*InR-2, *Nv*IR	No	T^{1441} (S^{1366})
	4) *Si*InR-2, *Am*InR-2, *Nv*IR, *DIR*, *MIR*	No	S^{1366}
cAMP-Dependent protein kinase phosphorylation sites	1) All analyzed insulin receptors	None found	None found
	2) *Si*InR-1, *Am*InR-1		
	3) *Si*InR-2, *Am*InR-2, *Nv*IR		P^{1440} (G^{1352})
	4) *Si*InR-2, *Am*InR-2, *Nv*IR, *DIR*, *MIR*		G^{1352}

Additionally, some sites conserved among group 3 were also found in DIR and MIR (residues listed in group 4: *Si*InR-2, *Am*InR-2, *Nv*IR, DIR and MIR). These differential conservation of post-translational modification sites between InR-1 and InR-2 (groups 2-4, Table 5.1), suggests that specific sites may be important for differential regulation of InR-1 and InR-2 signaling when both are expressed in the same tissues.

In the genomes of the carpenter ant *Camponotus floridanus* and the ponerine ant *Harpegnathos saltator*, four and five insulin receptor genes were identified, respectively [139]; however, we determined that only two of them in each species are similar in sequence and in predicted protein structure to the insulin receptor. Two insulin receptors are also annotated from the draft genome of the fire ant [3] and the argentine ant [138], and we found two by BLAST search in the genome of the leaf-cutter ant [140] and the harvester ant [141]. Phylogenetic relationships between insect insulin receptors were analyzed in a tree rooted with insulin receptor (Daf2) from the nematode *Caenorhabditis elegans* insulin receptor (Daf2) (Figure 5.4). The tree shows that InR-1 and InR-2 form two distinct clusters and each cluster contains one of the insulin receptor from ants and the honey bee. The InR-2 cluster appears to be the most ancestral in insects and included receptors from Diptera, Lepidoptera, and Hymenoptera, each in a separate sub-cluster. In the Hymenoptera InR-2 subcluster, *Si*InR-2 was grouped with one of the insulin receptors found in each of the other ant species, and then grouped with the insulin receptor from the honey bee (*Am*InR-1) and wasp (*Nv*IR). The InR-1 cluster contained only hymenopteran receptors. The presence of two receptor paralogs was also predicted in the genomes of the beetle *Tribolium castaneum* and the aphid

Acyrthosiphon pisum; however, these predictions are still incomplete. We did not include these receptors into our analyses because wrong sequences may produce incorrect cladograms.

Pairwise alignments of amino acid sequences from each *Si*InR with other insulin receptors (*Nv*IR; *DIR*; *Am*InR-1; *Am*InR-2, this study), respectively, also show that *Si*InR-1 shares high percentage of homology with AmInR-1, and *Si*InR-2 shares high homology with *Am*InR-2 (Figure 5.5; underlined percentages of identity and similarity). Pairwise alignments of sequences from single domains of each *Si*InR with their counterparts from listed insulin receptors were also analyzed. Higher homologies were observed in the L-1, L-2, Fn3-1, Fn3-3, and TK domains (Figure 5.5, shaded boxes). Alignment of the amino acid sequences of insulin receptors from *S. invicta* (*Si*InR-1 and *Si*InR-2), *A. mellifera* (*Am*InR-1 and *Am*InR-2), and *N. vitripennis* (*Nv*IR) also shows conserved residues are present in the ligand-binding loops (L-1 and L-2) and in the tyrosine kinase (TK) domain (Figure 5.6).

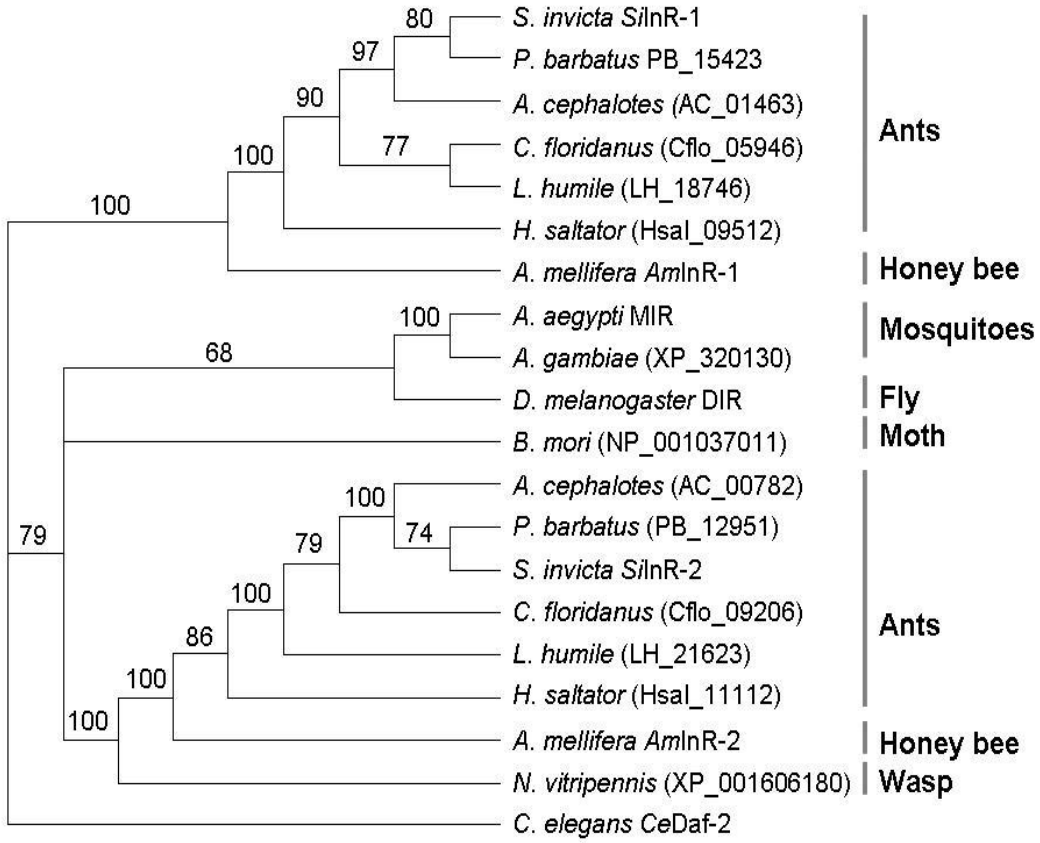

Figure 5.4. Bootstrap analysis of insect insulin receptors. The amino acid sequences were aligned with ClustalW and a rectangular cladogram was generated with 10,000 bootstrap replicates and 50% majority-rule consensus using the program PAUP 4.0. Bootstrap values over 50% are shown at branch points. Sequences analyzed include insulin receptors from *S. invicta Si*InR-1 (JF304723) and *Si*InR-2 (JF304722), *D. melanogaster* (DIR; NP524436), *A. gambiae* (XP_320130), *A. aegypti* (MIR; AAB17094), *Bombyx mori* (NP_001037011), *N. vitripennis* (*Nv*IR; XP_001606180), *C. floridanus* (Cflo_05946 and Cflo_09206), *P. barbatus* (PB_15423 and PB_12951), *Atta cephalotes* (AC_01463 and AC_00782), *Linepithema humile* (LH_18746 and LH_21623), *Harpegnathos saltator* (Hsal_09512 and Has_l11112), *A. mellifera Am*InR-1 (XP_394771) and *Am*InR-2 (BK008012), and *C. elegans* Daf2 (NP_497650). The tree was rooted with the *C. elegans* insulin receptor Daf2.

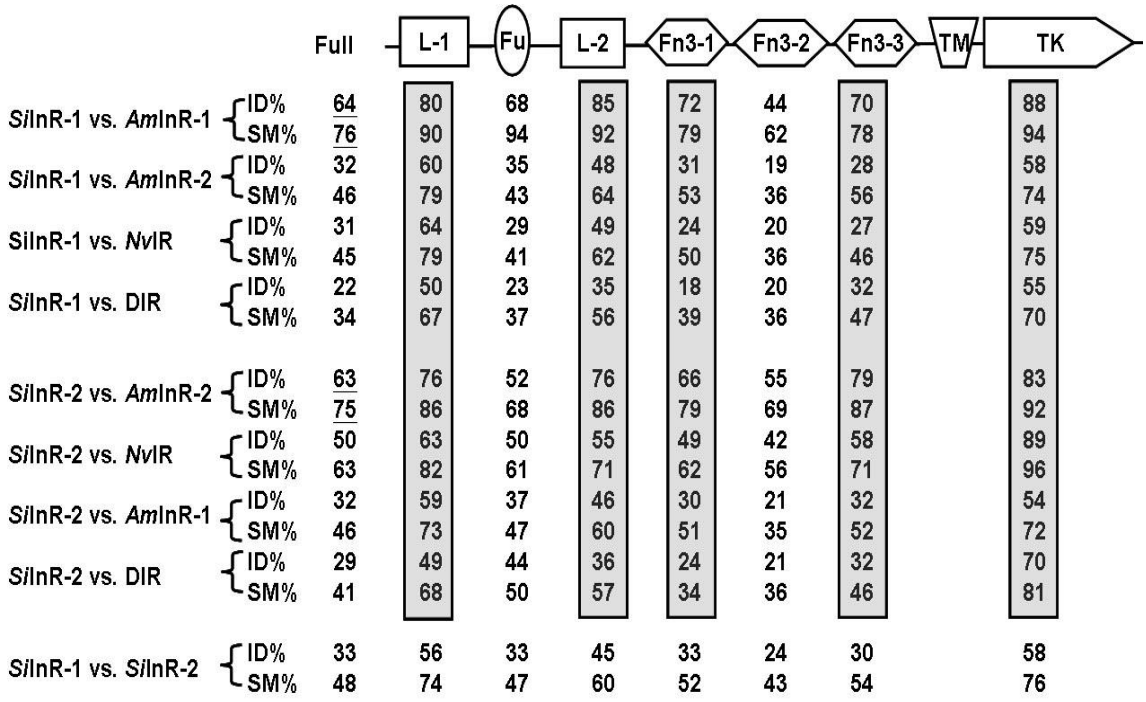

Figure 5.5. Identity and similarity between *Si*InR-1 and *Si*InR-2, and comparisions to other insect insulin receptors. Amino acid sequences from each *Si*InR were compared with their counterparts from the honey bee (*Am*InR-1; *Am*InR-2, this study), *Nasonia* (*Nv*IR), and *Drosophila* (DIR), respectively (labeled "Full"), by pairwise alignment algorithms provided by EMBOSS. Sequences from single domains of each *Si*InR were also compared with their counterparts from *Am*InR-1, *Am*InR-2, *Nv*IR, and *DIR*, respectively. The ligand-binding loops (L-1 and L-2), and the furin-like cysteine rich region (Fu), fibronectin type 3 domains (Fn3-1, Fn3-2, and Fn3-3), and tyrosine kinase domain (TK) are labeled in the top panel. Numbers below each domain indicate the percentage of identity (ID) or similarity (SIM) between two sequences on the left. Higher similarity and identity were observed in L-1, L-2, Fn3-1, Fn3-3, and TK domains (labeled with box). The Fu and Fn3-2 domains show less identity and similarity between pairs. TM: transmembrane region.

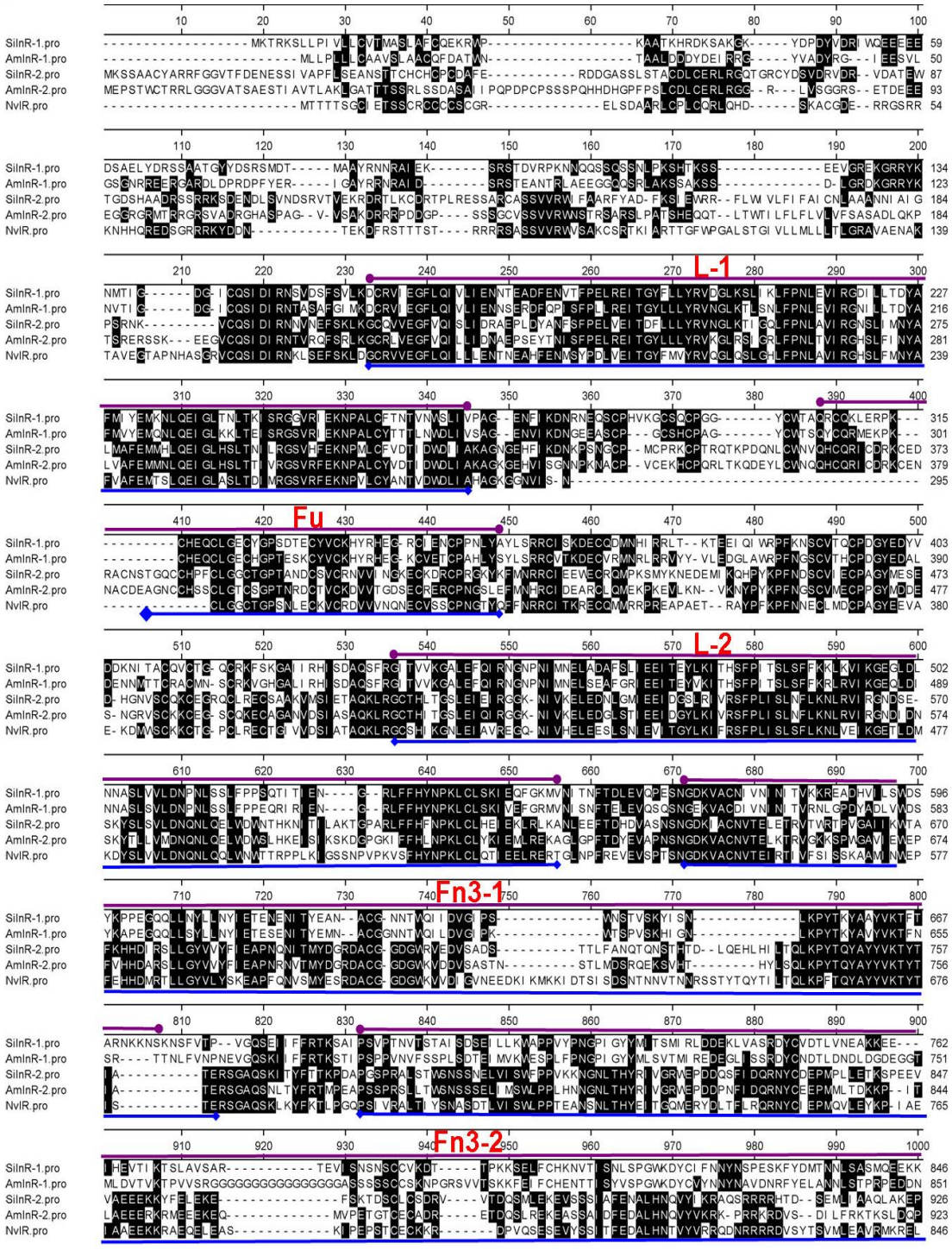

Figure 5.6. The alignment of the amino acid sequences of insulin receptors from *S. invicta* (*Si*InR-1; *Si*InR-2), *A. mellifera* (*Am*InR-1; *Am*InR-2, this study), and *N. vitripennis* (*Nv*IR) showing structural features. Domains in the *Si*InR-1 are indicated with a purple line (with dot) above the sequence and domains in the *Si*InR-2 are indicated with a blue line (with diamond) below the sequences. Conserved regions can be found in the ligand-binding loops (L-1 and L-2) and tyrosine kinase (TK) domain.

Semi-Q RT-PCR analyses the expression of two insulin receptors

We next compared the developmental profile of *Si*InRs by semi-Q RT-PCR using specific primers for *Si*InR-1, *Si*InR-2 and β-actin (as the internal control) to calculate relative receptor expression level (Table 5.2). The *Si*InR-1 expression level was significantly higher in eggs than in most of tested stages, except 4th instar larvae of workers and virgin queens and males (E, Figure 5.7). For *Si*InR-2, expression level was significantly higher in the eggs than in all of other stages (E, Figure 5.7). Expression levels for each receptor were compared between reproductives (R) and workers (W) from the last instar (4th) larvae to the adult stage. Last instar (4th) larvae of reproductives and their pharate pupae (p-pupae; R) had significantly lower transcript levels of both receptors than the workers at the same stages (Figures 5.7A and 5.7B, respectively). Such differences between workers and reproductives (RF; RM) were not observed within the white or dark pupae stages, except for transcript levels of InR-2 in white pupae in which receptor levels were higher in females (W and RF) than in reproductive males (Figure 5.7B). When comparing white and dark pupae stages within each caste, the white pupae had higher levels of *Si*InRs than the dark pupae (or showed a trend towards higher *Si*InR transcript) in all castes (Figures 5.7A and 5.7B).

In adults, the expression levels of both receptors in whole bodies of virgin queens and males were significant higher than their respective expression in whole bodies of workers (Figures 5.7A and 5.7B). These results are in agreement with the fact that reproductive adults may have higher receptor expression levels in gonads, increasing the

relative transcript abundance in whole bodies (Figures 5.7A and 5.7B), while workers are completely sterile with no ovaries.

We then compared the overall level of expression between the two receptors throughout development (Figure 5.7A vs. 5.7B; Table 5.3). The *Si*InR-2 transcripts are more abundant than those for *Si*InR-1, with significance differences for eggs and workers in all stages analyzed except dark pupae. In reproductives, we only observed this significantly higher *Si*InR-2 expression in the white pupae of female reproductives (and not in 4th instar larvae, the pharate pupae or adults of reproductives) perhaps pointing to the physiological significance of *Si*InR-2 signaling during this specifically critical pupal developmental period.

Table 5.2. Primers used for amplification of *S. invicta* insulin receptors (*Si*InR-1 and *Si*InR-2). The primer set "Si-IR2-f10 and SiIR2-r16" were used to amplify *Si*InR-1. The primer set "Si-IR1-f20 and SiIR1-r11" were used to amplify *Si*InR-2.

Gene	Primer	Sequences
β-actin	*Si*-actin-f1	5'-AGCAATGATCTTGATCTTGATGGTTGAGGG-3'
	Si-actin-r1	5'-GTCTCCCACACCGTACCCATTTATGAG-3'
*Si*InR-1	Si-IR2-f10	5'-CCACGGATGTCAGGCCGAAAAATAATCAGC-3'
	Si-IR2-r16	5'-TAACCGCCAGGACATTGCGAACATCCTTTC-3'
*Si*InR-2	Si-IR1-f20	5'-AATGGCGAAGGTTTCTCTGGATCGTTCTCTTC-3'
	Si-IR1-r11	5'-GGTTTCGTCTGTCTTGTTGGGCATTTTCTAG-3'

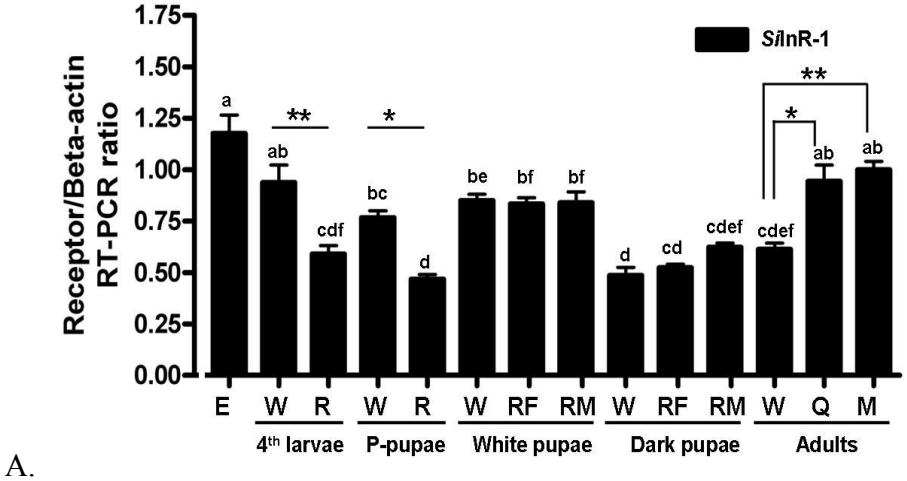

A.

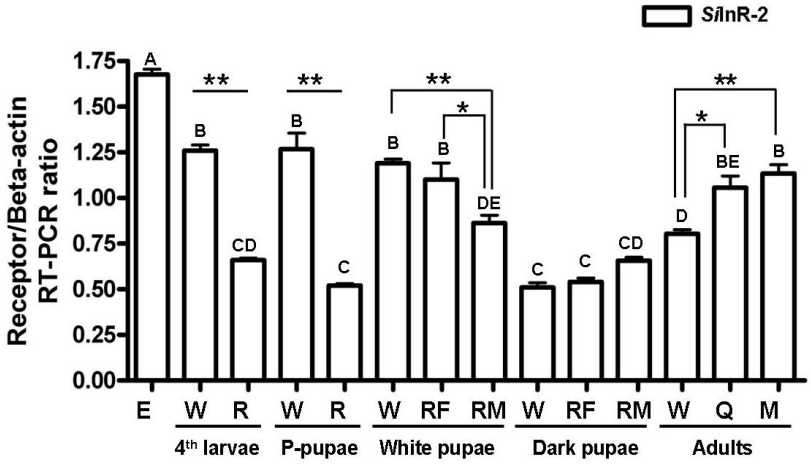

B.

Figure 5.7. Semi-Q RT-PCR expression analyses of fire ant insulin receptors *Si*InR-1 and *Si*InR-2 in different castes and developmental stages. A and B: The relative amount of *Si*InR-1 (A) and *Si*InR-2 (B) transcripts in the whole body of ants in comparison to amplified β-actin transcripts are shown. Eggs (E), 4th instar larvae (4thL) and pharate pupae (P-pupae) of workers (W) and immature reproductives (R), white pupae and dark pupae or workers, immature reproductive females (RF) and males (RM), as well as adult workers, virgin queens (Q), and males (M) were tested. Three sets of independent samples per developmental stage were analyzed. Results of *Si*InR-1/β-actin ratio (A) and *Si*InR-2/β-actin ratio (B) are shown. Data in the same figure were analyzed together. Statistically significant differences are indicated above each bar with small letters for *Si*InR-1 (A) and capital letters for *Si*InR-2 (B). Stars represent significant differences between castes in the same developmental stages (ANOVA, Tukey multiple comparison test, *, $P<0.05$, **, $P<0.01$). Comparisons of SiInR-1 vs. *Si*InR-2 expression for each life stage and cast were analyzed by t-test (see Table 5.3).

The relative expression of *Si*InRs from both virgin and mated queens was also estimated by semi-Q RT-PCR in the following tissues: 1) Brain-CC-CA (enriched in brains but containing some of two neurohemal organs, corpora cardiaca and corpora allata); 2) the ovary; 3) the abdominal fat body; 4) the gut. The highest expression levels of both *Si*InRs in virgin queens (Figure 5.8A) and mated queens (Figure 5.8B) were found in the ovaries of queens. In virgin queens, the expression levels of both *Si*InRs in ovary are significantly higher than their respective levels in the brain-CC-CA and in the gut, but not than in abdominal fat bodies (Figure 5.8A). In virgin queens the fat body expressed significantly higher levels of both receptors than in gut (Figure 5.8A). This correlates with the known storage of energy resources in the fat body of virgin queens. In mated queens, the expression levels of both *Si*InRs in the ovaries are significantly higher than their respective expression in all tested tissues (Figure 5.8B). The ovaries become the target of vitellogenin acquisition and the level of both receptors in the fat body is low and similar to expression in the gut. We also independently compared the expression level of *Si*InR-1 and *Si*InR-2 in different tissues (Figure 5.8C) between virgin (data from figure 5.8A) and mated queens (data from figure 5.8B). In the brain-CC-CA, the expression of *Si*InR-1 in virgin queens is significantly lower than its expression in the mated queens ($p \leq 0.05$) (Figure 5.8C). On the contrary, in the abdominal fat body the expression of *Si*InR-1 in virgin queens is significantly higher than its expression in the mated queens. The expression of *Si*InR-2 was not significantly different between queens.

Table 5.3. Relative transcript expression ratios (with receptor to actin) of *Si*InR-1 (Figure 5.7A) and *Si*InR-2 (Figure 5.7B) were compared within stages and castes and analyzed with t-test. *: $p \leq 0.05$; **: $p \leq 0.01$; ns, no statistical significant differences were found.

Developmental stages	Castes	t-test *Si*InR-1<*Si*InR-2
Eggs (E)		*
4th instar larvae (4thL)	Worker	*
	Immature reproductive	ns
pharate pupae (P-pupae)	Worker	**
	Immature reproductive	ns
White pupae	Worker	**
	Immature reproductive female (RF)	*
	Immature reproductive male (RM)	ns
Dark pupae	Worker	ns
	Immature reproductive female (RF)	ns
	Immature reproductive male (RM)	ns
Adult	Worker	**
	Virgin queen	ns
	Male	ns

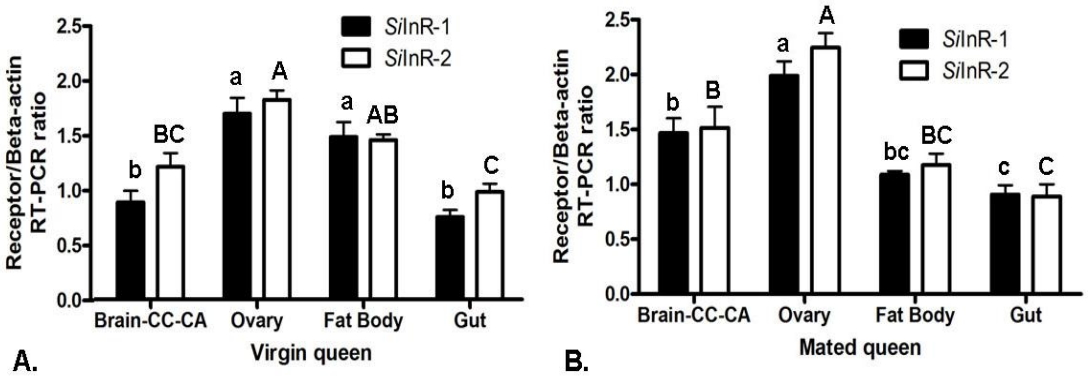

	Brain-CC-CA	Ovary	Fat body	Gut
SiInR-1	MQ > VQ*	MQ = VQ	MQ < VQ*	MQ = VQ
SiInR-2	MQ = VQ	MQ = VQ	MQ = VQ	MQ = VQ

C.

Figure 5.8. Semi-Q RT-PCR expression analyses of fire ant *Si*InR-1 and *Si*InR-2 in different tissues of virgin and mated queens. Relative amounts of *Si*InR-1 and *Si*InR-2 transcripts with respect to β-actin transcripts in virgin (panel A) and mated (panel B) queens are shown. cDNAs of the brain with corpora cardiaca/ corpora allata (brain-CC-CA), ovaries, abdominal fat body, and gut from virgin or mated queens were tested. **A:** In virgin queens, *Si*InR-1 had significantly higher expression in the ovaries and fat body than in the brain-CC-CA and gut. The *Si*InR-2 had significantly higher expression in the ovaries than in the brain-CC-CA and gut but not different than the expression in the fat body. **B:** In the mated queens both *Si*InRs had higher expression in the ovaries than in all other tested tissues. In both virgin (panel A) and mated (panel B) queens, three sets of independent samples per tissue were analyzed. Data for *Si*InR-1 and *Si*InR-2 were analyzed separately in each figure. Statistically significant differences are indicated above each bar with small letters for *Si*InR-1 and capital letters for *Si*InR-2 (ANOVA, Tukey multiple comparison test). **C.** *Si*InR-1 and *Si*InR-2 transcripts levels were compared between virgin (data from panel A) and mated (data from panel B) queens for the four tissues and analyzed with t-test (*: $p \leq 0.05$). Mated queens had significantly higher expression of *Si*InR-1 in brain-CC-CA and lower expression of *Si*InR-1 in fate body than virgin queens; no statistically significant differences were found between queens for ovary and gut (not shown). For *Si*InR-2, no statistically significant differences were found between queens for all tissues (not shown).

Discussion

Two insulin receptors in social insects

We describe the cloning and the transcriptional expression analyses of two putative fire ant insulin receptors, *Si*InR-1 and *Si*InR-2, which are the third and fourth insulin receptors cDNA cloned from insects, and the first cloned from social insects. Although there is evidence for revising the nomenclature of the insect insulin receptors annotated so far, until this occurs, and in order to avoid confusion in the literature, the nomenclature of *Si*InRs was based on their sequence similarity to the honey bee insulin receptors previously designated *Am*InR-1 and *Am*InR-2. The amino acid sequences of *Si*InRs are characterized by several conserved features of the insulin receptor family. In both *Si*InRs, sequence structural analyses (Figures 5.1 to 5.3), phylogenetic tree analysis (Figure 5.4), and pairwise alignments (Figure 5.5) clearly identify these two receptors as insulin receptor orthologs. The predicted structure of the two *Si*InRs is slightly different from that of the cloned insect insulin receptors *DIR* and *MIR*. The *Si*InR-2 does not have a predicted signal peptide sequence at the N-terminus like the *Si*InR-1 and *MIR* have; rather, the *Si*InR-2 has a putative membrane anchoring sequence far downstream from the start codon in the N-terminus, similar to the *DIR* [106,107]. In addition, both *Si*InRs do not have an extra C-terminal extension with four extra NPXY motifs in the β-subunit like the *DIR* has [272], nor do they have a long 3'UTR like the *MIR* has [62]. The conserved predicted sites for post-translational modifications in both *Si*InRs and other insulin receptors from dipterans and hymenopterans (Table 5.1) suggest that these

conserved sites might be important for the regulation of receptor function across insect orders. Positions found to be only conserved within the InR-1 receptors or within the InR-2 receptors (Table 5.1) indicate the possibility of differential modification and regulation between the two insulin receptors, of importance specifically when both proteins may be expressed in the same tissues.

The cladogram shows that the two fire ant insulin receptors are grouped into two different clusters (Figure 5.4), similarly to receptors from other ants and the honey bee. This result suggests that gene duplication from an ancestral gene might have occurred, resulting in two insulin receptor paralogs in these insects. Why some insects carry an extra insulin receptor and how they coordinate them to regulate downstream pathways are both still unknown. However, the presence of two insulin receptors may represent a functional redundancy strategy to ensure accurate development and/or provide functional diversity in multiple tissues. Functional diversity for the insulin pathway is likely provided by the diverse insulin-like peptides (ILPs) present in each species, the number of ILP genes varying from a few to many [267,274]. In *Drosophila*, the presence of one insulin receptor for multiple ligands (*Drosophila ILP*1-7) indicates that the diverse functions of IIS might be due to the diversification of the ligands; that is, ligands may modulate IIS pathway outcomes. The synergy, redundancy and compensation of the expression between these different ILPs were recently demonstrated [116,117]. In genome sequences of the honey bee and the fire ant, however, there are only two ILPs present. Our finding that also two insulin receptors are found in fire ants and other ant species suggests that two insulin receptors might provide a similar diversity of

regulatory functions for the IIS. In parasites of humans, the blood flukes *Schistosoma mansoni* and *S. japonicum*, have two insulin receptors that are differentially localized in ovaries and may have different functions [275,276]. This also opens the possibility that two receptor genes, may contribute to functional diversification in social insects, similar to mammals, including the possibility of hybrid receptor forms. Further localization of both *Si*InRs in fire ants will clarify this possibility.

SiInRs expressed in different ant's life stages and queen tissues

In fire ants, both *Si*InRs expressed throughout life stages, different castes, and in different queen tissues indicating that IIS pathway is important. The high transcriptional expression level of both *Si*InRs in laid eggs confirms that they may play an important role in embryo development. This was demonstrated in *Drosophila*, in which loss of *DIR* function resulted in embryonic lethality [107]. In fire ant workers the levels of each receptor remained relatively constant from 4th instar larvae through white pupae, however, in reproductives there is a significant increase in receptor levels between pre-pupae and white pupae stages (Figure 5.7). When comparing the transcriptional expression between *Si*InRs within stages (Table 5.3), the expression levels of the *Si*InR-2 were more abundant than the *Si*InR-1 in most stages. Statistically significant higher expression of *Si*InR-2 over *Si*InR-1 was observed in eggs and throughout worker stages except dark pupae; however, in reproductive females the higher expression of *Si*InR-2 is only observed in the white pupae. This indicates that specifically *Si*InR-2 signaling may be more important for regulation during this developmental period.

Our results of *Si*InRs transcriptional expression analyses can be interpreted in the context of the different fire ant castes which represent diverse phenotypes with respect to nutritional condition, body size and reproductive ability (Figure 5.9A). Although queens and workers are both females and diploid, queens are larger and highly reproductive while workers are polymorphic (of variable size) and completely sterile. In addition, queens are well fed while workers receive less food and nutrition. The average weight of 4th instar larvae and pharate pupae of reproductives in the colonies is ~10 times higher than the respective weight of workers at the same developmental stages. Based on the known role of the IIS pathway in regulating insect growth and body size, it would reasonable to hypothesize that the expression of both *Si*InRs would be higher in reproductive larvae than in worker larvae. However, the transcriptional expression of both *Si*InRs in larvae and pharate pupae of reproductives is significantly lower than in workers at the same respective stages. The *Si*InR expression in these stages of ants is, therefore, not correlated with their body size and nutritional status. The InRs in fire ants do not appear to have the same role in the regulation of body size as in solitary insects such as *Drosophila* [108,109]. Our results more closely resemble findings in honey bees in which receptor expression in queen larvae, although not statistically different than in worker larvae (in both 4th and 5th instars), show a lower receptor expression trend [137]. However, we have not yet analyzed the receptor protein expression in fire ants and it remains possible that discrepancies may exist between transcript and protein expression levels.

Figure 5.9. Relationship between the transcriptional expression level of insulin receptors and fire ant physiology. Arrow sizes represent the relative amount (or egg number) of listed attributes compared between castes (A) or queen mated status (B). Arrows with upward diagonal texture represent relative receptor transcript levels. **A:** The relative nutritional status, body size, and reproductive potential and InRs expression levels in virgin queens vs. workers are compared. The transcriptional expression of both *Si*InRs is negatively correlated to nutrition status and body size in virgin queens vs. worker ants, indicating a functional difference in social insects vs. solitary insects (e.g., *Drosophila*) for these attributes. For reproduction, the insulin pathway appears to have a conserved function in all insect groups. Workers have no reproductive ability (presented by dash). Therefore, the high expression of *Si*InRs in the whole body of queens is mainly due to their expression in ovaries for reproductive functions. **B.** The JH level, ovarian development, eggs laid, energy usage, and *Si*In-R1 levels in virgin vs. mated queens are compared. In virgin queens, low juvenile hormone (JH) titer prevents ovarian growth resulting in low reproductive capacity. Lower *Si*InR-1 level in the brain-CC-CA (brain with corpora cardiaca and corpora allata) in virgin queens vs mated queens appears to be associated with lower JH titer in virgin queens. Higher *Si*InR-1 expression in the fat body of virgin queens corresponds to storage of reserves for flight and future colony founding. In mated queens, higher *Si*InR-1 expression in the brain-CC-CA correlates with higher JH synthesis, which in turn promotes ovarian growth and high egg production [24,46,46,158]. The decreased level of *Si*InR-1 in the fat body in mated queens reveals a functional switch of this organ from storage in virgin queens to vitellogenin synthesis. In the ovary, both virgin and mated queens have high expression of both receptors which are not statistically significantly different between queens.

A.

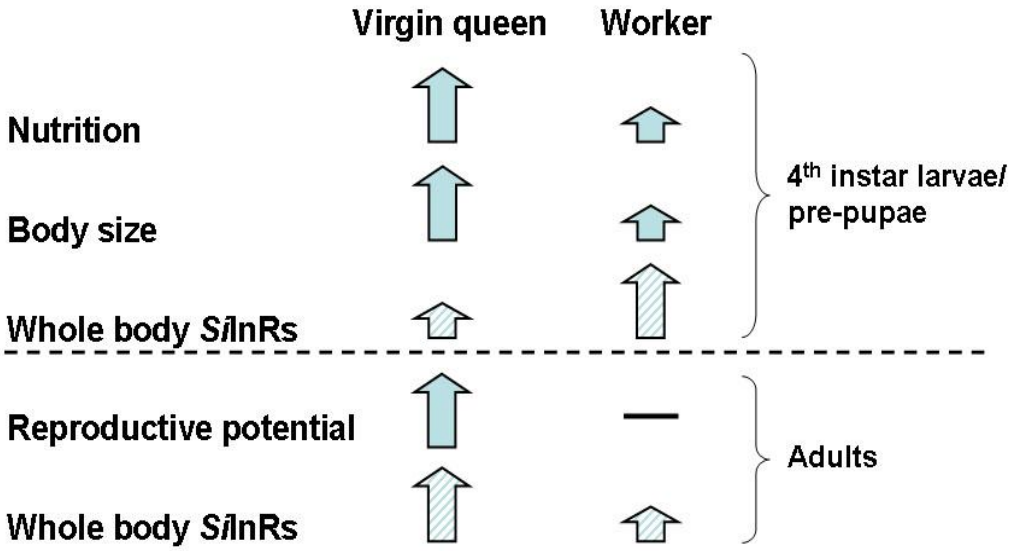
Virgin queen
Worker
Nutrition
Body size
Whole body SiInRs
4th instar larvae/ pre-pupae
Reproductive potential
Whole body SiInRs
Adults

B.

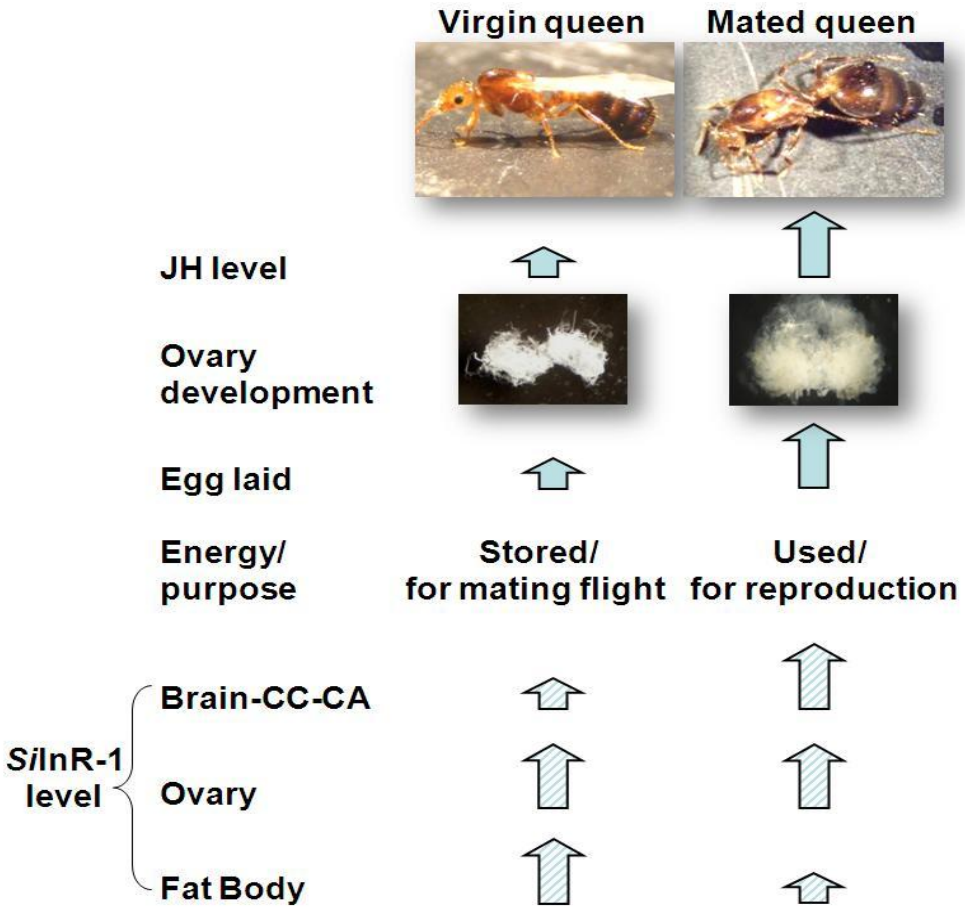
Virgin queen
Mated queen
JH level
Ovary development
Egg laid
Energy/ purpose
Stored/ for mating flight
Used/ for reproduction
SiInR-1 level
Brain-CC-CA
Ovary
Fat Body

In virgin queens within the colony, a primer pheromone released from mated queens suppresses their corpora allata activity and the corresponding production of JH. JH is the major gonadotropin in fire ants [46,46] and therefore low JH titers suppress ovary development [154,155]. Virgin queens have the ability to remain inside the colony for long periods of time until physiological and environmental requirements are met for their participation in the mating flight. However, ovary development during this time proceeds slowly, with the final localization of the Vg receptor at the oocyte membrane [192]. Virgin queens accumulate large energy reserves during this maturation period because upon mating, they will not eat until the new colony is established. The relationships among JH level, reproductive ability, nutritional stores utilization and *Si*InRs transcriptional expression in queen tissues (fat body, brain and ovary), between virgin and mated queens is summarized (Figure 5.9B). The IIS pathway is thought to be the upstream regulator of JH synthesis in insects [66,111,125,126]. In fire ant virgin queens, the observed lower expression of *Si*InR-1 in the brain-CC-CA vs. mated queens (Figure 5.8C) may reflect the low activity of the insulin pathway, with the consequent low JH synthesis and titer in virgin queens [158]. On the contrary, the mated queen in a mature colony has higher expression of the *Si*InR-1 in the brain-CC-CA correlating with the putative downstream stimulation of JH synthesis and high titer of JH in hemolymph, which in turn triggers vitellogenesis. In both queens, we observed significantly high expression of both *Si*InRs in the ovaries than in most other tested tissues (except virgin queen fat body), suggesting that *Si*InRs are important for ovary development and reproduction. Because both virgin and mated queens are well nourished, it appears that

nutritional status is not associated with their reverse, differential expression of *Si*InR-1 in brains-CC-CA (being lower in virgin than in mated queens) and fat body (being higher in virgin than in mated queens) (Figure 5.9B). However the metabolic status of the fat body may be different between queens because in virgin queens the fat body has a preponderant storage function while in mated queens is dedicated to synthesis and export of vitellogenin. Thus, we hypothesize that in virgin queens within the colony the queen primer pheromone deactivates or suppresses the insulin pathway-regulated JH synthesis. However the insulin pathway is active in fat body, with significantly higher expression of *Si*InR-1, likely associated with fat body nutrient storage and growth during the maturation period [143]. High *Si*InR-1 expression in virgin queen fat body makes biological sense because insulin plays an anabolic role in the fat body of insects promoting lipid accumulation [277]. In mated queens, however, lower *Si*InRs levels reflect a functional change in the fat body for vitellogenesis, and storage may not be required because the queen is constantly fed by workers. This reduced receptor expression in fat body may be reflective of IIS pathway reduced function, contributing to high longevity in mated queens.

In summary, by investigating the insulin pathway in a species of ant in which workers have no reproductive ability, the different functions of the insulin pathway in nutrition and reproduction can be more clearly distinguished in different castes and tissues. Testable new hypotheses emerging from our study are that *Si*InR-1 plays roles in queen physiology (including fat body energy metabolism) and reproduction, and *Si*InR-2 plays roles in body size growth and development. The differential expression of

*Si*InRs reveals caste-specific regulation for workers and reproductives, and highlights the physiological significance of this IIS pathway in the regulation of queen physiology and behavior. Our results on the IIS pathway in fire ants contributes new knowledge to the understanding of other social hymenopterans specially of ant species in which workers have no reproductive capacity.

Materials and Methods

Insects

S. invicta were reared as described in Chapter II. For determining receptor expression across developmental stages and castes, larvae (4^{th} instar), pupae (pharate, white, and dark pupae), and adults of both workers and reproductives were collected from more than 6 colonies. It is difficult to distinguish the sex of reproductive larvae and pharate pupae; therefore, reproductives were pooled in these two stages. Female and male reproductive pupae (white and dark) and adults were individually collected. In addition, eggs were also collected from colonies.

Virgin queens that were likely sexually mature (with liquid-filled crops and prominent fat bodies in their abdomens indicating high nutritional status) and mated queens within colonies were chosen for these studies. For receptor tissue expression in queens, the brain-CC-CA (enriched in brains but containing some of two neurohemal organs, corpora cardiaca and corpora allata and devoid of fat body), ovaries, abdominal fat bodies, and guts were dissected individually from both virgin queens and mated

queens. During dissection, successfully mated queens were identified by observing an inseminated large and white spermatheca; only inseminated queens were used as 'mated queens'.

To measure the size difference between castes, 4th instar larvae and pharate pupae were collected individually for both workers and reproductives castes and each group had 40 ants. Total weight for each group was measured and then divided by 40 to calculate their average individual's weight. The average weight for reproductive 4th instar larvae is 0.0297g, for reproductive pharate pupae is 0.0185g, for worker 4th instar larvae is 0.00246g, and for worker pharate pupae is 0.00205g.

Identification of the honey bee insulin receptor-2 (AmInR-2)

Two genes, *Am*InR-2 (XM_001121597) and *Am*IGF-1R (XM_001121628) had been predicted from the same contig (NW_001253271.1) in NCBI (http://www.ncbi.nlm.nih.gov/). These two genes are located next to each other with wrongly predicted 3'end in *Am*InR-2 and 5'end in *Am*IGF-1R. The splice site prediction tool from the Berkeley *Drosophila* Genome Project (http://www.fruitfly.org/ seqtools/splice.html) was used to identify potential exon−intron boundaries in this contig. Identified ORF-containing exons were manually arranged using DNASTAR software (DNASTAR Inc.) and translated *in silico*. The new corrected *Am*InR-2 sequence (TPA GenBank number: BK008012) was used in subsequent analyses.

RT-PCR and RACE

Amino acid sequences from *D. melanogaster* DIR (NP_524436), *A. aegypti* MIR (AAB17094), *N. vitripennis Nv*IR (XP_001606180), *A. mellifera Am*InR-1 (XP_394771) and *Am*InR-2 (BK008012) were aligned using DNASTAR software to identified conserved regions. Sequences in the LB domain and the TK domain were highly conserved among these receptors. Degenerate primer sets were designed first based on the nucleotide sequence alignment of the TK domain from *Nv*IR (XM_001606130), *Am*InR-1 (XM_00394771), and *Am*InR-2 (this work). Mated queen ovaries mRNA was isolated using the DynaBeads® mRNA Direct kit (Invitrogen) and then cDNA was synthesized using 0.5 µg mRNA and oligo-dT_{20} primer using SuperScript™ III First-Strand Synthesis System (Invitrogen) as per manufacturer's specifications. To amplify initial insulin receptor fragments from mated queen ovary cDNA, temperature gradient PCR reactions were performed with degenerate primers. PCR mix contained 2µl cDNA (50 x dilution), 1 µl Advantage® 2 Polymerase (Clontech, Mountain View, CA, USA), 0.4 µM of each primer, 400 µM of dNTPs, 1 x reaction buffer. Gradient PCR parameters were 94 °C for 2 min; 39 cycles of 94 °C for 30 s, 55-60 °C for 1 min, and 72 °C for 2 min; 72 °C for 10 min. A secondary reaction with nested primers was preformed when necessary. PCR products were purified using QIAEX II Gel Extraction kit (Qiagen), and cloned into pCR2.1 Vector (Invitrogen). Competent cells (DH5α, Invitrogen) containing the plasmid were grown and cloned products were isolated by QIAprep Spin Miniprep Kit (Qiagen) and sequenced by the Gene Technology Laboratory (Texas A&M University, College Station, TX). All cDNA fragments were

sequenced at least twice. Two different insulin receptor fragments of similar size (~400bp, named arbitrarily IR-1 and IR-2, respectively) were obtained. IR-1 was later found to be part of *Si*InR-2 gene and IR-2 was found to be part of *Si*InR-1 gene. We then followed with RT-PCR reactions, each combining specific and degenerate primers to obtain further sequence towards the 3' and 5' ends to obtain these two large genes. To obtain the sequence of the *Si*InR-1, degenerate primer sets were also designed for the LB domain. After specific sequence was obtained, a similar RT-PCR strategy as described above was followed to obtain the complete receptor cDNA sequence.

To obtain full-length cDNA, RNA ligase-mediated (RLM)-cDNA was synthesized using GeneRacer™ Kit (Invitrogen) with ovarian mRNA (0.1 μg) as a template following manufacturer's instructions. The 5' and 3' end of receptors were obtained using RLM-cDNA (2μl of 50 x dilution) with specific primers designed based on the *Si*InR-1 and *Si*InR-2 cDNA fragments obtained above. Touchdown-gradient PCR was used and the parameters were 94 °C for 2 min; 10 cycles of 94 °C for 30 sec, 72 °C for 1 min (-0.5 °C each cycle), 72 °C for 1.5 min ; 25 cycles of 94 °C for 30 sec, 60-70 °C for 1 min, 72 °C for 1.5 min; 72 °C for 10 min. The resulting bands were purified, cloned and sequenced as described above.

Sequence analyses

DNASTAR software was used for analyzing sequences obtained from the sequence center. The BLAST search algorithms at NCBI and Hymenoptera Genome Database (http://hymenopteragenome.org/) were used to identify insulin receptor

sequences from other organisms. Molecular weights for the *Si*InRs were predicted by the Compute pI/Mw program provided by ExPASy (http://ca.expasy.org/tools/). The SMART program provided by EMBL (http://smart.embl-heidelberg.de/) was used for identification of modular domains that were adjusted by eye, when necessary. Transmembrane region predictions were made using the TMHMM V2.0 (http://www.cbs.dtu.dk/services/TMHMM/). The SigCleave program from EMBOSS (http://emboss.bioinformatics.nl/cgi-bin/ emboss/sigcleave) and SignalP 3.0 program (http://www.cbs.dtu.dk/services/) were used to predict the N-terminus signal peptide. The PeptideCutter program from ExPASy (http://ca.expasy.org/tools/peptidecutter/) was used to identify potential cleaving enzymes in receptor Fn3-2 region. Amino acid sequences of *Si*InR-1 (JF304723) and *Si*InR-2 (JF304722), *DIR*, *MIR*, *Am*InR-1, *Am*InR-2 and *Nv*IR were aligned using DNASTAR software. Post-translational modification sites in these sequences were predicted using the PPSEARCH program (http://www.ebi.ac.uk/Tools/ protein.html) and sites were compared in the alignment.

To characterize the identity and similarity between each *Si*InRs (*Si*InR-1 and *Si*InR-2) and other insect insulin receptors, each domain from *Si*InR-1 and *Si*InR-2 was compared with the respective domain from *Nv*IR, DIR, *Am*InR-1, *Am*InR-2 (BK008012), by EMBOSS pairwise alignment algorithms (http://www.ebi.ac.uk/Tools/emboss/align/ index.html) and the percentage of identity and similarity were obtained.

For construction of the cladogram, the multiple sequence alignment of insulin receptors was constructed with the ClustalW (http://align.genome.jp/) based on the BLOSUM protein score matrix. These sequences include insulin receptors from *S.*

invicta *Si*InR-1 (JF304723) and *Si*InR-2 (JF304722), *D. melanogaster* (DIR; NP524436), *A. gambiae* (XP_320130), *A. aegypti* (MIR; AAB17094), *B. mori* (NP_001037011), *N. vitripennis* (*Nv*IR; XP_001606180), *C. floridanus* (Cflo_05946 and Cflo_09206), *P. barbatus* (PB_15423 and PB_12951), *A. cephalotes* (AC_01463 and AC_00782), *L. humile* (LH_18746 and LH_21623), *H. saltator* (Hsal_09512 and Has_l11112), *A. mellifera* *Am*InR-1 (XP_394771) and *Am*InR-2 (this work), and *C. elegans* Daf2 (NP_497650). Aligned sequence consensus were imported into PAUP 4.0b10 [278] and alignment gaps were treated as missing data. A neighbor-joining tree was generated and rooted using the *Ce*Daf-2, insulin receptor from nematode *C. elegans*.

Semi-quantitative RT-PCR (semi-Q RT-PCR)

To determine the transcriptional expression pattern of *Si*InRs in the fire ant, ants at different developmental stages and castes (~50 mg/each replication) and tissues from mated and virgin queens (~40 queens/each replication) were collected and their mRNA was extracted as previously mentioned above. The concentration and purity of mRNA was measured by nanodrop (Thermo Scientific, Wilmington, DE). cDNA was synthesized using mRNA (0.1 μg) and oligo-dT20 primer as previously mentioned. Semi-Q RT-PCR methodology was used to determine the gene expression level. Several specific primer sets and the optimal number of PCR amplification cycles for *Si*InR-1 and *Si*InR-2 were tested through preliminary runs. After tested, primer sets Si-IR2-f10/Si-IR2-r16 and Si-IR1f20/Si-IR1r11 were selected to specific amplify *Si*InR-1 (613bp) and *Si*InR-2 (583bp), respectively. PCR amplifications contained 2 μl of the diluted cDNA

(2 X dilution), 0.4 μM of each primer, 400 μM of dNTPs, 1 x reaction buffer and 1 μl Taq DA polymerase in a final volume of 50 μl. PCR parameters were 94 °C for 3 min, 30 cycles of 94 °C for 30 s, 60 °C for 60 s, and 72 °C for 40 s. The β-actin was used as an endogenous control. A fire ant β-actin fragment (557 bp) was originally obtained from PCR amplification of fire ant ovarian cDNA using degenerate primers, Act-3F and Act-4R for obtained the tick β-actin [279]. In semi-Q RT-PCR assays, primer set *Si*-actin-f1 and *Si*-actin-r1 was used to specific amplify the fire ant β-actin (519bp) as the internal control. PCR conditions for amplification of actin cDNA were identical to the receptor PCR amplification except that 22 cycles were used. One-tenth of the reaction (5 μl) was analyzed by agarose gel (1%) electrophoresis. Transcript abundance was determined based on the intensity of the amplified PCR bands using image J program. Relative mRNA expression levels from each of the samples were presented as the ratio of the band intensities of the receptor RT-PCR product over the corresponding β-actin RT-PCR product. The expression ratio in the same RT-PCR sample was averaged from two gels to limit the bias. Three replicates for each sample were analyzed using one-way ANOVA followed by a Tukey multiple comparison test. T-test was used for analyzing receptor expression between two receptors or between virgin and mated queens. Statistical analyses and graphs were performed using prism 4.0 (GraphPad, San Diego, CA, USA).

CHAPTER VI

CONCLUSIONS

Insect reproduction is controlled by complicated gene networks which are regulated by hormones and modulated by environmental stimuli. Juvenile hormone and/or ecdysone are believed to directly induce vitellogenesis. Neuropeptide hormones from the central nervous system appear to be upstream of these direct inducers present in the neuroendocrine system, and they may also be released into the hemolymph and act directly on peripheral tissues. This dissertation provides novel contributions to the understanding of insect reproductive physiology, biology of receptors from three different receptor superfamilies, and the possible roles of these receptors involved in endocrine control mechanisms in the red imported fire ant. These three receptors included the Vg receptor, sNPF receptor, and insulin receptors. The role of these receptor signaling pathways in essential physiological processes makes it an important subject for study in social insects, especially ants, in which the control of both feeding and reproduction is complex and poorly understood.

Our results on these receptors provide novel information for subsequent studies on the regulatory network hierarchy and overall coordination of pathways that control fire ant reproduction. Previously, only the transcript expression levels of Vg and sNPF receptors were known from the fire ant queen. To our knowledge, our work in chapter III is the first report of successful RNA interference of a VgR in hymenopterans and is the first report of successful RNA interference in any ant species. Chapter III describes

the first cellular localization of a sNPF receptor in the brain, SEG, and ovaries of any adult insect. In chapter V, the molecular characterization of two fire ant insulin receptors is studied in the fire ant for the first time. Insulin receptors cloned in this dissertation are the first cloned cDNA of insulin receptors from social insects. Therefore, studies in this dissertation not only fulfill knowledge of fire ant reproductive physiology, but also provide novel information helpful for other insect orders.

Contributions of this dissertation are summarized (Figure 6.1). First, this dissertation focuses on one critical step during vitellogenesis, the expression of a *Si*VgR in the ovaries of fire ant queens which is directly involved in oocyte development and egg production. We found that correct localization for functional *Si*VgR at the oocyte membrane did not occur until 12 days post-eclosion in virgin queens (Figure 6.1, labeled with 3). This time period in virgin queens coincides with the two weeks of maturation time required before a mating flight. Thus, the significant finding is that the previously undefined "maturation period" of virgin queens within the colony involves the correct localization of the *Si*VgR in the oocyte membrane. This correct localization appears to be a potential marker for the sexual maturation of queens and their readiness to fly for dispersal. The temporal expression analysis of the *Si*VgR protein in queens before and after mating shows that successfully mating, and not flight only, induces high *Si*VgR protein expression and subsequently egg production in mated queens. We next established the technique of RNA interference to silence gene expression in queen ovaries.

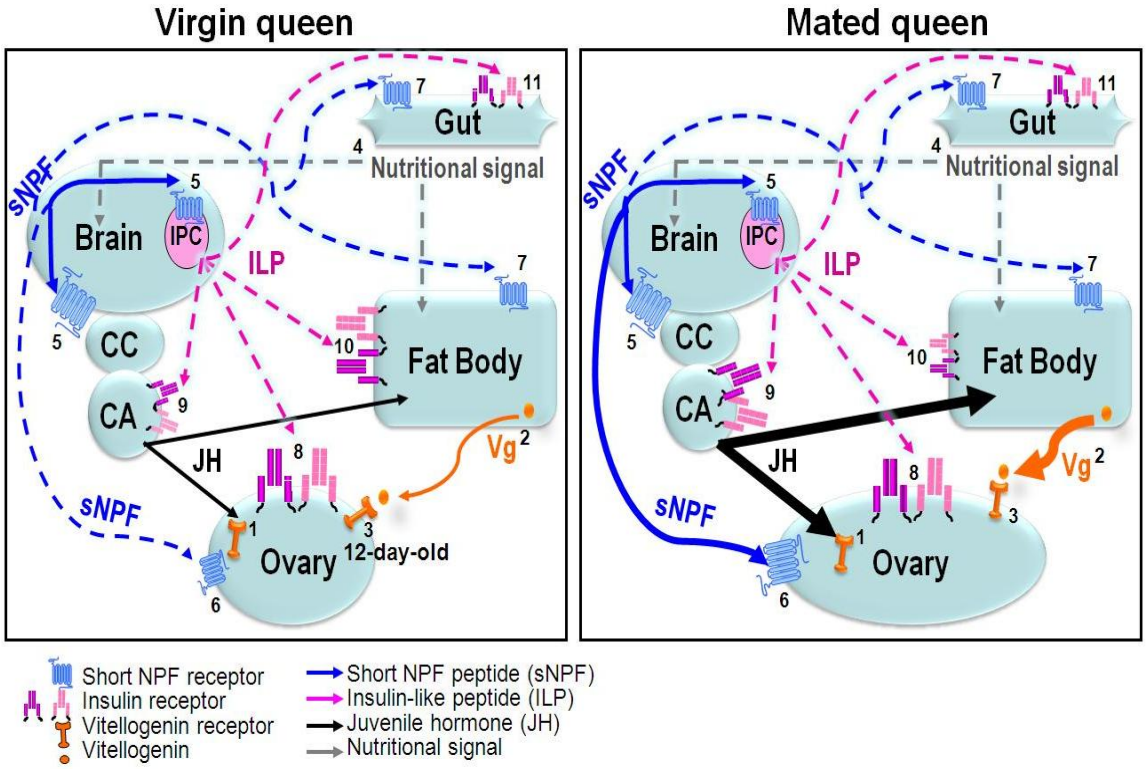

Figure 6.1. New information provided by this dissertation in the hormonal control of fire ant reproduction. Previously it was known that the mated queens have higher JH level than virgin queens. JH increases *Si*VgR transcripts[1] in the ovary and stimulates vitellogenesis[2] in the fat body [24,46,55,155,157]. In the ovaries of virgin queens within a colony, the correct localization for functional *Si*VgR at the oocyte membrane did not occur until 12 days post-eclosion; in the ovaries of mated queens within a colony, the *Si*VgR protein is highly expressed[3]. In the honey bee and fire ant, nutritional signals[4] regulate sNPF receptor expression [68,96] and also regulate vitellogenesis [68]. In the fire ant, this was demonstrated by starvation of mated queens resulting in reduced sNPF receptor transcripts in queen brains and reduced egg laying [68]. The localization of the sNPF receptor in many important regions of queen brain[5] including potential insulin-producing cells (IPC) links the receptor signaling pathway to behaviors such as foraging, learning, and food consumption. The sNPF receptor is also expressed in the mated queen ovaries and may involve in oocyte development[6]. The sNPF receptor transcripts were also detected in the fat body and the gut of queens [68]; however, we did not detect the receptor protein expression in these two tissues using western blot[7]. The expression level of insulin receptors is high in the ovaries of both queens and suggests that insulin receptors are important for ovary development in queens[8]. In the brain-CC-CA, lower *Si*InR-1 level is associated with lower juvenile hormone (JH) titer in virgin vs. mated queens[9], and higher *Si*InR-1 expression in the mated queen correlates with higher JH synthesis[9] (thick arrows), which in turn promotes ovarian growth. High *Si*InR-1 expression in the fat body of virgin queens[10] (smaller receptor icons) corresponds to storage of reserves for flight and future colony founding; however, the decreased level of *Si*InR-1 in the fat body in mated queens reveals a functional switch of this organ from storage to vitellogenin synthesis. Insulin receptors transcripts were also expressed in the fat body of both virgin and mated queens, however, the expression level was similar in virgin queens vs. mated queens. Dashed lines represent unknown pathways. CC: corpora cardiaca; CA: corpora allata.

We showed that queen ovaries can be atrophied by silencing the expression of the *Si*VgR. This is the first demonstration of the potential to manipulate reproduction in ants and has opened up the possibility of dissecting the gene networks that control reproduction and cast differentiation in fire ants.

Next, we targeted the potential upstream endocrine regulators in fire ant reproduction. Two candidate receptors were investigated: the sNPF receptor and insulin receptors (summarized in Figure 6.1). In insects, studies regarding the signaling pathways for sNPF and insulin-like peptides were until recently only on a very limited member of insect orders. Most of studies are obtained through the advantage of using transgenic flies; however, flies perform differently in many physiological and behavioral aspects when compared to social insects. Therefore, it is important to establish new knowledge of those two signaling pathways for fire ants.

With respect to the sNPF signaling pathway, we present evidence that the sNPF peptide(s) not only functions as neurotransmitter(s) or neuromodulator(s) within the brain and SEG (Figure 6.1, labeled with 5), but also might act as neurohormone(s) targeting the ovaries (Figure 6.1, labeled with 6). A comprehensive investigation of the localization of the sNPF receptor in the queen brain and SEG described in this dissertation, contributes to understanding the activity of the sNPF peptide in the brain of insects. This knowledge is especially important for social insects that display complex social and learning behaviors. The sNPF receptor signal present in several neuropils might link the receptor signaling pathway to behaviors such as foraging, learning, and food consumption. The presence of sNPF receptor in the oocyte suggests that the sNPF

signal transduction cascade may potentially play a new role in the oocyte pole and perhaps is also involved in oocyte development.

The insulin signaling pathway is a fundamental pathway that influences growth, reproduction, and longevity in solitary insects, and relates to division of labor, caste differentiation, foraging behavior, and also longevity in social insects (honey bee). We provide evidence that two insulin receptors are present in the fire ant. Sequence analyses showed that several post-translational modification sites are differentially conserved between *Si*InR-1 and *Si*InR-2 and other correspondingly social hymenopteran insulin receptors suggesting that functional diversification regulation may be present for the two receptors. This is the first such comparison providing evidence for the possible post-translational differential regulation in both receptors. The transcriptional expression analyses of two insulin receptors revealed that the abundance of both receptors was negatively correlated with body size and nutritional status in the larvae and pharate pupae of two castes, workers and reproductives. Thus, the IIS pathway may affect growth in fire ants differently than in *Drosophila*. In virgin and mated queens, the transcriptional expression pattern of both receptors in different tissues appears to correlate with tissue requirements for queen reproductive physiology and behaviors (Figure 6.1, labeled with 8-11). Toward the end of this project, the first fire ant genome draft was released and partial predicted sequences of two insulin receptor sequences are annotated [3], supporting our findings of two insulin receptor genes.

The sNPF and insulin signaling pathways may involve in many physiological functions in fire ants including feeding behavior, JH level, and reproduction. Therefore,

the studies of sNPF receptor and insulin receptors will not only further our understanding of the coordination and regulation of fire ant reproduction, but also will provide knowledge in the many other physiological processes that may affect colony functions. RNA interference of these two receptors will help to validate the function of these two types of receptors.

Still, several questions remain to be answered to fully understand the role of sNPF and insulin signaling pathway in the endocrine control of reproduction and in other, yet unknown functions. These and other studies will be facilitated by the development of novel specific antibodies and neuronal markers as the annotation of the fire ant genome is completed.

REFERENCES

1. Holldobler B & Wilson EO (1990) *The Ants*. Harvard University Press, Cambridge, MA.

2. Wilson EO & Holldobler B (2005) The rise of the ants: a phylogenetic and ecological explanation. *Proc Natl Acad Sci U S A* **102**, 7411-7414.

3. Wurm Y, Wang J, Riba-Grognuz O, Corona M, Nygaard S, Hunt BG, Ingram KK, Falquet L, Nipitwattanaphon M, Gotzek D, Dijkstra MB, Oettler J, Comtesse F, Shih CJ, Wu WJ, Yang CC, Thomas J, Beaudoing E, Pradervand S, Flegel V, Cook ED, Fabbretti R, Stockinger H, Long L, Farmerie WG, Oakey J, Boomsma JJ, Pamilo P, Yi SV, Heinze J, Goodisman MA, Farinelli L, Harshman K, Hulo N, Cerutti L, Xenarios I, Shoemaker D & Keller L (2011) The genome of the fire ant *Solenopsis invicta*. *Proc Natl Acad Sci U S A* **108**, 5679-5684.

4. Vander Meer RK, Morel L & Lofgren CS (1992) A comparison of queen oviposition rates from monogyne and polygyne fire ant, *Solenopsis invicta,* colonies. *Physiol Entomol* **17**, 384-390.

5. Raikhel AS & Dhadialla TS (1992) Accumulation of yolk proteins in insect oocytes. *Annu Rev Entomol* **37**, 217-251.

6. Sappington TW & Raikhel AS (1998) Molecular characteristics of insect vitellogenins and vitellogenin receptors. *Insect Biochem Mol Biol* **28**, 277-300.

7. Swevers L, Raikhel AS, Sappington TW, Shirk P & Iatrou K (2005) Vitellogenesis and post-vitellogenic maturation of the insect ovarian follicle. In *Comprehensive Molecular Insect Science* **3** (Gilbert LI, Iatrou K & Gill SS, eds), pp. 87-155. Elsevier, Amsterdam, The Netherlands.

8. Polzonetti-Magni AM, Mosconi G, Soverchia L, Kikuyama S & Carnevali O (2004) Multihormonal control of vitellogenesis in lower vertebrates. *Int Rev Cytol* **239**, 1-46.

9. Goldstein JL, Anderson RG & Brown MS (1979) Coated pits, coated vesicles, and receptor-mediated endocytosis. *Nature* **279**, 679-685.

10. Schonbaum CP, Perrino JJ & Mahowald AP (2000) Regulation of the vitellogenin receptor during *Drosophila melanogaster* oogenesis. *Mol Biol Cell* **11**, 511-521.

11. Snigirevskaya ES, Sappington TW & Raikhel AS (1997) Internalization and recycling of vitellogenin receptor in the mosquito oocyte. *Cell Tissue Res* **290**, 175-183.

12. Snigirevskaya ES & Raikhel AS (2004) Receptor mediated endocytosis in insect oocytes. In *Progress in Vitellogenesis. Reproductive Biology of Invertebrates* **7**, Part B (Raikhel AS & Sappington TW, eds), pp. 199-228. Science Publishers, Enfield, NH.

13. Bujo H, Hermann M, Kaderli MO, Jacobsen L, Sugawara S, Nimpf J, Yamamoto T & Schneider WJ (1994) Chicken oocyte growth is mediated by an eight ligand binding repeat member of the LDL receptor family. *EMBO J* **13**, 5165-5175.

14. Okabayashi K, Shoji H, Nakamura T, Hashimoto O, Asashima M & Sugino H (1996) cDNA cloning and expression of the Xenopus laevis vitellogenin receptor. *Biochem Biophys Res Commun* **224**, 406-413.

15. Davail B, Pakdel F, Bujo H, Perazzolo LM, Waclawek M, Schneider WJ & Le MF (1998) Evolution of oogenesis: the receptor for vitellogenin from the rainbow trout. *J Lipid Res* **39**, 1929-1937.

16. Li A, Sadasivam M & Ding JL (2003) Receptor-ligand interaction between vitellogenin receptor (VtgR) and vitellogenin (Vtg), implications on low density lipoprotein receptor and apolipoprotein B/E. The first three ligand-binding repeats of VtgR interact with the amino-terminal region of Vtg. *J Biol Chem* **278**, 2799-2806.

17. Hiramatsu N, Chapman RW, Lindzey JK, Haynes MR & Sullivan CV (2004) Molecular characterization and expression of vitellogenin receptor from white perch (*Morone americana*). *Biol Reprod* **70**, 1720-1730.

18. Mitchell III RD, Ross E, Osgood C, Sonenshine DE, Donohue KV, Khalil SM, Thompson DM & Michael RR (2007) Molecular characterization, tissue-specific expression and RNAi knockdown of the first vitellogenin receptor from a tick. *Insect Biochem Mol Biol* **37**, 375-388.

19. Boldbaatar D, Battsetseg B, Matsuo T, Hatta T, Umemiya-Shirafuji R, Xuan X & Fujisaki K (2008) Tick vitellogenin receptor reveals critical role in oocyte development and transovarial transmission of *Babesia* parasite. *Biochem Cell Biol* **86**, 331-344.

20. Tiu SH, Benzie J & Chan SM (2008) From hepatopancreas to ovary: molecular characterization of a shrimp vitellogenin receptor involved in the processing of vitellogenin. *Biol Reprod* **79**, 66-74.

21. Grant B & Hirsh D (1999) Receptor-mediated endocytosis in the *Caenorhabditis elegans* oocyte. *Mol Biol Cell* **10**, 4311-4326.

22. Schonbaum CP, Lee S & Mahowald AP (1995) The *Drosophila* yolkless gene encodes a vitellogenin receptor belonging to the low density lipoprotein receptor superfamily. *Proc Natl Acad Sci U S A* **92**, 1485-1489.

23. Sappington TW, Hays AR & Raikhel AS (1995) Mosquito vitellogenin receptor: purification, developmental and biochemical characterization. *Insect Biochem Mol Biol* **25**, 807-817.

24. Chen ME, Lewis DK, Keeley LL & Pietrantonio PV (2004) cDNA cloning and transcriptional regulation of the vitellogenin receptor from the imported fire ant, *Solenopsis invicta* Buren (Hymenoptera: Formicidae). *Insect Mol Biol* **13**, 195-204.

25. Shu YH, Wang JW, Lu K, Zhou JL, Zhou Q & Zhang GR (2011) The first vitellogenin receptor from a Lepidopteran insect: molecular characterization, expression patterns and RNA interference analysis. *Insect Mol Biol* **20**, 61-73.

26. Tufail M & Takeda M (2005) Molecular cloning, characterization and regulation of the cockroach vitellogenin receptor during oogenesis. *Insect Mol Biol* **14**, 389-401.

27. Ciudad L, Piulachs MD & Belles X (2006) Systemic RNAi of the cockroach vitellogenin receptor results in a phenotype similar to that of the *Drosophila* yolkless mutant. *FEBS J* **273**, 325-335.

28. Tufail M & Takeda M (2007) Molecular cloning and developmental expression pattern of the vitellogenin receptor from the cockroach, *Leucophaea maderae*. *Insect Biochem Mol Biol* **37**, 235-245.

29. Schneider WJ (1996) Vitellogenin receptors: oocyte-specific members of the low-density lipoprotein receptor supergene family. *Int Rev Cytol* **166**, 103-137.

30. Goldstein JL, Brown MS, Anderson RG, Russell DW & Schneider WJ (1985) Receptor-mediated endocytosis: concepts emerging from the LDL receptor system. *Annu Rev Cell Biol* **1**, 1-39.

31. Guidugli-Lazzarini KR, Nascimento AM, Tanaka ED, Piulachs MD, Hartfelder K, Bitondi MG & Simoes ZLP (2008) Expression analysis of putative vitellogenin and lipophorin receptors in honey bee (*Apis mellifera* L.) queens and workers. *J Insect Physiol* **54**, 1138-1147.

32. Tufail M & Takeda M (2009) Insect vitellogenin/lipophorin receptors: molecular structures, role in oogenesis, and regulatory mechanisms. *J Insect Physiol* **55**, 87-103.

33. Sappington TW, Kokoza VA, Cho WL & Raikhel AS (1996) Molecular characterization of the mosquito vitellogenin receptor reveals unexpected high homology to the *Drosophila* yolk protein receptor. *Proc Natl Acad Sci U S A* **93**, 8934-8939.

34. Ciudad L, Belles X & Piulachs MD (2007) Structural and RNAi characterization of the German cockroach lipophorin receptor, and the evolutionary relationships of lipoprotein receptors. *BMC Mol Biol* **8**, 53.

35. Chen ME (2003) cDNA cloning and transcriptional regulation of the vitellogenin receptor from the imported fire ant, *Solenopsis invicta* Buren (Hymenoptera: Formicidae). Ph.D. Dissertation, Department of Entomology, Texas A&M University, College Station.

36. Cho KH, Cheon HM, Kokoza V & Raikhel AS (2006) Regulatory region of the vitellogenin receptor gene sufficient for high-level, germ line cell-specific ovarian expression in transgenic *Aedes aegypti* mosquitoes. *Insect Biochem Mol Biol* **36**, 273-281.

37. Raikhel AS, Brown MR & Belles X (2005) Hormonal control of reproductive processes. In *Comprehensive Molecular Insect Science* **3** (Gilbert LI, Iatrou K & Gill SS, eds), pp. 433-491. Elsevier, Amsterdam, The Netherlands.

38. Shapiro JP & Hagedorn HH (1982) Juvenile hormone and the development of ovarian responsiveness to a brain hormone in the mosquito, *Aedes aegypti*. *Gen Comp Endocrinol* **46**, 176-183.

39. Gilbert LI, Serafin RB, Watkins NL & Richard DS (1998) Ecdysteroids regulate yolk protein uptake by *Drosophila melanogaster* oocytes. *J Insect Physiol* **44**, 637-644.

40. Li C, Kapitskaya MZ, Zhu J, Miura K, Segraves W & Raikhel AS (2000) Conserved molecular mechanism for the stage specificity of the mosquito vitellogenic response to ecdysone. *Dev Biol* **224**, 96-110.

41. Raikhel AS, Kokoza VA, Zhu J, Martin D, Wang SF, Li C, Sun G, Ahmed A, Dittmer N & Attardo G (2002) Molecular biology of mosquito vitellogenesis: from basic studies to genetic engineering of antipathogen immunity. *Insect Biochem Mol Biol* **32**, 1275-1286.

42. Hurd H, Ellams KM, Major M & Webb TJ (1997) The interplay between patency, microsomal Na(+)/K(+) ATPase activity and juvenile hormone, in *Tenebrio molitor* parasitized by *Hymenolepsis diminuta*. *J Insect Physiol* **43**, 337-343.

43. Telfer WH & Woodruff RI (2002) Ion physiology of vitellogenic follicles. *J Insect Physiol* **48**, 915-923.

44. Pszczolkowski MA, Peterson A, Srinivasan A & Ramaswamy SB (2005) Pharmacological analysis of ovarial patency in *Heliothis virescens*. *J Insect Physiol* **51**, 445-453.

45. Pszczolkowski MA, Olson E, Rhine C & Ramaswamy SB (2008) Role for calcium in the development of ovarial patency in *Heliothis virescens*. *J Insect Physiol* **54**, 358-366.

46. Burns SN, Teal PE, Vander Meer RK, Nation JL & Vogt JT (2002) Identification and action of juvenile hormone III from sexually mature alate females of the red imported fire ant, *Solenopsis invicta*. *J Insect Physiol* **48**, 357-365.

47. Bloch G, Borst DW, Huang Z, Robinson GE, Cnaani J & Hefetz A (2000) Juvenile hormone titers, juvenile hormone biosynthesis, ovarian development and social environment in *Bombus terrestris*. *J Insect Physiol* **46**, 47-57.

48. Geva S, Hartfelder K & Bloch G (2005) Reproductive division of labor, dominance, and ecdysteroid levels in hemolymph and ovary of the bumble bee *Bombus terrestris*. *J Insect Physiol* **51**, 811-823.

49. Brent C, Peeters C, Dietemann V, Crewe R & Vargo E (2006) Hormonal correlates of reproductive status in the queenless ponerine ant, *Streblognathus peetersi*. *J Comp Physiol A Neuroethol Sens Neural Behav Physiol* **192**, 315-320.

50. Sommer K, Hölldobler B & Rembold H (1993) Behavioral and physiological aspects of reproductive control in Diacamma species from Malaysia (Formicidae, Ponerinae). *Ethology* **94**, 162-170.

51. Guidugli KR, Nascimento AM, Amdam GV, Barchuk AR, Omholt S, Simoes ZL & Hartfelder K (2005) Vitellogenin regulates hormonal dynamics in the worker caste of a eusocial insect. *FEBS Lett* **579**, 4961-4965.

52. Bloch G, Sullivan JP & Robinson GE (2002) Juvenile hormone and circadian locomotor activity in the honey bee *Apis mellifera*. *J Insect Physiol* **48**, 1123-1131.

53. Hartfelder K & Emlen DJ (2005) Endocrine control of insect polyphenism. In *Comprehensive Molecular Insect Science* **3** (Gilbert LI, Iatrou K & Gill SS, eds), pp. 651-703. Elsevier, Amsterdam, The Netherlands.

54. Hartfelder K, Bitondi MM, Santana WC & Simoes ZL (2002) Ecdysteroid titer and reproduction in queens and workers of the honey bee and of a stingless bee: loss of

ecdysteroid function at increasing levels of sociality? *Insect Biochem Mol Biol* **32**, 211-216.

55. Robinson GE & Vargo EL (1997) Juvenile hormone in adult eusocial Hymenoptera: gonadotropin and behavioral pacemaker. *Arch Insect Biochem Physiol* **35**, 559-583.

56. Kuczer M, Rosinski G & Konopinska D (2007) Insect gonadotropic peptide hormones: some recent developments. *J Pept Sci* **13**, 16-26.

57. Cerstiaens A, Benfekih L, Zouiten H, Verhaert P, De Loof A & Schoofs L (1999) Led-NPF-1 stimulates ovarian development in locusts. *Peptides* **20**, 39-44.

58. Lee KS, Kwon OY, Lee JH, Kwon K, Min KJ, Jung SA, Kim AK, You KH, Tatar M & Yu K (2008) *Drosophila* short neuropeptide F signalling regulates growth by ERK-mediated insulin signaling. *Nat Cell Biol* **10**, 468-475.

59. Kaplan DD, Zimmermann G, Suyama K, Meyer T & Scott MP (2008) A nucleostemin family GTPase, NS3, acts in serotonergic neurons to regulate insulin signaling and control body size. *Genes Dev* **22**, 1877-1893.

60. Garofalo RS & Rosen OM (1988) Tissue localization of *Drosophila melanogaster* insulin receptor transcripts during development. *Mol Cell Biol* **8**, 1638-1647.

61. Riehle MA & Brown MR (2002) Insulin receptor expression during development and a reproductive cycle in the ovary of the mosquito *Aedes aegypti*. *Cell Tissue Res* **308**, 409-420.

62. Graf R, Neuenschwander S, Brown MR & Ackermann U (1997) Insulin-mediated secretion of ecdysteroids from mosquito ovaries and molecular cloning of the insulin receptor homologue from ovaries of bloodfed *Aedes aegypti*. *Insect Mol Biol* **6**, 151-163.

63. Helbling P & Graf R (1998) Localization of the mosquito insulin receptor homolog (MIR) in reproducing yellow fever mosquitoes (*Aedes aegypti*). *J Insect Physiol* **44**, 1127-1135.

64. Riehle MA & Brown MR (1999) Insulin stimulates ecdysteroid production through a conserved signaling cascade in the mosquito *Aedes aegypti*. *Insect Biochem Mol Biol* **29**, 855-860.

65. Roy SG, Hansen IA & Raikhel AS (2007) Effect of insulin and 20-hydroxyecdysone in the fat body of the yellow fever mosquito, *Aedes aegypti*. *Insect Biochem Mol Biol* **37**, 1317-1326.

66. Tu MP, Yin CM & Tatar M (2005) Mutations in insulin signaling pathway alter juvenile hormone synthesis in *Drosophila melanogaster*. *Gen Comp Endocrinol* **142**, 347-356.

67. Tu MP, Yin CM & Tatar M (2002) Impaired ovarian ecdysone synthesis of *Drosophila melanogaster* insulin receptor mutants. *Aging Cell* **1**, 158-160.

68. Chen ME & Pietrantonio PV (2006) The short neuropeptide F-like receptor from the red imported fire ant, *Solenopsis invicta* Buren (Hymenoptera: Formicidae). *Arch Insect Biochem Physiol* **61**, 195-208.

69. Borovsky D (2003) Trypsin-modulating oostatic factor: a potential new larvicide for mosquito control. *J Exp Biol* **206**, 3869-3875.

70. de Bono M & Bargmann CI (1998) Natural variation in a neuropeptide Y receptor homolog modifies social behavior and food response in *C. elegans*. *Cell* **94**, 679-689.

71. Macosko EZ, Pokala N, Feinberg EH, Chalasani SH, Butcher RA, Clardy J & Bargmann CI (2009) A hub-and-spoke circuit drives pheromone attraction and social behaviour in *C. elegans*. *Nature* **458**, 1171-1175.

72. Clynen E & Schoofs L (2009) Peptidomic survey of the locust neuroendocrine system. *Insect Biochem Mol Biol* **39**, 491-507.

73. Kreshchenko ND, Sedelnikov Z, Sheiman IM, Reuter M, Maule AG & Gustafsson MK (2008) Effects of neuropeptide F on regeneration in *Girardia tigrina* (Platyhelminthes). *Cell Tissue Res* **331**, 739-750.

74. Hummon AB, Richmond TA, Verleyen P, Baggerman G, Huybrechts J, Ewing MA, Vierstraete E, Rodriguez-Zas SL, Schoofs L, Robinson GE & Sweedler JV (2006) From the genome to the proteome: uncovering peptides in the *Apis* brain. *Science* **314**, 647-649.

75. Kuo LE, Kitlinska JB, Tilan JU, Li L, Baker SB, Johnson MD, Lee EW, Burnett MS, Fricke ST, Kvetnansky R, Herzog H & Zukowska Z (2007) Neuropeptide Y acts directly in the periphery on fat tissue and mediates stress-induced obesity and metabolic syndrome. *Nat Med* **13**, 803-811.

76. Dumont Y, Chabot JG & Quirion R (2004) Receptor autoradiography as mean to explore the possible functional relevance of neuropeptides: focus on new agonists and antagonists to study natriuretic peptides, neuropeptide Y and calcitonin gene-related peptides. *Peptides* **25**, 365-391.

77. Hokfelt T, Stanic D, Sanford SD, Gatlin JC, Nilsson I, Paratcha G, Ledda F, Fetissov S, Lindfors C, Herzog H, Johansen JE, Ubink R & Pfenninger KH (2008) NPY and its involvement in axon guidance, neurogenesis, and feeding. *Nutrition* **24**, 860-868.

78. De Loof A, Baggerman G, Breuer M, Claeys I, Cerstiaens A, Clynen E, Janssen T, Schoofs L & Vanden BJ (2001) Gonadotropins in insects: an overview. *Arch Insect Biochem Physiol* **47**, 129-138.

79. Wu Q, Zhao Z & Shen P (2005) Regulation of aversion to noxious food by *Drosophila* neuropeptide Y- and insulin-like systems. *Nat Neurosci* **8**, 1350-1355.

80. Lee G, Bahn JH & Park JH (2006) Sex- and clock-controlled expression of the neuropeptide F gene in *Drosophila*. *Proc Natl Acad Sci U S A* **103**, 12580-12585.

81. Xu J, Li M & Shen P (2010) A G-protein-coupled neuropeptide Y-like receptor suppresses behavioral and sensory response to multiple stressful stimuli in *Drosophila*. *J Neurosci* **30**, 2504-2512.

82. Krashes MJ, DasGupta S, Vreede A, White B, Armstrong JD & Waddell S (2009) A neural circuit mechanism integrating motivational state with memory expression in *Drosophila*. *Cell* **139**, 416-427.

83. Dierick HA & Greenspan RJ (2007) Serotonin and neuropeptide F have opposite modulatory effects on fly aggression. *Nat Genet* **39**, 678-682.

84. Lingo PR, Zhao Z & Shen P (2007) Co-regulation of cold-resistant food acquisition by insulin- and neuropeptide Y-like systems in *Drosophila melanogaster*. *Neuroscience* **148**, 371-374.

85. Wu Q, Wen T, Lee G, Park JH, Cai HN & Shen P (2003) Developmental control of foraging and social behavior by the *Drosophila* neuropeptide Y-like system. *Neuron* **39**, 147-161.

86. Wen T, Parrish CA, Xu D, Wu Q & Shen P (2005) *Drosophila* neuropeptide F and its receptor, NPFR1, define a signaling pathway that acutely modulates alcohol sensitivity. *Proc Natl Acad Sci U S A* **102**, 2141-2146.

87. Wu Q, Zhang Y, Xu J & Shen P (2005) Regulation of hunger-driven behaviors by neural ribosomal S6 kinase in *Drosophila*. *Proc Natl Acad Sci U S A* **102**, 13289-13294.

88. Gonzalez R & Orchard I (2009) Physiological activity of neuropeptide F on the hindgut of the blood-feeding hemipteran, *Rhodnius prolixus*. *J Insect Sci* **9**, 1-14.

89. Schoofs L, Clynen E, Cerstiaens A, Baggerman G, Wei Z, Vercammen T, Nachman R, De Loof A & Tanaka S (2001) Newly discovered functions for some myotropic neuropeptides in locusts. *Peptides* **22**, 219-227.

90. Nässel DR & Winther AM (2010) *Drosophila* neuropeptides in regulation of physiology and behavior. *Prog Neurobiol* **92**, 42-104.

91. Nässel DR, Enell LE, Santos JG, Wegener C & Johard HA (2008) A large population of diverse neurons in the *Drosophila* central nervous system expresses short neuropeptide F, suggesting multiple distributed peptide functions. *BMC Neurosci* **9**, 90.

92. Lee KS, You KH, Choo JK, Han YM & Yu K (2004) *Drosophila* short neuropeptide F regulates food intake and body size. *J Biol Chem* **279**, 50781-50789.

93. Lee KS, Hong SH, Kim AK, Ju SK, Kwon OY & Yu K (2009) Processed short neuropeptide F peptides regulate growth through the ERK-insulin pathway in *Drosophila melanogaster*. *FEBS Lett* **583**, 2573-2577.

94. Huybrechts J, De Loof A & Schoofs L (2004) Diapausing Colorado potato beetles are devoid of short neuropeptide F I and II. *Biochem Biophys Res Commun* **317**, 909-916.

95. Brockmann A, Annangudi SP, Richmond TA, Ament SA, Xie F, Southey BR, Rodriguez-Zas SR, Robinson GE & Sweedler JV (2009) Quantitative peptidomics reveal brain peptide signatures of behavior. *Proc Natl Acad Sci U S A* **106**, 2383-2388.

96. Ament SA, Velarde RA, Kolodkin MH, Moyse D & Robinson GE (2011) Neuropeptide Y-like signalling and nutritionally mediated gene expression and behaviour in the honey bee. *Insect Mol Biol* **20**, 335-345.

97. Marciniak P, Grodecki S, Konopinska D & Rosinski G (2008) Structure-activity relationships for the cardiotropic action of the Led-NPF-I peptide in the beetles *Tenebrio molitor* and *Zophobas atratus*. *J Pept Sci* **14**, 329-334.

98. Kahsai L, Kapan N, Dircksen H, Winther AM & Nässel DR (2010) Metabolic stress responses in *Drosophila* are modulated by brain neurosecretory cells that produce multiple neuropeptides. *PLoS One* **5**, e11480.

99. Kahsai L, Martin JR & Winther AM (2010) Neuropeptides in the *Drosophila* central complex in modulation of locomotor behavior. *J Exp Biol* **213**, 2256-2265.

100. Garczynski SF, Brown MR & Crim JW (2006) Structural studies of *Drosophila* short neuropeptide F: Occurrence and receptor binding activity. *Peptides* **27**, 575-582.

101. Yamanaka N, Yamamoto S, Zitnan D, Watanabe K, Kawada T, Satake H, Kaneko Y, Hiruma K, Tanaka Y, Shinoda T & Kataoka H (2008) Neuropeptide receptor transcriptome reveals unidentified neuroendocrine pathways. *PLoS ONE* **3**, e3048.

102. Mertens I, Meeusen T, Huybrechts R, De Loof A & Schoofs L (2002) Characterization of the short neuropeptide F receptor from *Drosophila melanogaster*. *Biochem Biophys Res Commun* **297**, 1140-1148.

103. Feng G, Reale V, Chatwin H, Kennedy K, Venard R, Ericsson C, Yu K, Evans PD & Hall LM (2003) Functional characterization of a neuropeptide F-like receptor from *Drosophila melanogaster*. *Eur J Neurosci* **18**, 227-238.

104. Garczynski SF, Crim JW & Brown MR (2007) Characterization and expression of the short neuropeptide F receptor in the African malaria mosquito, *Anopheles gambiae*. *Peptides* **28**, 109-118.

105. Wu Q & Brown MR (2006) Signaling and function of insulin-like peptides in insects. *Annu Rev Entomol* **51**, 1-24.

106. Ruan Y, Chen C, Cao Y & Garofalo RS (1995) The *Drosophila* insulin receptor contains a novel carboxyl-terminal extension likely to play an important role in signal transduction. *J Biol Chem* **270**, 4236-4243.

107. Fernandez R, Tabarini D, Azpiazu N, Frasch M & Schlessinger J (1995) The *Drosophila* insulin receptor homolog: a gene essential for embryonic development encodes two receptor isoforms with different signaling potential. *EMBO J* **14**, 3373-3384.

108. Chen C, Jack J & Garofalo RS (1996) The *Drosophila* insulin receptor is required for normal growth. *Endocrinology* **137**, 846-856.

109. Brogiolo W, Stocker H, Ikeya T, Rintelen F, Fernandez R & Hafen E (2001) An evolutionarily conserved function of the *Drosophila* insulin receptor and insulin-like peptides in growth control. *Curr Biol* **11**, 213-221.

110. Bohni R, Riesgo-Escovar J, Oldham S, Brogiolo W, Stocker H, Andruss BF, Beckingham K & Hafen E (1999) Autonomous control of cell and organ size by CHICO, a *Drosophila* homolog of vertebrate IRS1-4. *Cell* **97**, 865-875.

111. Tatar M, Kopelman A, Epstein D, Tu MP, Yin CM & Garofalo RS (2001) A mutant *Drosophila* insulin receptor homolog that extends life-span and impairs neuroendocrine function. *Science* **292**, 107-110.

112. LaFever L & Drummond-Barbosa D (2005) Direct control of germline stem cell division and cyst growth by neural insulin in *Drosophila*. *Science* **309**, 1071-1073.

113. Rulifson EJ, Kim SK & Nusse R (2002) Ablation of insulin-producing neurons in flies: growth and diabetic phenotypes. *Science* **296**, 1118-1120.

114. Broughton SJ, Piper MD, Ikeya T, Bass TM, Jacobson J, Driege Y, Martinez P, Hafen E, Withers DJ, Leevers SJ & Partridge L (2005) Longer lifespan, altered metabolism, and stress resistance in *Drosophila* from ablation of cells making insulin-like ligands. *Proc Natl Acad Sci U S A* **102**, 3105-3110.

115. Ikeya T, Galic M, Belawat P, Nairz K & Hafen E (2002) Nutrient-dependent expression of insulin-like peptides from neuroendocrine cells in the CNS contributes to growth regulation in *Drosophila*. *Curr Biol* **12**, 1293-1300.

116. Gronke S, Clarke DF, Broughton S, Andrews TD & Partridge L (2010) Molecular evolution and functional characterization of *Drosophila* insulin-like peptides. *PLoS Genet* **6**, e1000857.

117. Broughton S, Alic N, Slack C, Bass T, Ikeya T, Vinti G, Tommasi AM, Driege Y, Hafen E & Partridge L (2008) Reduction of DILP2 in *Drosophila* triages a metabolic phenotype from lifespan revealing redundancy and compensation among DILPs. *PLoS One* **3**, e3721.

118. Zhang H, Liu J, Li CR, Momen B, Kohanski RA & Pick L (2009) Deletion of *Drosophila* insulin-like peptides causes growth defects and metabolic abnormalities. *Proc Natl Acad Sci U S A* **106**, 19617-19622.

119. Yang CH, Belawat P, Hafen E, Jan LY & Jan YN (2008) *Drosophila* egg-laying site selection as a system to study simple decision-making processes. *Science* **319**, 1679-1683.

120. Clancy DJ, Gems D, Harshman LG, Oldham S, Stocker H, Hafen E, Leevers SJ & Partridge L (2001) Extension of life-span by loss of CHICO, a *Drosophila* insulin receptor substrate protein. *Science* **292**, 104-106.

121. Richard DS, Rybczynski R, Wilson TG, Wang Y, Wayne ML, Zhou Y, Partridge L & Harshman LG (2005) Insulin signaling is necessary for vitellogenesis in *Drosophila melanogaster* independent of the roles of juvenile hormone and ecdysteroids: female sterility of the *chico*^{1} insulin signaling mutation is autonomous to the ovary. *J Insect Physiol* **51**, 455-464.

122. Williams KD, Busto M, Suster ML, So AK, Ben-Shahar Y, Leevers SJ & Sokolowski MB (2006) Natural variation in *Drosophila melanogaster* diapause due to the insulin-regulated PI3-kinase. *Proc Natl Acad Sci U S A* **103**, 15911-15915.

123. Scanga SE, Ruel L, Binari RC, Snow B, Stambolic V, Bouchard D, Peters M, Calvieri B, Mak TW, Woodgett JR & Manoukian AS (2000) The conserved PI3'K/PTEN/Akt signaling pathway regulates both cell size and survival in *Drosophila*. *Oncogene* **19**, 3971-3977.

124. Verdu J, Buratovich MA, Wilder EL & Birnbaum MJ (1999) Cell-autonomous regulation of cell and organ growth in *Drosophila* by Akt/PKB. *Nat Cell Biol* **1**, 500-506.

125. Belgacem YH & Martin JR (2006) Disruption of insulin pathways alters trehalose level and abolishes sexual dimorphism in locomotor activity in *Drosophila*. *J Neurobiol* **66**, 19-32.

126. Belgacem YH & Martin JR (2007) Hmgcr in the corpus allatum controls sexual dimorphism of locomotor activity and body size via the insulin pathway in *Drosophila*. *PLoS ONE* **2**, e187.

127. Caldwell PE, Walkiewicz M & Stern M (2005) Ras activity in the *Drosophila* prothoracic gland regulates body size and developmental rate via ecdysone release. *Curr Biol* **15**, 1785-1795.

128. Colombani J, Bianchini L, Layalle S, Pondeville E, Dauphin-Villemant C, Antoniewski C, Carre C, Noselli S & Leopold P (2005) Antagonistic actions of ecdysone and insulins determine final size in *Drosophila*. *Science* **310**, 667-670.

129. Mirth C, Truman JW & Riddiford LM (2005) The role of the prothoracic gland in determining critical weight for metamorphosis in *Drosophila melanogaster*. *Curr Biol* **15**, 1796-1807.

130. Walkiewicz MA & Stern M (2009) Increased insulin/insulin growth factor signaling advances the onset of metamorphosis in *Drosophila*. *PLoS One* **4**, e5072.

131. Gu SH, Lin JL, Lin PL & Chen CH (2009) Insulin stimulates ecdysteroidogenesis by prothoracic glands in the silkworm, *Bombyx mori*. *Insect Biochem Mol Biol* **39**, 171-179.

132. Maniere G, Rondot I, Bullesbach EE, Gautron F, Vanhems E & Delbecque JP (2004) Control of ovarian steroidogenesis by insulin-like peptides in the blowfly (*Phormia regina*). *J Endocrinol* **181**, 147-156.

133. Brown MR, Clark KD, Gulia M, Zhao Z, Garczynski SF, Crim JW, Suderman RJ & Strand MR (2008) An insulin-like peptide regulates egg maturation and metabolism in the mosquito *Aedes aegypti*. *Proc Natl Acad Sci U S A* **105**, 5716-5721.

134. Arik AJ, Rasgon JL, Quicke KM & Riehle MA (2009) Manipulating insulin signaling to enhance mosquito reproduction. *BMC Physiol* **9**, 15.

135. Slaidina M, Delanoue R, Gronke S, Partridge L & Leopold P (2009) A *Drosophila* insulin-like peptide promotes growth during nonfeeding states. *Dev Cell* **17**, 874-884.

136. Francis VA, Zorzano A & Teleman AA (2010) dDOR is an EcR coactivator that forms a feed-forward loop connecting insulin and ecdysone signaling. *Curr Biol* **20**, 1799-1808.

137. de Azevedo SV & Hartfelder K (2008) The insulin signaling pathway in honey bee (*Apis mellifera*) caste development - differential expression of insulin-like peptides and insulin receptors in queen and worker larvae. *J Insect Physiol* **54**, 1064-1071.

138. Smith CD, Zimin A, Holt C, Abouheif E, Benton R, Cash E, Croset V, Currie CR, Elhaik E, Elsik CG, Fave MJ, Fernandes V, Gadau J, Gibson JD, Graur D, Grubbs KJ, Hagen DE, Helmkampf M, Holley JA, Hu H, Viniegra AS, Johnson BR, Johnson RM, Khila A, Kim JW, Laird J, Mathis KA, Moeller JA, Munoz-Torres MC, Murphy MC, Nakamura R, Nigam S, Overson RP, Placek JE, Rajakumar R, Reese JT, Robertson HM, Smith CR, Suarez AV, Suen G, Suhr EL, Tao S, Torres CW, van WE, Viljakainen L, Walden KK, Wild AL, Yandell M, Yorke JA & Tsutsui ND (2011) Draft genome of the globally widespread and invasive Argentine ant (*Linepithema humile*). *Proc Natl Acad Sci U S A* **108**, 5673-5678.

139. Bonasio R, Zhang G, Ye C, Mutti NS, Fang X, Qin N, Donahue G, Yang P, Li Q, Li C, Zhang P, Huang Z, Berger SL, Reinberg D, Wang J & Liebig J (2010) Genomic comparison of the ants *Camponotus floridanus* and *Harpegnathos saltator*. *Science* **329**, 1068-1071.

140. Suen G, Teiling C, Li L, Holt C, Abouheif E, Bornberg-Bauer E, Bouffard P, Caldera EJ, Cash E, Cavanaugh A, Denas O, Elhaik E, Fave MJ, Gadau J, Gibson JD, Graur D, Grubbs KJ, Hagen DE, Harkins TT, Helmkampf M, Hu H, Johnson BR, Kim J, Marsh SE, Moeller JA, Munoz-Torres MC, Murphy MC, Naughton MC, Nigam S, Overson R, Rajakumar R, Reese JT, Scott JJ, Smith CR, Tao S, Tsutsui ND, Viljakainen L, Wissler L, Yandell MD, Zimmer F, Taylor J, Slater SC, Clifton SW, Warren WC, Elsik CG, Smith CD, Weinstock GM, Gerardo NM & Currie CR (2011) The genome sequence of the leaf-cutter ant *Atta cephalotes* reveals insights into its obligate symbiotic lifestyle. *PLoS Genet* **7**, e1002007.

141. Smith CR, Smith CD, Robertson HM, Helmkampf M, Zimin A, Yandell M, Holt C, Hu H, Abouheif E, Benton R, Cash E, Croset V, Currie CR, Elhaik E, Elsik CG, Fave MJ, Fernandes V, Gibson JD, Graur D, Gronenberg W, Grubbs KJ, Hagen DE, Viniegra AS, Johnson BR, Johnson RM, Khila A, Kim JW, Mathis KA, Munoz-Torres MC, Murphy MC, Mustard JA, Nakamura R, Niehuis O, Nigam S, Overson RP, Placek JE, Rajakumar R, Reese JT, Suen G, Tao S, Torres CW, Tsutsui ND, Viljakainen L, Wolschin F & Gadau J (2011) Draft genome of the red harvester ant *Pogonomyrmex barbatus*. *Proc Natl Acad Sci U S A* **108**, 5667-5672.

142. Wilson EO (1971) *The Insect Societies*. Harvard University Press, Cambridge. MA.

143. Vinson SB, Pietrantonio PV, Lu HL & Coates CJ (2008) The physiology of reproduction in the imported fire ant, *Solenipsis invicta* Buren. In *Recent Advances in Insect Physiology, Toxicology and Molecular Biology* (Liu N, ed), pp. 153-171. Research Signpost, Kerala, India.

144. Tschinkel WR (2008) *The Fire Ants*. Harvard University Press, Cambridge, MA.

145. Barker JF (1979) Endocrine basis of wing casting and flight muscle histolysis in the fire ant *Solenopsis invicta*. *Experientia* **35**, 552-554.

146. Davis WL, Jones RG & Farmer GR (1989) Insect hemolymph factor promotes muscle histolysis in *Solenopsis*. *Anat Rec* **224**, 473-478.

147. Tian H, Vinson S.B. & Coates CJ (2004) Differential gene expression between alate and dealate queens in the red imported fire ant, *Solenopsis invicta* Buren (Hymenoptera: Formicidae). *Insect Biochem Mol Biol* **34**, 937-949.

148. Burns SN, Vander Meer RK & Teal PEA (2005) The effect of age and social environment on dealation in *Solenopsis invicta* (Hymenoptera: Formicidae) female alates. *Florida Entomol* **88**, 452-457.

149. Keller L & Ross KG (1993) Phenotypic plasticity and "cultural transmission" of alternative social organizations in the fire ant *Solenopsis invicta*. *Behav Ecol Sociobiol* **33**, 121-129.

150. Harshman LG & Zera AJ (2007) The cost of reproduction: the devil in the details. *Trends Ecol Evol* **22**, 80-86.

151. Voss SH & Blum M.S. (1987) Trophic and embryonated egg production in founding colonies of the fire ant *Solenopsis invicta* (Hymenoptera: Formicidae). *Sociobiology* **13**, 271-278.

152. Fletcher DJ & Blum MS (1981) Pheromonal control of dealation and oogenesis in virgin queen fire ants. *Science* **212**, 73-75.

153. Barker JF (1978) Neuroendocrine regulation of oocyte maturation in the imported fire ant *Solenopsis invicta*. *Gen Comp Endocrinol* **35**, 234-237.

154. LeConte Y & Hefetz A (2008) Primer pheromones in social Hymenoptera. *Annu Rev Entomol* **53**, 523-542.

155. Vargo EL & Laurel M (1994) Studies on the mode of action of a queen primer pheromone of the fire ant *Solenopsis invicta*. *J Insect Physiol* **40**, 601-610.

156. Vargo EL (1998) Primer pheromones in ants. In *Pheromone Communication in Social Insects: Ants, Wasps, Bees, and Termites* (Vander Meer RK, Breed MD, Winston ML & Espelie KE, eds), pp. 293-313. Westview Press, Boulder, CO.

157. Kearney GP, Toom PM & Blomquist GL (1977) Induction of de-alation in virgin female *Solenopsis invicta* with juvenile hormones. *Ann Entomol Soc Am* **70**, 699-701.

158. Brent CS & Vargo EL (2003) Changes in juvenile hormone biosynthetic rate and whole body content in maturing virgin queens of *Solenopsis invicta*. *J Insect Physiol* **49**, 967-974.

159. Boulay R, Hooper-Bui LM & Woodring J (2001) Oviposition and oogenesis in virgin fire ant females *Solenopsis invicta* are associated with a high level of dopamine in the brain. *Physiol Entomol* **26**, 294-299.

160. The Honeybee Genome Sequencing Consortium (2006) Insights into social insects from the genome of the honeybee *Apis mellifera*. *Nature* **443**, 931-949.

161. Lu HL & Pietrantonio PV (2011) Insect insulin receptors: insights from the sequence and caste expression analyses of two cloned hymenopteran insulin receptor cDNAs from the fire ant. *Insect Mol Biol* **Accepted**,

162. Wurm Y, Wang J & Keller L (2010) Changes in reproductive roles are associated with changes in gene expression in fire ant queens. *Mol Ecol* **19**, 1200-1211.

163. Werren JH, Richards S, Desjardins CA, Niehuis O, Gadau J, Colbourne JK, Bekeboom LW, Desplan C, Elsik CG, Grimmelikhuijzen CJ, Kitts P, Lynch JA, Murphy T, Oliveira DC, Smith CD, van de Zande L, Worley KC, Zdobnov EM, Aerts M, Albert S, Anaya VH, Anzola JM, Barchuk AR, Behura SK, Bera AN, Berenbaum MR, Bertossa RC, Bitondi MM, Bordenstein SR, Bork P, Bornberg-Bauer E, Brunain M, Cazzamali G, Chaboub L, Chacko J, Chavez D, Childers CP, Choi JH, Clark ME, Claudianos C, Clinton RA, Cree AG, Cristino AS, Dang PM, Darby AC, de Graaf DC, Devreese B, Dinh HH, Edwards R, Elango N, Elhaik E, Ermolaeva O, Evans JD, Foret S, Fowler GR, Gerlach D, Gibson JD, Gilbert DG, Graur D, Grunder S, Hagen DE, Han Y, Hauser F, Hultmark D, Hunter HC, Hurst

GD, Jhangian SN, Jiang H, Johnson RM, Jones AK, Junier T, Kadowaki T, Kamping A, Kapustin Y, Kechavarzi B, Kim J, Kim J, Kiryutin B, Koevoets T, Kovar CL, Kriventseva EV, Kucharski R, Lee H, Lee SL, Lees K, Lewis LR, Loehlin DW, Logsdon JM, Jr., Lopez JA, Lozado RJ, Maglott D, Maleszka R, Mayampurath A, Mazur DJ, McClure MA, Moore AD, Morgan MB, Muller J, Munoz-Torres MC, Muzny DM, Nazareth LV, Neupert S, Nguyen NB, Nunes FM, Oakeshott JG, Okwuonu GO, Pannebakker BA, Pejaver VR, Peng Z, Pratt SC, Predel R, Pu LL, Ranson H, Raychoudhury R, Rechtsteiner A, Reese JT, Reid JG, Riddle M, Robertson HM, Romero-Severson J, Rosenberg M, Sackton TB, Sattelle DB, Schluns H, Schmitt T, Schneider M, Schuler A, Schurko AM, Shuker DM, Simoes ZL, Sinha S, Smith Z, Solovyev V, Souvorov A, Springauf A, Stafflinger E, Stage DE, Stanke M, Tanaka Y, Telschow A, Trent C, Vattathil S, Verhulst EC, Viljakainen L, Wanner KW, Waterhouse RM, Whitfield JB, Wilkes TE, Williamson M, Willis JH, Wolschin F, Wyder S, Yamada T, Yi SV, Zecher CN, Zhang L & Gibbs RA (2010) Functional and evolutionary insights from the genomes of three parasitoid *Nasonia* species. *Science* **327**, 343-348.

164. Sappington TW & Raikhel AS (2004) Insect vitellogenin/yolk protein receptors. In *Progress in Vitellogenesis, Reproductive Biology of Invertebrates* **7**, Part B (Raikhel AS & Sappington TW, eds), pp. 229-264. Science Publishers, Enfield, NH.

165. Amdam GV, Norberg K, Hagen A & Omholt SW (2003) Social exploitation of vitellogenin. *Proc Natl Acad Sci U S A* **100**, 1799-1802.

166. Hafer J & Ferenz HJ (1991) Locust vitellogenin receptor: an acidic glycoprotein with N- and O-linked oligosaccharides. *Comp Biochem Physiol* **100B**, 579-586.

167. Hafer J, Fischer A & Ferenz HJ (1992) Identification of the yolk receptor protein in oocytes of *Nereis virens* (Annelida, Polychaeta) and comparison with the locust vitellogenin receptor. *J Comp Physiol B* **162**, 148-152.

168. Hafer J & Ferenz HJ (1994) Yolk formation in *Locusta migratoria* and *Schistocerca gregaria*: Related ligands and oocyte receptors. *Arch Insect Biochem Physiol* **25**, 107-120.

169. Warrier S & Subramoniam T (2002) Receptor mediated yolk protein uptake in the crab *Scylla serrata*: crustacean vitellogenin receptor recognizes related mammalian serum lipoproteins. *Mol Reprod Dev* **61**, 536-548.

170. Toth AL & Robinson GE (2007) Evo-devo and the evolution of social behavior. *Trends Genet* **23**, 334-341.

171. Smith CR, Toth AL, Suarez AV & Robinson GE (2008) Genetic and genomic analyses of the division of labour in insect societies. *Nat Rev Genet* **9**, 735-748.

172. Richard DS, Gilbert M, Crum B, Hollinshead DM, Schelble S & Scheswohl D (2001) Yolk protein endocytosis by oocytes in *Drosophila melanogaster*: immunofluorescent localization of clathrin, adaptin and the yolk protein receptor. *J Insect Physiol* **47**, 715-723.

173. Seehuus S-C, Norbert K, Krekling T, Fondrk K & Amdam GV (2007) Immumogold localization of vitellogenin in the ovaries, hypopharyngeal glands and head fat bodies of honey bee workers, *Apis mellifera*. *J Insect Sci* **7**, 52.

174. Cho KH & Raikhel AS (2001) Organization and developmental expression of the mosquito vitellogenin receptor gene. *Insect Mol Biol* **10**, 465-474.

175. Obin MS & Vander Meer RK (1994) Alate semiochemicals release worker behavior during fire ant nuptial flights. *J Entomol Sci* **29**, 143-151.

176. Alonso AE & Vander Meer R.K. (1997) Source of alate excitant pheromones in the red imported fire ant *Solenopsis invicta* (Hymenoptera: Formicidae). *J Insect Behav* **10**, 541-555.

177. Culi J & Mann RS (2003) Boca, an endoplasmic reticulum protein required for wingless signaling and trafficking of LDL receptor family members in *Drosophila*. *Cell* **112**, 343-354.

178. Wilhelm JE, Buszczak M & Sayles S (2005) Efficient protein trafficking requires trailer hitch, a component of a ribonucleoprotein complex localized to the ER in *Drosophila*. *Dev Cell* **9**, 675-685.

179. Sommer B, Oprins A, Rabouille C & Munro S (2005) The exocyst component Sec5 is present on endocytic vesicles in the oocyte of *Drosophila melanogaster*. *J Cell Biol* **169**, 953-963.

180. Lewis DK, Campbell JQ, Sowa SM, Chen M, Vinson SB & Keeley LL (2001) Characterization of vitellogenin in the red imported fire ant, *Solenopsis invicta* (Hymenoptera: Apocrita: Formicidae). *J Insect Physiol* **47**, 543-551.

181. Glancey BM, Stringer CE & Bishop PM (1973) Trophic egg production in the imported fire ant, *Solenopsis invicta*. *J Georgia Entomol Soc* **8**, 217-220.

182. Azizi T, Johnston JS & Vinson SB (2008) Initiation of flight muscle apoptosis and wing casting in the red imported fire ant, *Solenopsis invicta*. *Physiol Entomol* **34**, 79-85.

183. Kubli E (2003) Sex-peptides: seminal peptides of the *Drosophila* male. *Cell Mol Life Sci* **60**, 1689-1704.

184. Yapici N, Kim YJ, Ribeiro C & Dickson BJ (2008) A receptor that mediates the post-mating switch in *Drosophila* reproductive behaviour. *Nature* **451**, 33-37.

185. Goodman WG & Granger NA (2005) The Juvenile Hormones. In *Comprehensive Molecular Insect Science* **3** (Gilbert LI, Iatrou K & Gill SS, eds), pp. 320-385. Elsevier, Amsterdam, The Netherlands.

186. Zhu J, Chen L & Raikhel AS (2003) Posttranscriptional control of the competence factor betaFTZ-F1 by juvenile hormone in the mosquito *Aedes aegypti*. *Proc Natl Acad Sci U S A* **100**, 13338-13343.

187. Chen JS, Snowden K, Mitchell F, Sokolova J, Fuxa J & Bradleigh VS (2004) Sources of spores for the possible horizontal transmission of *Thelohania solenopsae* (Microspora: Thelohaniidae) in the red imported fire ants, *Solenopsis invicta*. *J Invertebr Pathol* **85**, 139-145.

188. Drees BM & Ellison SL (1998) Collecting and maintaining colonies of red imported fire ants for study. *Fire Ant Plan Fact Sheet* #008; Department of Entomology, Texas A&M University, College Station.

189. Schultz J, Milpetz F, Bork P & Ponting CP (1998) SMART, a simple modular architecture research tool: identification of signaling domains. *Proc Natl Acad Sci U S A* **95**, 5857-5864.

190. Letunic I, Goodstadt L, Dickens NJ, Doerks T, Schultz J, Mott R, Ciccarelli F, Copley RR, Ponting CP & Bork P (2002) Recent improvements to the SMART domain-based sequence annotation resource. *Nucleic Acids Res* **30**, 242-244.

191. Saksena S, Shao Y, Braunagel SC, Summers MD & Johnson AE (2004) Cotranslational integration and initial sorting at the endoplasmic reticulum translocon of proteins destined for the inner nuclear membrane. *Proc Natl Acad Sci U S A* **101**, 12537-12542.

192. Lu HL, Vinson SB & Pietrantonio PV (2009) Oocyte membrane localization of vitellogenin receptor coincides with queen flying age, and receptor silencing by RNAi disrupts egg formation in fire ant virgin queens. *FEBS J* **276**, 3110-3123.

193. Belles X (2010) Beyond *Drosophila*: RNAi in vivo and functional genomics in insects. *Annu Rev Entomol* **55**, 111-128.

194. Azorsa DO, Mousses S & Caplen NJ (2006) Gene silencing through RNA interference: potential for terapeutics and functional genomics. In *Peptide Nucleic Acids, Morpholinos and Related Antisense Biomolecules* (Jason CG & During MJ, eds), pp. 252-264. Kluwer Academic/Plenum Publishers, New York.

195. Fire A, Xu S, Montgomery MK, Kostas SA, Driver SE & Mello CC (1998) Potent and specific genetic interference by double-stranded RNA in *Caenorhabditis elegans*. *Nature* **391**, 806-811.

196. Cruz J, Mane-Padros D, Belles X & Martin D (2006) Functions of the ecdysone receptor isoform-A in the hemimetabolous insect *Blattella germanica* revealed by systemic RNAi *in vivo*. *Dev Biol* **297**, 158-171.

197. Hatta T, Umemiya R, Liao M, Gong H, Harnnoi T, Tanaka M, Miyoshi T, Boldbaatar D, Battsetseg B, Zhou J, Xuan X, Tsuji N, Taylor D & Fujisaki K (2007) RNA interference of cytosolic leucine aminopeptidase reduces fecundity in the hard tick, *Haemaphysalis longicornis*. *Parasitol Res* **100**, 847-854.

198. Elalayli M, Hall JD, Fakhouri M, Neiswender H, Ellison TT, Han Z, Roon P & Lemosy EK (2008) Palisade is required in the *Drosophila* ovary for assembly and function of the protective vitelline membrane. *Dev Biol* **319**, 359-369.

199. Pelisson A, Sarot E, Payen-Groschene G & Bucheton A (2007) A novel repeat-associated small interfering RNA-mediated silencing pathway downregulates complementary sense gypsy transcripts in somatic cells of the *Drosophila* ovary. *J Virol* **81**, 1951-1960.

200. Zhu X & Stein D (2004) RNAi-mediated inhibition of gene function in the follicle cell layer of the *Drosophila* ovary. *Genesis* **40**, 101-108.

201. Lynch JA & Desplan C (2006) A method for parental RNA interference in the wasp *Nasonia vitripennis*. *Nat Protoc* **1**, 486-494.

202. Amdam GV, Norberg K, Page RE, Jr., Erber J & Scheiner R (2006) Downregulation of vitellogenin gene activity increases the gustatory responsiveness of honey bee workers (*Apis mellifera*). *Behav Brain Res* **169**, 201-205.

203. Amdam GV, Simoes ZL, Guidugli KR, Norberg K & Omholt SW (2003) Disruption of vitellogenin gene function in adult honeybees by intra-abdominal injection of double-stranded RNA. *BMC Biotechnol* **3**, 1.

204. Farooqui T, Vaessin H & Smith BH (2004) Octopamine receptors in the honeybee (*Apis mellifera*) brain and their disruption by RNA-mediated interference. *J Insect Physiol* **50**, 701-713.

205. Cormack BP, Valdivia RH & Falkow S (1996) FACS-optimized mutants of the green fluorescent protein (GFP). *Gene* **173**, 33-38.

206. Ma Y, Creanga A, Lum L & Beachy PA (2006) Prevalence of off-target effects in *Drosophila* RNA interference screens. *Nature* **443**, 359-363.

207. Perrimon N & Mathey-Prevot B (2007) Matter arising: off-targets and genome-scale RNAi screens in *Drosophila*. *Fly (Austin)* **1**, 1-5.

208. Gordon KH & Waterhouse PM (2007) RNAi for insect-proof plants. *Nat Biotechnol* **25**, 1231-1232.

209. DiMario PJ & Mahowald AP (1987) Female sterile (1) yolkless: a recessive female sterile mutation in *Drosophila melanogaster* with depressed numbers of coated pits and coated vesicles within the developing oocytes. *J Cell Biol* **105**, 199-206.

210. Christie AE (2008) *In silico* analyses of peptide paracrines/hormones in Aphidoidea. *Gen Comp Endocrinol* **159**, 67-79.

211. Gard AL, Lenz PH, Shaw JR & Christie AE (2009) Identification of putative peptide paracrines/hormones in the water flea *Daphnia pulex* (Crustacea; Branchiopoda; Cladocera) using transcriptomics and immunohistochemistry. *Gen Comp Endocrinol* **160**, 271-287.

212. Hauser F, Neupert S, Williamson M, Predel R, Tanaka Y & Grimmelikhuijzen CJ (2010) Genomics and peptidomics of neuropeptides and protein hormones present in the parasitic wasp *Nasonia vitripennis*. *J Proteome Res* **9**, 5296-5310.

213. Spittaels K, Verhaert P, Shaw C, Johnston RN, Devreese B, Van BJ & De Loof A (1996) Insect neuropeptide F (NPF)-related peptides: isolation from Colorado potato beetle (*Leptinotarsa decemlineata*) brain. *Insect Biochem Mol Biol* **26**, 375-382.

214. Predel R, Russell WK, Russell DH, Lopez J, Esquivel J & Nachman RJ (2008) Comparative peptidomics of four related hemipteran species: pyrokinins, myosuppressin, corazonin, adipokinetic hormone, sNPF, and periviscerokinins. *Peptides* **29**, 162-167.

215. Riehle MA, Garczynski SF, Crim JW, Hill CA & Brown MR (2002) Neuropeptides and peptide hormones in *Anopheles gambiae*. *Science* **298**, 172-175.

216. Reale V, Chatwin HM & Evans PD (2004) The activation of G-protein gated inwardly rectifying K^+ channels by a cloned *Drosophila melanogaster* neuropeptide F-like receptor. *Eur J Neurosci* **19**, 570-576.

217. Rollmann SM, Yamamoto A, Goossens T, Zwarts L, Callaerts-Vegh Z, Callaerts P, Norga K, Mackay TF & Anholt RR (2007) The early developmental gene

Semaphorin 5c contributes to olfactory behavior in adult *Drosophila*. *Genetics* **176**, 947-956.

218. Luer K & Technau GM (2009) Single cell cultures of *Drosophila* neuroectodermal and mesectodermal central nervous system progenitors reveal different degrees of developmental autonomy. *Neural Dev* **4**, 30.

219. Schurmann FW & Erber J (1990) FMRFamide-like immunoreactivity in the brain of the honeybee (*Apis mellifera*). A light-and electron microscopical study. *Neuroscience* **38**, 797-807.

220. Sinakevitch I, Niwa M & Strausfeld NJ (2005) Octopamine-like immunoreactivity in the honey bee and cockroach: comparable organization in the brain and subesophageal ganglion. *J Comp Neurol* **488**, 233-254.

221. Chapman RF (1969) *The Insects: Structure and Function*. Cambridge University Press, New York, NY.

222. Veenstra JA (2009) Peptidergic paracrine and endocrine cells in the midgut of the fruit fly maggot. *Cell Tissue Res* **336**, 309-323.

223. Johard HA, oishii T, ircksen H, usumano P, ouyer F, elfrich-Förster C & Nässel DR (2009) Peptidergic clock neurons in *Drosophila*: ion transport peptide and short neuropeptide F in subsets of dorsal and ventral lateral neurons. *J Comp Neurol* **516**, 59-73.

224. Johard HA, Enell LE, Gustafsson E, Trifilieff P, Veenstra JA & Nässel DR (2008) Intrinsic neurons of *Drosophila* mushroom bodies express short neuropeptide F: relations to extrinsic neurons expressing different neurotransmitters. *J Comp Neurol* **507**, 1479-1496.

225. Carlsson MA, Diesner M, Schachtner J & Nässel DR (2010) Multiple neuropeptides in the *Drosophila* antennal lobe suggest complex modulatory circuits. *J Comp Neurol* **518**, 3359-3380.

226. Kim YJ, Zitnan D, Cho KH, Schooley DA, Mizoguchi A & Adams ME (2006) Central peptidergic ensembles associated with organization of an innate behavior. *Proc Natl Acad Sci U S A* **103**, 14211-14216.

227. Park D, Veenstra JA, Park JH & Taghert PH (2008) Mapping peptidergic cells in *Drosophila*: where DIMM fits in. *PLoS One* **3**, e1896.

228. Eichmuller S, Hammer M & Schafer S (1991) Neurosecretory cells in the honeybee brain and suboesophageal ganglion show FMRFamide-like immunoreactivity. *J Comp Neurol* **312**, 164-174.

229. Cao C & Brown MR (2001) Localization of an insulin-like peptide in brains of two flies. *Cell Tissue Res* **304**, 317-321.

230. Fahrbach SE (2006) Structure of the mushroom bodies of the insect brain. *Annu Rev Entomol* **51**, 209-232.

231. Gronenberg W (1999) Modality-specific segregation of input to ant mushroom bodies. *Brain Behav Evol* **54**, 85-95.

232. Seid MA, Harris KM & Traniello JF (2005) Age-related changes in the number and structure of synapses in the lip region of the mushroom bodies in the ant *Pheidole dentata*. *J Comp Neurol* **488**, 269-277.

233. Farris SM, Abrams AI & Strausfeld NJ (2004) Development and morphology of class II Kenyon cells in the mushroom bodies of the honey bee, *Apis mellifera*. *J Comp Neurol* **474**, 325-339.

234. Strausfeld NJ (2002) Organization of the honey bee mushroom body: representation of the calyx within the vertical and gamma lobes. *J Comp Neurol* **450**, 4-33.

235. Mobbs P (1982) The brain of the honey bee *Apis mellifera*. *Philosophical Transactions of the Royal Society B: Biological Sciences* **298**, 309-354.

236. Balling A, Technau GM & Heisenberg M (1987) Are the structural changes in adult *Drosophila* mushroom bodies memory traces? Studies on biochemical learning mutants. *J Neurogenet* **4**, 65-73.

237. Strauss R (2002) The central complex and the genetic dissection of locomotor behaviour. *Curr Opin Neurobiol* **12**, 633-638.

238. Fussnecker BL, Smith BH & Mustard JA (2006) Octopamine and tyramine influence the behavioral profile of locomotor activity in the honey bee (*Apis mellifera*). *J Insect Physiol* **52**, 1083-1092.

239. Hardie SL, Zhang JX & Hirsh J (2007) Trace amines differentially regulate adult locomotor activity, cocaine sensitivity, and female fertility in *Drosophila melanogaster*. *Dev Neurobiol* **67**, 1396-1405.

240. Seid MA & Wehner R (2008) Ultrastructure and synaptic differences of the boutons of the projection neurons between the lip and collar regions of the mushroom bodies in the ant, *Cataglyphis albicans*. *J Comp Neurol* **507**, 1102-1108.

241. Schachtner J, Schmidt M & Homberg U (2005) Organization and evolutionary trends of primary olfactory brain centers in Tetraconata (Crustacea+Hexapoda). *Arthropod Struct Dev* **34**, 257-299.

242. Marin EC, Jefferis GS, Komiyama T, Zhu H & Luo L (2002) Representation of the glomerular olfactory map in the *Drosophila* brain. *Cell* **109**, 243-255.

243. Kreissl S, Eichmuller S, Bicker G, Rapus J & Eckert M (1994) Octopamine-like immunoreactivity in the brain and subesophageal ganglion of the honeybee. *J Comp Neurol* **348**, 583-595.

244. Schroter U, Malun D & Menzel R (2007) Innervation pattern of suboesophageal ventral unpaired median neurones in the honeybee brain. *Cell Tissue Res* **327**, 647-667.

245. Barron AB, Schulz DJ & Robinson GE (2002) Octopamine modulates responsiveness to foraging-related stimuli in honey bees (*Apis mellifera*). *J Comp Physiol A Neuroethol Sens Neural Behav Physiol* **188**, 603-610.

246. Barron AB & Robinson GE (2005) Selective modulation of task performance by octopamine in honey bee (*Apis mellifera*) division of labour. *J Comp Physiol A Neuroethol Sens Neural Behav Physiol* **191**, 659-668.

247. Barron AB, Maleszka R, Vander Meer RK & Robinson GE (2007) Octopamine modulates honey bee dance behavior. *Proc Natl Acad Sci U S A* **104**, 1703-1707.

248. Giray T, Galindo-Cardona A & Oskay D (2007) Octopamine influences honey bee foraging preference. *J Insect Physiol* **53**, 691-698.

249. Hunt GJ (2007) Flight and fight: a comparative view of the neurophysiology and genetics of honey bee defensive behavior. *J Insect Physiol* **53**, 399-410.

250. Schulz DJ & Robinson GE (2001) Octopamine influences division of labor in honey bee colonies. *J Comp Physiol A* **187**, 53-61.

251. Spivak M, Masterman R, Ross R & Mesce KA (2003) Hygienic behavior in the honey bee (*Apis mellifera* L.) and the modulatory role of octopamine. *J Neurobiol* **55**, 341-354.

252. Vander Meer RK, Preston CA & Hefetz A (2008) Queen regulates biogenic amine level and nestmate recognition in workers of the fire ant, *Solenopsis invicta*. *Naturwissenschaften* **95**, 1155-1158.

253. Vaccari S, Horner K, Mehlmann LM & Conti M (2008) Generation of mouse oocytes defective in cAMP synthesis and degradation: endogenous cyclic AMP is essential for meiotic arrest. *Dev Biol* **316**, 124-134.

254. Sheng Y, Wang L, Liu XS, Montplaisir V, Tiberi M, Baltz JM & Liu XJ (2005) A serotonin receptor antagonist induces oocyte maturation in both frogs and mice: evidence that the same G protein-coupled receptor is responsible for maintaining meiosis arrest in both species. *J Cell Physiol* **202**, 777-786.

255. Rios-Cardona D, Ricardo-Gonzalez RR, Chawla A & Ferrell JE, Jr. (2008) A role for GPRx, a novel GPR3/6/12-related G-protein coupled receptor, in the maintenance of meiotic arrest in *Xenopus laevis* oocytes. *Dev Biol* **317**, 380-388.

256. Edson MA, Lin YN & Matzuk MM (2010) Deletion of the novel oocyte-enriched gene, *Gpr149*, leads to increased fertility in mice. *Endocrinology* **151**, 358-368.

257. Shmueli A, Cohen-Gazala O & Neuman-Silberberg FS (2002) Gurken, a TGF-alpha-like protein involved in axis determination in *Drosophila*, directly binds to the EGF-receptor homolog Egfr. *Biochem Biophys Res Commun* **291**, 732-737.

258. Bastock R & Strutt D (2007) The planar polarity pathway promotes coordinated cell migration during *Drosophila* oogenesis. *Development* **134**, 3055-3064.

259. Chintapalli VR, Wang J & Dow JA (2007) Using FlyAtlas to identify better *Drosophila melanogaster* models of human disease. *Nat Genet* **39**, 715-720.

260. Lu HL, Kersch C & Pietrantonio PV (2010) The kinin receptor is expressed in the Malpighian tubule stellate cells in the mosquito *Aedes aegypti* (L.): A new model needed to explain ion transport? *Insect Biochem Mol Biol* **41**, 135-140.

261. Belfiore A, Frasca F, Pandini G, Sciacca L & Vigneri R (2009) Insulin receptor isoforms and insulin receptor/insulin-like growth factor receptor hybrids in physiology and disease. *Endocr Rev* **30**, 586-623.

262. Piper MD, Selman C, McElwee JJ & Partridge L (2008) Separating cause from effect: how does insulin/IGF signalling control lifespan in worms, flies and mice? *J Intern Med* **263**, 179-191.

263. Taguchi A & White MF (2008) Insulin-like signaling, nutrient homeostasis, and life span. *Annu Rev Physiol* **70**, 191-212.

264. Giannakou ME & Partridge L (2007) Role of insulin-like signalling in Drosophila lifespan. *Trends Biochem Sci* **32**, 180-188.

265. Baker KD & Thummel CS (2007) Diabetic larvae and obese flies-emerging studies of metabolism in *Drosophila*. *Cell Metab* **6**, 257-266.

266. Wolschin F, Mutti NS & Amdam GV (2010) Insulin receptor substrate influences female caste development in honeybees. *Biol Lett* **7**, 112-115.

267. Wheeler DE, Buck N & Evans JD (2006) Expression of insulin pathway genes during the period of caste determination in the honey bee, *Apis mellifera*. *Insect Mol Biol* **15**, 597-602.

268. Patel A, Fondrk MK, Kaftanoglu O, Emore C, Hunt G, Frederick K & Amdam GV (2007) The making of a queen: TOR pathway is a key player in diphenic caste development. *PLoS One* **2**, e509.

269. Corona M, Velarde RA, Remolina S, Moran-Lauter A, Wang Y, Hughes KA & Robinson GE (2007) Vitellogenin, juvenile hormone, insulin signaling, and queen honey bee longevity. *Proc Natl Acad Sci U S A* **104**, 7128-7133.

270. Okada Y, Miyazaki S, Miyakawa H, Ishikawa A, Tsuji K & Miura T (2010) Ovarian development and insulin-signaling pathways during reproductive differentiation in the queenless ponerine ant *Diacamma* sp. *J Insect Physiol* **56**, 288-295.

271. Ascunce MS, Yang CC, Oakey J, Calcaterra L, Wu WJ, Shih CJ, Goudet J, Ross KG & Shoemaker D (2011) Global invasion history of the fire ant *Solenopsis invicta*. *Science* **331**, 1066-1068.

272. Poltilove RM, Jacobs AR, Haft CR, Xu P & Taylor SI (2000) Characterization of *Drosophila* insulin receptor substrate. *J Biol Chem* **275**, 23346-23354.

273. Zhang B, Tavare JM, Ellis L & Roth RA (1991) The regulatory role of known tyrosine autophosphorylation sites of the insulin receptor kinase domain. An assessment by replacement with neutral and negatively charged amino acids. *J Biol Chem* **266**, 990-996.

274. Kondo H, Ino M, Suzuki A, Ishizaki H & Iwami M (1996) Multiple gene copies for bombyxin, an insulin-related peptide of the silkmoth *Bombyx mori*: structural signs for gene rearrangement and duplication responsible for generation of multiple molecular forms of bombyxin. *J Mol Biol* **259**, 926-937.

275. You H, Zhang W, Jones MK, Gobert GN, Mulvenna J, Rees G, Spanevello M, Blair D, Duke M, Brehm K & McManus DP (2010) Cloning and characterisation of *Schistosoma japonicum* insulin receptors. *PLoS One* **5**, e9868.

276. Khayath N, Vicogne J, Ahier A, BenYounes A, Konrad C, Trolet J, Viscogliosi E, Brehm K & Dissous C (2007) Diversification of the insulin receptor family in the helminth parasite *Schistosoma mansoni*. *FEBS J* **274**, 659-676.

277. DiAngelo JR & Birnbaum MJ (2009) Regulation of fat cell mass by insulin in *Drosophila melanogaster*. *Mol Cell Biol* **29**, 6341-6352.

278. Swofford D (2002) *PAUP*. Phylogenetic Analysis Using Parsimony (*and Other Methods).* Sinauer Associates, Sunderland, MA.

279. Holmes SP, He H, Chen AC, lvie GW & Pietrantonio PV (2000) Cloning and transcriptional expression of a leucokinin-like peptide receptor from the southern cattle tick, *Boophilus microplus* (Acari: Ixodidae). *Insect Mol Biol* **9**, 457-465.

APPENDIX

List of abbreviations:

*Si*VgR	*Solenopsis invicta* vitellogenin receptor
VgR	Vitellogenin receptor
LDLR	Low-density lipoprotein receptor
JH	Juvenile hormone
Vg	Vitellogenin
RNAi	RNA interference
dsRNA	Double-stranded RNA
EGFP	Enhanced green fluorescent protein
sNPF	Short neuropeptide F;
CNS	Central nervous system
mCa	Medial calyces
lCa	Lateral calyces
sP, slP, smP, iP, ilP, imP, respectively.	The superior, the superior lateral, superior medial, inferior, inferior lateral, and inferior medial protocerebrum, respectively.
SEG	Subesophageal ganglion.
*Si*InR	*Solenopsis invicta* insulin receptor
IIS	Insulin/insulin-like growth factor signaling
RTK	Receptor Tyrosine Kinase
LB domain	Ligand Binding domain
TK domain	Tyrosine Kinase domain

VITA

NAME: Hsiao-ling Lu

ADDRESS: Department of Entomology
c/o Dr. Patricia Pietrantonio
Texas A&M University
College Station, TX 77843-2475

EMAIL ADDRESS: nancylu0311@hotmail.com

EDUCATION:
2011 Ph.D. Entomology, Texas A&M University.
2002 M.S. Entomology, National Chung-Hsing University.
2000 B.S. Entomology, National Chung-Hsing University.

PEER REVIEWED PUBLICATIONS (2005-2011):

1. Lu, H.L. & Pietrantonio, P.V. 2011. Insect insulin receptors: insights from sequence and caste expression analyses of two cloned hymenopteran insulin receptors cDNAs from the fire ant. (Accepted. *Insect Molecular Biology*).
2. Lu, H.L., Pietrantonio, P.V. 2011. The distribution of short neuropeptide F receptor in queen brain and ovaries of fire ant. *BMC Neuroscience.* 12:57.
3. Lu, H.L., Kersch, C., Taneja-Bageshwar, S., Pietrantonio, P.V. 2011. A calcium bioluminescence assay for functional analysis of mosquito (*Aedes aegypti*) and tick (*Rhipicephalus microplus*) G protein-Coupled Receptors. *JoVE.*
4. Lu, H.L., Kersch, C., Pietrantonio, P.V. 2010. The kinin receptor is expressed in the Malpighian tubule stellate cells in the mosquito *Aedes aegypti* (L.): A new model needed to explain ion transport? *Insect Biochem. Mol. Biol.* 41: 135-140.
5. Lu, H.L., Vinson, S.B., Pietrantonio, P.V. 2009. Oocyte membrane localization of vitellogenin receptor coincides with queen flying age and receptor silencing by RNAi disrupts egg formation in fire ant virgin queens. *FEBS Journal* 276: 3110–3123.

BOOK CHAPTER:

Vinson, S.B. Pietrantonio, P.V., Lu, H.L., Coates, C.J. 2008. The physiology of reproduction in the imported fire ant, *Solenopsis invicta* Buren. In *Recent Advances in insect physiology, toxicology and molecular biology* (Liu N, ed), pp. 153-171. Research Signpost, Kerala, India.

SELECTED AWARDS AND SCHOLARSHIPS:

2011 John Henry Comstock Graduate Student Award. ESA.
2010 Sigma Xi Grants-in-Aid of Research Award.
2008, 2009 1st place winner of 11th and 12th Student Research Week. TAMU.
2008 2nd place winner of the 11th Entomology Graduate Student Forum. TAMU.
2007 3rd place winner of the 10th Entomology Graduate Student Forum. TAMU.
2005 Scholarship from Mark Lu Educational Foundation of Hualien ($17,000).